The Role of Ribosome Biogenesis in *Arabidopsis thaliana* Root Development and Epidermal Patterning

by

Yana Marie Wieckowski

**A dissertation submitted in partial fulfillment
of the requirements for the degree of
Doctor of Philosophy
(Molecular, Cellular and Developmental Biology)
in The University of Michigan
2011**

Doctoral Committee:

Professor John W. Schiefelbein, Chair
Professor Steven E. Clark
Assistant Professor Scott E. Barolo
Assistant Professor Erik E. Nielsen

ACKNOWLEDGEMENTS

This thesis represents the culmination of my academic career to date - without the support of my family, friends and colleagues it would not be in existence.

First and foremost, I would like to express my sincere gratitude to my advisor Dr. John Schiefelbein for his continuous support of my PhD study and research. Your guidance, patience, motivation, enthusiasm, and immense knowledge helped me in all the time of research and writing of this thesis. Thank you for providing a great environment for learning and development, both personally and professionally.

I'd also like to thank my committee members, Scott Barolo, Steve Clark and Erik Nielsen for their valuable comments and encouragement throughout this process. I could not have asked for a better committee.

I would like to thank present and former lab members Su-Hwan Kwak, Christa Barron, Angela Bruex, Christine Bernhardt, Aaron Sluis, Myeong Min Lee and Amy Zheng for stimulating discussions (both about science and not), helpful advice, and support throughout my time at Michigan. In particular, I would like to extend a special thanks to Su-Hwan for being a wonderful friend and mentor. Without your help, this thesis would not have been possible.

I would also like to thank the Cellular Biotechnology Training Program for

partial financial support during my PhD tenure as well as for providing me with a glimpse into different fields of biology, both in academia and in industry.

I would like to express my gratitude to the members of the Maddock lab, especially Dr. Janine Maddock and Dr. Ryszard Zielke, for help with the primer extension experiment. Thank you for welcoming me into your lab as I navigated through the uncharted territory of giant acrylamide gels and radioactivity.

A sincere thank you goes out to my fellow classmates and plant lab colleagues. To the incoming class of 2005, in particular Emily Petty, Karishma Collette and Gizem Kalay, thank you for your support over the years. We navigated the first years, survived prelims and are moving on together - best of luck to you all! To my plant lab colleagues, especially Jennifer Gagne, Nicola Harrison-Lowe, Amy Szumlanski and Lindsay Gish, thank you for help and support both in science and in life. I'm forever indebted to your helpful discussions and technical support - as well as necessary diversions (of the eating, coffee-drinking, and crafting kind). A special thanks to all of you who enthusiastically braved the East Coast wet wedding of 2008.

It goes without saying that I would not be where I am today without the love, support and encouragement from my family. Somehow I emerged from a family of engineers, a trait that skipped over me right to my brother. While Danny was dissecting computer parts in the basement, I was more interested in pond scum collected from Wyassup Lake. Thank you for recognizing my passion and for nurturing it over the years. Mom, Dad and Dan - you are a constant source inspiration. I dedicate this thesis to you.

To all my wonderful in-laws – thank you for your support and love; and for welcoming me wholeheartedly into your crazy family. A special thanks to “Big Stimpy” for your enthusiast discussions and editing help while I was writing this thesis.

Lastly, to my other half - I know in my heart that I could not have done this without your unwavering love and support. You patiently listened to my doubts as experiments repeatedly failed or yielded unexpected results, and cheered me on when things finally came together. . . . . so far it’s been quite an adventure, I can’t wait to see where it takes us next.

TABLE OF CONTENTS

LIST OF FIGURES

LIST OF TABLES

LIST OF ABBREVIATIONS

BAC	bacterial artificial chromosome
CAPS	cleaved amplified polymorphic sequence
CPC	CAPRICE
dCAPS	derived cleaved amplified polymorphic sequence
DIM1A	DIM1-like protein A
DNA	deoxyribonucleic acid
EGL3	ENHANCER OF GLABRA3
ETC1	ENHANCER OF TRY AND CPC 1
GL2	GLABRA2
GL3	GLABRA3
GFP	green fluorescent protein
GUS	β-Glucoronidase
H-cell	hair cell
H-file	hair cell file
Kb	kilobase
Ler	Landsberg erecta
Mb	megabase
N-cell	non-hair cell
N-file	non-hair cell file
PCR	polymerase chain reaction
RNA	ribonucleic acid
rRNA	ribosomal RNA
SAM	S-adenosyl-L-methionine
sno-RNP	small nucleolar ribonucleoprotein
SCM	SCRAMBLED
SSLP	simple-sequence-length polymorphisms
TRY	TRIPTYCHON
TTG1	TRANSPARENT TESTA GLABRA 1
WER	WEREWOLF
WS	Wassilewskija
WT	wild type

Note: Arabidopsis genes are represented by uppercase, italics font; mutations by lowercase, italics; and proteins by uppercase, non-italicized.

ABSTRACT

The Role of Ribosome Biogenesis in *Arabidopsis thaliana* Root Development and Epidermal Patterning

by

Yana Marie Wieckowski

Chair: John W. Schiefelbein

The establishment of distinct patterns of gene expression is essential to the differentiation of specialized cell types during the development of multicellular organisms. To investigate the regulatory networks involved in this cell fate specification, one can turn to the *Arabidopsis* root epidermis, where a position-dependent pattern of hair and non-hair cells serves as a pertinent and accessible model. Recent studies have implicated ribosomal protein and ribosome assembly factors in regulation of gene expression during development, however, the connection between ribosome biogenesis and root cell-type patterning has previously never been investigated. To that end, this thesis research explores the connection and function of a highly conserved ribosome biogenesis factor with respect to the development and epidermal patterning of the *Arabidopsis* root

epidermis.

The *Arabidopsis DIM1A* gene was identified in a genetic screen for genes required for position-dependent expression of non-hair fate regulator *GLABRA2*. Our analysis has revealed that functional DIM1A is required for generation of distinct gene expression patterns in developing root-hair and non-hair cells. In addition to defects in root epidermal patterning, the *dim1A* mutant displays reduced root meristem cell division rate and deficient leaf size, shape, vascular patterning and trichome branching. Furthermore, *DIM1A* promoter activity and gene product are enriched in rapidly dividing plant tissues, supporting a role for *DIM1A* in *Arabidopsis* development and cell differentiation.

The Dim1/KsgA family of dimethylases are a highly conserved enzymes involved in post-transcriptional modification of ribosomal RNA (rRNA) and pre-rRNA processing. While the two small subunit RNA base modifications they catalyze are present in almost every known organism, the functional significance of these modifications is currently unknown. My experimental evidence indicates that the *dim1A* mutant lacks the two 18S rRNA modifications without affecting pre-rRNA processing. In conclusion, I propose that DIM1A and the post-transcriptional rRNA modification it catalyzes are important for generating well-defined patterns of gene expression necessary for establishment of the two distinct cell fates in the *Arabidopsis* root epidermis.

CHAPTER 1

Introduction: *Arabidopsis thaliana* Root Development and Eukaryotic Ribosome Biogenesis

Development and Patterning of the *Arabidopsis* Root Epidermis

Patterning of distinct cell types is one of the most fundamental processes that occur during the development of multicellular organisms. As such, a growing body of research has been undertaken with the aim of uncovering the intricacies of cell patterning using a variety of model organisms and experimental approaches. An ideal system possesses a simple and easily visible pattern; robust and rapid growth; easy experimental manipulation; and powerful molecular and genomic resources. Given these prerequisites, the *Arabidopsis* root epidermis has emerged over the last twenty years as a leading model for studying cell pattern formation (Grierson and Schiefelbein, 2002, Ueda *et al.*, 2005, Guimil and Dunand, 2006, Schellmann *et al.*, 2007, Schiefelbein *et al.*, 2009).

The *Arabidopsis* root epidermis contains two types of cells, root-hair cells

and non-hair cells, which arise in a stereotyped pattern influenced by cell position. Because only two cell types are specified, root epidermal pattern formation is reduced to an either-or decision, making it an ideal system for studying cell fate specification during development. Furthermore, root hairs are visible shortly after germination, and complete loss of hairs does not affect viability or fertility, making it a quick and robust model system to work with. An extensive body of research has characterized the development of *Arabidopsis* root epidermal cells from origin to maturity (Dolan *et al.*, 1994, Dolan *et al.*, 1993, Scheres *et al.*, 1994), providing a solid foundation for the study of cell fate specification. These cells are formed continuously in cell files, which means that a complete developmental timeline may be observed along the axis of growth at any point in time. An increasing array of genetic, molecular and genomic resources, including publicly available microarray databases of root tissue of specific cell types and from a variety of mutants, aid in analysis and identification of genes and proteins. The analysis of root hair patterning in *Arabidopsis* has enriched our understanding of molecular-genetic regulation of cell fate specification and ongoing research continues to glean new information.

Arabidopsis root post-embryonic growth and development

The *Arabidopsis* primary root is elegantly organized in concentric rings of cells surrounding a central vascular region. A transverse root section reveals four layers (from outside inward): the epidermis, cortex, endodermis and pericycle surrounding the vascular tissue (phloem, xylem and procambium) (Fig.

1.1a) (Dolan *et al.*, 1993). Stereotyped divisions of a small population of stem cells at the tip of the root combined with lack of cell movement give rise to clonally-related cells organized in files along the axis of root growth (Dolan *et al.*, 1993).

Epidermal cells arise from a group of 16 epidermal/lateral root cap (LRC) stem cells (Dolan *et al.*, 1993, Dolan *et al.*, 1994) maintained by four adjacent cells, called the quiescent center (QC), which serve as the stem cell niche (Fig. 1.2) (van den Berg *et al.*, 1997). Each epidermal/LRC stem cell divides periclinally, generating an outer cell (the LRC daughter cell) as well as an inner cell. The inner cell divides transversely generating the epidermal daughter cell as well as regenerating the stem cell (Fig. 1.2) (Dolan *et al.*, 1993, Dolan *et al.*, 1994). After epidermal cells are generated, they undergo rapid cell division in the meristem division zone (Fig. 1.3). Each meristematic epidermal cell will divide transversely on average five to six times, which serves to generate additional cells in each file. Typically, a seedling root will have 16-24 epidermal cell files - one file from each of the 16 original stem cells, and additional files generated by occasional longitudinal divisions (Dolan *et al.*, 1994, Berger *et al.*, 1998b).

Upon exiting the meristem region, root cells cease division and rapidly elongate in the direction of root growth until their final cell dimensions are reached (Fig. 1.3.). When elongation ceases, root hairs emerge from the epidermis (Dolan *et al.*, 1994). Mature hair cells possess long, tubular outgrowths approximately 22 microns in diameter and one millimeter or more in length (Fig. 1.3a) (Grierson and Schiefelbein, 2002). Root hairs are not

multicellular structures, but rather are tip-growing protrusions that emerge at the end of the cell nearest the root tip (Grierson and Schiefelbein, 2002). Root hairs vastly increase the surface area of the root and are thought to aid plants in nutrient acquisition, water uptake, anchorage and microbe interaction (Hofer, 1991).

Root epidermal patterning: to be or not to be a hair cell

Most angiosperms possess both hair cells and non-hair cells in their root epidermis. Among these species, three patterns of epidermal cell types have been identified: alternating pattern, random pattern and position-dependent striped pattern (Reviewed in Dolan and Costa, 2001). The alternating pattern, which is widespread among monocots but present in only a few dicot species, results from asymmetric epidermal cell divisions that give rise to a large non-hair cell and a small hair cell (Clowes, 2000). Widespread amongst dicots and found in some monocots, plants with a randomly patterned epidermis develop hair cells on all, none or a subset of epidermal cells - the final distribution influenced primarily by environmental conditions (Cormack, 1937, 1947, Clowes, 2000, Pemberton *et al.*, 2001). Lastly, the position-dependent striped pattern, in which hair cell files alternate with non-hair cell files, is found in a few families of dicots, including *Brassicaceae* (Cormack, 1935, Clowes, 2000, Dolan and Costa, 2001, Pemberton *et al.*, 2001).

Hair and non hair cells: how are they different?

Epidermal cells in *Arabidopsis,* a model plant from the family *Brassicaceae*,

are organized in position-dependent stripes relative to the anticlinal cortical cell wall (ACCW), the boundary between adjacent cortical cell files. Cells located over the ACCW (H position cells) make root hairs and those located over a single cortical cell file (N position cells) do not (Fig. 1.1) (Dolan *et al.*, 1993, Galway *et al.*, 1994). This striped pattern has been shown by both clonal analysis (Berger *et al.*, 1998b) and laser-ablation studies (Berger *et al.*, 1998a) to be regulated by positional information as apposed to lineage.

Morphological differences between the two types of epidermal cells are not limited to the simple presence or absence of a root hair, and are in fact discernible long before any evidence of root hair emergence. In *Arabidopsis*, H-position cells have greater cytoplasmic density (Dolan *et al.*, 1994, Galway *et al.*, 1994), variant cell surface features (Dolan *et al.*, 1994, Freshour *et al.*, 1996), delayed vacuolation (Galway *et al.*, 1994), and distinct chromatin organization (Costa and Shaw, 2006, Xu *et al.*, 2005), all characteristics attributed to greater metabolic activity involved in production of a root hair (Cutter, 1978). Additionally, H files contain more cells with reduced cell length compared to cells in N files, a consequence of a greater rate of cell division (Berger *et al.*, 1998b, Dolan *et al.*, 1994, Massucci *et al.*, 1996). Taken together, it is evident that epidermal cells are programmed early during post-embryonic development to follow their distinct developmental paths. Nevertheless, until exit from the meristem and the onset of elongation, they are capable of switching fates if their position relative to underlying cortical cells changes (Berger *et al.*, 1998a)

The genetics behind root epidermal cell fate specification

Molecular genetic research has unveiled an intricate regulatory network that guides *Arabidopsis* root meristem epidermal cell fate specification. With the influence of positional information, this molecular machinery within epidermal cells utilizes lateral inhibition and feedback mechanisms to regulate cell-type specific expression of root hair morphogenesis genes. From what is know of the molecular nature of root epidermal cell fate specification in *Arabidopsis*, *GLABRA2* (*GL2*) is the most downstream player and it often used as a readout of the integrity of upstream signaling. GL2, a homeodomain transcription factor (Rerie *et al.*, 1994), is required for non-hair cell differentiation (Massucci *et al.*, 1996). Loss of *GL2* expression results in specification of root-hair cells in all positions, resulting in a hairy root phenotype (Fig. 1.4a) (Massucci *et al.*, 1996, Di Cristina *et al.*, 1996). Interestingly, loss of *GL2* does not affect all aspects of hair cell differentiation - cells develop early characteristics (vacuolation, cell size, cytoplasmic density) in accordance with their position (Massucci *et al.*, 1996). The *GL2* gene is expressed in a position-dependent manner in developing non-hair cells as early as two to three cells above the epidermal/lateral root cap initial cell (Fig. 1.4b) (Massucci *et al.*, 1996). Preferential *GL2* expression in N position cells appears to be critical for non-hair specification, as *GL2* expression in the cells in the H position causes them to develop as non-hair cells. The GL2 protein negatively regulates transcription of root-hair morphogenesis genes and positively regulates non-hair cell specific genes to promote the non-hair cell fate (Massucci *et al.*, 1996, Lee and Schiefelbein, 1999, 2002). Putative GL2 targets

include: *ROOT HAIR DEFECTIVE 6 (RHD6)*, which encodes a basic helix-loop-helix (bHLH) transcription factor involved in root hair initiation (Menand *et al.*, 2007), and *PHOSPHOLIPASE Dζ1 (PLDζ1)*, which plays a role in hair outgrowth and elongation (Ohashi *et al.*, 2003). GL2 has been shown to bind the promoter and prevent expression of *PLDζ1* (Ohashi *et al.*, 2003), supporting its role in downregulation of hair gene expression.

Four genes, *WEREWOLF* (*WER*), *GLABRA3* (*GL3*), *ENHANCER OF GLABRA3* (*EGL3*) and *TRANSPARENT TESTA GLABRA 1* (*TTG1*), are positive regulators of the non-hair cell fate, and are essential for all aspects of non-hair cell development, as loss-of-function mutations result in every epidermal cells developing both early and late characteristics of hair cells (Fig. 1.4a) (Bernhardt *et al.*, 2003, Lee and Schiefelbein, 1999, Galway *et al.*, 1994, Massucci *et al.*, 1996). The four encoded proteins preferentially accumulate in N position cells and are thought to act together as a core transcriptional complex to generate a spatially-distinct expression pattern of *GL2* in cells in the N position.

The WER protein belongs to the R2R3 family of MYB-domain transcription factors and contains two MYB repeats and an acidic transcriptional activation domain (Lee and Schiefelbein, 1999). *WER* is expressed highly in developing root-hair and non-hair cells, later becoming restricted mainly to non-hair cells (Fig. 1.4b) (Lee and Schiefelbein, 1999). WER is nuclear-localized and has been shown to influence *GL2* expression by binding to MYB-binding sites in the *GL2* promoter (Koshino-Kimura *et al.*, 2005). Accordingly, the *WER* loss-of-function mutation effectively abolishes *GL2* promoter activity and transcript accumulation

(Lee and Schiefelbein, 1999). *WER* also plays a role in positively reinforcing the core transcriptional complex in developing non-hair cells through direct transcriptional activation of a highly related R2R3 MYB protein, MYB23 (Kang *et al.*, 2009). The MYB23 protein is functionally equivalent to WER and is thought to contribute to increased production of the WER/MYB23-GL3/EGL3-TTG transcriptional complex in developing non-hair cells (Kang *et al.*, 2009). This positive feedback loop ensures robust formation of the epidermal cell-type pattern.

The core transcriptional complex genes *GL3* and *EGL3*, which encode highly related bHLH proteins, are also necessary for *GL2* expression and non-hair cell fate specification. Interestingly, the TTG-GL3/EGL3-WER core transcriptional complex suppresses expression of *GL3* and *EGL3* in cells in the N position, restricting promoter activity (Fig. 1.4b) and RNA accumulation to developing H position cells (Bernhardt *et al.*, 2005). However, GL3 protein is present primarily in developing non-hair cells, indicating that GL3 (and possibly EGL3 as well) moves from the H position cells to the N position cells, potentially as a additional feedback/lateral inhibition mechanism between epidermal cells (Bernhardt *et al.*, 2005).

It is interesting to note, that while GL3 and EGL3 are functionally similar in many ways, they also exhibit significant differences. For instance, the *gl3 egl3* double mutant has a dramatic increase in hair cells (due to misspecification of hair cells in the non-hair position), the *gl3* single mutant shows only has a moderate increase in hair cell frequency and the *egl3* single mutant has only a

slight increase in hair cell frequency (Bernhardt *et al.*, 2003). Furthermore, the effect of overexpression of *GL3* is not as strong as *EGL3* (Bernhardt *et al.*, 2003), an unexpected result considering the significance of their single mutant patterning defects. In addition, *EGL3* plays a role in regulation of seed coat mucilage and anthocyanin production, whereas *GL3* is not required for these biological functions (Zhang *et al.*, 2003).

The third core transcriptional complex member TTG1, a small protein containing WD40 repeats (Walker *et al.*, 1999), also is essential for specification of the non-hair fate. Overexpression of *GL3* and *EGL3* can overcome the effect of the *ttg1* mutation, but not the *wer* mutation (Bernhardt *et al.*, 2003), suggesting that *GL3* and *EGL3* act in parallel with *TTG1* and potentially downstream of *WER* in the non-hair specification pathway. *TTG1* has also been shown to be important for trichome formation, anthocyanin production, and seed coat mucilage (Koornneef, 1981, 1990). Interestingly, *TTG1*'s role in these varied biological processes all involve both a MYB and bHLH protein, suggesting a common mechanism for TTG1 action (Zhang *et al.*, 2003).

While the importance of the TTG-GL3/EGL3-WER core transcriptional complex for non-hair cell fate specification is most apparent, it also influences root-hair cell fate by promoting transcription of a three single-repeat R3 MYB-domain proteins, CAPRICE (CPC), TRIPTYCHON (TRY), and ENHANCER OF TRY AND CPC (ETC1), which are necessary for root-hair cell fate specification (Simon *et al.*, 2007, Bernhardt *et al.*, 2003, Lee and Schiefelbein, 2002, Wada *et al.*, 2002, Wada *et al.*, 1997, Schellmann *et al.*, 2002, Kirik *et al.*, 2004). WER,

TTG and GL3/EGL3 are necessary for *CPC*, *TRY* and *ETC1* gene expression (Lee and Schiefelbein, 2002, Wada *et al.*, 2002, Simon *et al.*, 2007, Bernhardt *et al.*, 2003) likely mediated through binding of WER to MYB binding sites within their promoters (as has been shown for *CPC*) (Koshino-Kimura *et al.*, 2005, Ryu *et al.*, 2005). The *cpc* single mutant has a moderate reduction in root-hair cell frequency (Fig. 1.4) (Wada *et al.*, 1997) and the *try* and *etc1* single mutants have slight to no affect on root hair frequency (Schellmann *et al.*, 2002, Kirik *et al.*, 2004). However, the *cpc try* double (Schellmann *et al.*, 2002) and *cpc try etc1* triple mutants completely lack root hairs, with the *etc1* mutation enhancing the *cpc try* root hair defective phenotype at the hypocotyl-root junction (Kirik *et al.*, 2004). Furthermore, functional *CPC*, *TRY* and *ETC1* genes are necessary to restrict *GL2* expression to cells in the N-position. *GL2* expression is expanded moderately in *cpc* (Wada *et al.*, 2002, Lee and Schiefelbein, 2002) slightly in *try* and *etc1,* and to almost every epidermal cell in the *cpc try* double and *cpc try etc1* triple mutants (Simon *et al.*, 2007). Conversion of all epidermal cells to non-hair cells is *WER*-dependent, as the *wer cpc try* triple mutant resembles the *wer* single mutant phenotypically, possessing hairs on every cell and lacking detectable *GL2::GUS* expression (Simon *et al.*, 2007). This suggests that CPC, TRY and ETC1 act downstream of the TTG-GL3/EGL3-WER core transcriptional complex to influence hair cell fate by downregulating expression of *GL2* in H-position cells.

Current research supports the role of the R3 MYB-domain proteins as part of a lateral inhibition pathway between epidermal cell types. While *CPC*, *TRY*

and *ETC1* are necessary for specifying the hair-cell fate, mRNA expression is detected only in developing cells in the N-position (Wada *et al.*, 2002, Schellmann *et al.*, 2002, Kirik *et al.*, 2004, Simon *et al.*, 2007). CPC protein is found in nuclei of both N-position and H-position cells, indicating that CPC (and possibly TRY and ETC1 as well) moves from one cell type to the other, likely through the plasmodesmata (Wada *et al.*, 2002, Kurata *et al.*, 2005). Altogether, it appears that the TTG-GL3/EGL3-WER core transcriptional complex promotes transcription of *CPC*, *TRY* and *ETC1* in N position cells, and that these R3 MYB proteins then move to H position cells acting as a lateral inhibitors to prevent specification of the non hair fate in cells in the H position.

While MYB proteins are known to bind both DNA and proteins in plants, loss of conserved amino acids required for MYB-protein binding to DNA indicates that CPC, TRY and ETC1 likely function through protein-protein interactions (Wada *et al.*, 2002). Furthermore, the *CPC*, *TRY* and *ETC1* gene products are highly related to the R2R3 MYB-domain protein WER, except for the absence of the acidic transcriptional activation domain (Wada *et al.*, 1997, Schellmann *et al.*, 2002, Kirik *et al.*, 2004). By constructing CPC-WER chimeric proteins, Tominaga et al (2007) showed that the WER R3 domain could functionally replace the CPC R3 domain as well as confer *GL2* promoter binding activity to the CPC protein. Together, molecular genetic and biochemical research suggests that through evolution the R3-single repeat MYB-domain proteins CPC, TRY and ETC1, lost functionality as transcription factors.

The positional control of root epidermal cell pattern

SCRAMBLED (SCM), a leucine-rich repeat receptor-like kinase (LRR-RLK), is necessary for the position-dependence of root epidermal cell fate specification. Loss-of-function mutations in *SCM* make a similar frequency of hair cells as wild-type, however there is a remarkable disconnect between cell fate and position (Kwak *et al.*, 2005). Interestingly, the epidermal cell molecular network establishes cell identity in the *scm* mutant as it does in wild-type, however transcription factor expression (and subsequently cell fate) is no longer directly connected to the cell position relative to underlying cortical cell junctions (Kwak *et al.*, 2005, Kwak and Schiefelbein, 2007). Still, the pattern of epidermal cells is not completely random, even in the presumed *scm* null mutant. A tendency for the cells to adopt fate based on their position hints at an auxiliary or parallel mechanism to the SCM signaling pathway influencing positional patterning.

SCM gene expression, mRNA accumulation and protein localization occur throughout the developing root tissue, with the exception of the lateral root cap (Kwak *et al.*, 2005, Kwak and Schiefelbein, 2008). In epidermal cells, the SCM protein is localized on the plasma membrane of both cell types, but is enriched in H position cells in the late division and early elongation zones (Kwak and Schiefelbein, 2008). Using tissue-specific promoters to drive RNA interference of *SCM* in wild-type plants and to drive *SCM* gene expression in *scm* mutant plants, Kwak et al (2008) found that *SCM* expression and accumulation in epidermal cells is both sufficient and necessary for epidermal patterning. Furthermore, to fully complement the *scm* cell-fate patterning defect, preferential *SCM* expression

in H position cells is necessary, as driving *SCM* expression using non-hair cell promoters caused aberrant patterning (Kwak and Schiefelbein, 2008).

Detailed genetic and expression studies indicate that the SCM signaling pathway influences epidermal cell fate through preferential inhibition of *WER* transcription in the H cell position. *WER* expression is moderately increased in the *scm* mutant background and in the *cpc scm* mutant background, in which the dampening effect of the CPC feedback loop is removed, there is an even greater increase in *WER* expression (Kwak and Schiefelbein, 2007). Additionally, overexpressing *SCM* results in a significant reduction in *WER* mRNA accumulation (Kwak and Schiefelbein, 2007). These and other findings imply that SCM influences the downstream transcription factor network by repressing *WER* transcription in H position cells (Kwak and Schiefelbein, 2007).

As *SCM* encodes a receptor-like kinase localized to the plasma membrane of epidermal cells it is likely to receive a positional signal and translate it to underlying epidermal cells (Kwak et al., 2005). Surprisingly, biochemical and genetic evidence indicate that while the carboxyl-terminal kinase domain is necessary for function, it most likely lacks catalytic activity (Chevalier *et al.*, 2005). Thus, SCM may act as an atypical receptor-like kinase, functioning through protein-protein interactions with a additional, active kinase (Chevalier *et al.*, 2005).

Chromatin modifications influence cell fate specification

Chromatin modification may act as a sensor switch to modulate patterning

signals. Initial evidence from Shu-Nong Bai and colleagues came in the way of altered position-dependent patterning after application of histone deacetylase compound TSA (Xu *et al.*, 2005). In addition, they specifically implicated a histone deacetylase protein, *HDA18*, in mediating epidermal patterning during development (Xu *et al.*, 2005).

Additional support for the importance of chromatin modifications in epidermal patterning came from Costa and Shaw (2006) through their use of three-dimensional fluorescence in situ hybridization (3D FISH) on intact root tissue. They found that wild-type plants display an “open” chromatin organization around the *GL2* locus in N position cells, where *GL2* is normally expressed, and a “closed” conformation in H position cells, where *GL2* expression is repressed. Furthermore, they observed that specific chromatin states around the *GL2* locus are not inherited, but rather are reset during mitosis and re-specified in the following G1 phase of the cell cycle in response to local positional information. This suggests that root meristem cells are constantly assessing their position relative to underlying cortical cells and rapidly respond to changes in position by remodeling chromatin around patterning gene loci (Costa and Shaw, 2006).

Position-dependent chromatin modifications may be mediated by the GEM1 protein, which was found to interact directly with TTG1 and affect histone methylation within the *GI2* and *CPC* promoters (Caro *et al.*, 2007). Analysis of the phenotypic effect of overexpression and knockout of *GEM1* suggest a possible direct role of repressing *GL2* and *CPC* expression, potentially in H position cells, to negatively influence the non-hair cell fate in H position cells. It is

tempting to speculate that the “open” and “closed” chromatin state around the *GL2* locus identified by Costa and Shaw may be regulated by GEM1.

Model of position-dependent epidermal patterning

Molecular genetic and biochemical evidence to date suggest a model for position-dependent fate specification in the *Arabidopsis* root epidermis (Fig. 1.5). Essential to becoming a non-hair cell is accumulation of the TTG-GL3/EGL3-WER core transcriptional activation complex. On the other hand, an epidermal cell will become a hair cell if it accumulates enough CPC/TRY/ETC1 to prevent core transcriptional complex formation by preventing WER from binding to TTG-GL3/EGL3. Therefore, a cell with greater relative abundance of WER than CPC will develop as a non-hair cell, and one with greater CPC will develop as a hair cell. In developing non-hair cells, the core transcriptional complex (TTG-GL3/EGL3-WER) promotes non-hair cell fate (through expression of *GL2*), lateral inhibition (through expression of *CPC/TRY/ETC1*), down-regulation of SCM accumulation, and intracellular feedback (through expression of *MYB23*). In developing hair cells, the lateral inhibitors (CPC/TRY/ETC1) promote hair cell fate by competing with WER for binding to TTG-GL3/EGL3 (Lee and Schiefelbein, 1999, 2002, Tominaga *et al.*, 2007), positively regulating *GL3/EGL3* expression, as well as strengthening preferential H position accumulation of SCM (Kwak and Schiefelbein, 2008).

At the core of the cell fate specification model is interaction between the different patterning gene products. Genetic evidence supports the role of WER,

TTG1 and GL3/EGL3 as a core transcriptional activation complex and suggests that competition between WER and CPC/TRY/ETC1 for binding to TTG-GL3/EGL3 complex may be essential for epidermal patterning (Larkin *et al.*, 2003, Ueda *et al.*, 2005, Pesch and Hulskamp, 2004). To support this model, protein interaction and competition have been shown both in yeast and plant cells. The GL3 and EGL3 proteins have been shown to interact with CPC, TRY, WER and TTG1 and are thought to bridge the interaction between the MYB-domain and WD40-repeat proteins (Payne *et al.*, 2000, Zhang *et al.*, 2003, Bernhardt *et al.*, 2003, Lee and Schiefelbein, 1999, Wada *et al.*, 2002). In support of this notion, the MYB-domain proteins WER, CPC, and TRY interact with a different region of the GL3 protein than TTG1 (Payne *et al.*, 2000, Zhang *et al.*, 2003). Additionally, TTG1 and the WER-equivalent MYB-domain protein GL1 cannot interact with each other (Payne *et al.*, 2000, Zhang *et al.*, 2003), however they each interact with GL3 and EGL3.

Furthermore, protein interaction analysis in yeast supports the model of the single-repeat MYB-domain proteins disrupting WER binding to the core transcriptional activation complex in cells in the H position. Tominaga et al (2007) used a yeast-three-hybrid experiment to demonstrate that the CPC protein inhibits WER interaction with GL3 or EGL3. Thus, it is likely that CPC, TRY, and ETC1 promote the cell fate by preventing WER from binding to TTG1-EGL3/GL3.

Feedback mechanisms also play an essential role in epidermal patterning by ensuring positional accuracy of patterning gene expression and localization.

One important feedback loop exists between GL3/EGL3 and CPC/TRY. GL3/EGL3 localization in N position cells is essential for *CPC* (and probably *TRY* and *ETC1*) expression (Bernhardt *et al.*, 2003), and CPC/TRY are essential in H position cells for *GL3/EGL3* expression (Bernhardt *et al.*, 2005), generating a positive intercellular feedback loop. Additionally, feedback is necessary for establishing preferential hair cell localization of the SCM receptor (Kwak and Schiefelbein, 2008). The core transcriptional activation complex negatively regulates *SCM* expression in N position cells and CPC/TRY positively regulate *SCM* expression in H-position cells (Kwak and Schiefelbein, 2008). Together, this intricate molecular network within epidermal cells establishes cell fate based on position and then strengthens cellular differences between cells in each position through lateral inhibition and multiple feedback loops.

Developmental timeline of epidermal patterning

Patterning genes are expressed in the proper position-dependent location beginning as early as the heart stage, suggesting that embryonic root epidermal cells have the same striped pattern before and after germination. *GL2* is first expressed throughout the epidermis of developing roots at late heart stage, and progressively becomes restricted to N position cells by the end of embryogenesis (Costa and Dolan, 2003). This suggests that pattern formation occurs between late heart stage and the mature stage of embryogenesis. Interestingly, in situ analysis does not detect *WER* or *CPC* expression at the heart stage (Costa and Dolan, 2003, Lin and Schiefelbein, 2001), but rather late torpedo stage (Costa

and Dolan, 2003). Functional WER, TTG1 (Lin and Schiefelbein, 2001), GL3/EGL3 (Bernhardt *et al.*, 2005), and CPC/TRY (Simon *et al.*, 2007) are required for N cell specific *GL2* expression in the embryo, suggesting similar molecular-genetic regulation in both the embryonic and post-embryonic root.

Unexpectedly, the *scm* mutant does not exhibit an alteration in expression of *GL2* in mature embryos or emerging roots from germinating seeds (which are from embryonic origin), implying that *SCM* is not required for embryonic epidermal patterning (Kwak and Schiefelbein, 2007). In fact, *GL2* expression patterning in the *scm* mutant background does not deviate from wild-type until three days post-germination (Kwak and Schiefelbein, 2007) or about the stage when root tip cells are derived from post-embryonic meristematic activity (Scheres *et al.*, 1994). This implicates an additional, unknown mechanism in embryonic position-dependent epidermal patterning.

Post-embryonically, patterning and positional information is continuously generated and processed, as a change in position late in the root meristem can result in a change in fate (Berger *et al.*, 1998a). SCM is necessary for establishing the pattern of meristem epidermal cells, not just maintaining a preset epidermal pattern established during embryogenesis, as may be implied from its lack of a role in embryonic root patterning (Kwak and Schiefelbein, 2007). Pattern analysis of epidermal clones, clonally-related files of cells generated by longitudinal division of a single epidermal cell, found the *scm* mutant to be significantly less effective at establishing two distinct cell fates in clones derived from developing hair cells (in which the clones would contain one new hair file

and one non-hair file) (Kwak and Schiefelbein, 2007). Thus, epidermal cells in the meristem continuously assess their position via the SCM-mediated signaling pathway during post-embryonic root development.

Root epidermal cell-type patterning – what's next?

Arabidopsis root epidermal patterning has been well studied and continues to provide insight into the molecular-genetic regulation of cell fate specification. Nevertheless, future research is needed to address many unanswered questions.

To fully understand the regulation of position-dependent pattern, it is essential to identify the putative SCM receptor ligand. Based on the specific organization of hair and non-hair cells relative to the underlying cortical cells, the SCM ligand is hypothesized to be asymmetrically distributed around the epidermis. However, the nature of the signal, where it is generated, and how it is translated to the epidermal cells is currently unknown. Additionally, it will be interesting to define the mechanism of signaling through the SCM pathway, as SCM has been shown to lack kinase activity (Chevalier *et al.*, 2005).

Also, in view of the fact that SCM is not required for position-dependent cell patterning in the embryonic epidermis and the *scm* mutant does not entirely abolish the cell pattern in the post-embryonic epidermis, additional patterning mechanisms beyond the SCM-signaling pathway are thought to exist (Kwak and Schiefelbein, 2007). The recent discovery of *scm*-like mutants *qky*, *doq* and *zet* may help answer some of these questions (Fulton *et al.*, 2009), however further research is needed to determine their precise role in root epidermal patterning.

Also of interest are the specific roles of redundant genes *GL3/EGL3* and *CPC/TRY/ETC1*. Not only do their loss-of-function root epidermal fate specification phenotypes differ (Bernhardt *et al.*, 2003, Bernhardt *et al.*, 2005, Schellmann *et al.*, 2002, Kirik *et al.*, 2004, Simon *et al.*, 2007), but new developments suggest that their genetic regulation (Simon *et al.*, 2007) and functions within the epidermal fate-specification pathway (Kwak and Schiefelbein, 2008) may also have diverged. Analysis at the transcriptome level may provide interesting insight to their slightly divergent, yet significantly overlapping functions.

Ribosome Biogenesis and the Role of a Conserved 18S RNA Modification

Ribosome biogenesis in eukaryotes

Ribosomes are essential components of all living organisms owing to their essential role in deciphering transcripts encoded by cellular genomes. Cells contain millions of ribosomes and expend an immense amount of resources and energy in generating and supporting this machinery.

Ribosomes are large ribonucleoprotein (RNP) complexes composed of two subunits: a large subunit (LSU), involved in polypeptide synthesis, and a small subunit (SSU), responsible for decoding messenger RNA (mRNA) transcribed from DNA. The internal composition and size of ribosomes varies between bacteria, fungi, plants and animals. In eukaryotes, the smaller 40S subunit consists of one 18S ribosomal RNA (rRNA) and approximately 30 proteins. The larger 60S subunit is composed of three rRNAs, a 25S-28S, 5.8S and 5S RNA, as well as about 40-50 proteins. The two subunits come together during translation initiation to form a functional 90S ribosome.

Ribosome biogenesis is a complex process requiring coordinated transcription, RNA processing, RNA modification, folding and complexing of RNA and ribosomal proteins. In eukaryotes, transcription and processing of ribosomal RNA as well as assembly of the ribonucleoprotein takes place in a sub-compartment of the nucleus called the nucleolus (Fig. 1.6). Transcripts encoding three of the four ribosomal RNA species are organized in multiple tandem copies

present on chromosomal sites, known as nucleolar organizer regions (NORs), sequestered in the nucleolus. The 18S, 5.8S and 25S/28S subunits are arranged within NORs as a unit, referred to as the "rDNA gene," and are transcribed by RNA polymerase I. Interestingly, in most eukaryotes the small 5S is located elsewhere in the genome, transcribed in the nucleoplasm by RNA polymerase III, and then imported into the nucleolus.

The rDNA gene is transcribed as a single, 35S/40S/45S (yeast/*Xenopus laevis*/higher eukaryotes) pre-rRNA, and then further processed to yield the individual subunits (Fig. 1.7). Individual rDNA genes are separated by non-transcribed spacers (NTS). Within a single rDNA gene, transcripts encoding the rRNA subunits are flanked on either end by external transcribed spacers (ETS) and are separated by internal transcribed spacers (ITS). Therefore, the transcribed pre-rRNA contains a 5' ETS region, the 18S, 5.8S and 25S-28S subunits separated by ITS1 (between the 18S and 5.8S) and ITS2 (between the 5.8S and 28S) and a 3' ETS region (Fig. 1.7).

Processing of the pre-rRNA to mature rRNAs requires a number of small nucleolar RNAs (snoRNAs) and nucleolar proteins (Venema and Tollervey, 1999, Fatica and Tollervey, 2002, Shaw and Jordan, 1995). After transcription, the pre-rRNA is endonucleolyticly cleaved at defined sites and then exonucleolytically trimmed to yield the three mature subunits (Fig. 1.7). The initial cleavages, which likely begin before transcription is complete, yield the 20S pre-rRNA, which is exported to the cytoplasm where it is processed to mature 18s rRNA (Udem and Warner, 1973). Subsequent processing events within ITS2 and the 3' ETS give

rise to the mature 5.8S and 28S rRNAs.

During processing, rRNA sequences undergo three types of nucleotide modifications: (1) conversion of uridine to pseudouridine, (2) 2'-O-methylation of ribose and (3) base modification. Uridine isomerization to pseudouridine and 2'-O-ribosome methylation are the most common rRNA modifications in eukaryotes, with over 100 of each kind found in most species (Maden, 1990, Ofengand and Bakin, 1997). In eukaryotes, most rRNA modifications occur co-transcriptionally (Kos and Tollervey, 2010) in the nucleolus, and are guided by trans-acting snoRNAs (Ganot *et al.*, 1997, Kiss-Laszlo *et al.*, 1996, Brown and Shaw, 1998). One notable exception is a conserved adenosine dimethylation of the 20S subunit rRNA that occurs in the cytoplasm (Brand *et al.*, 1977, Udem and Warner, 1973). Most rRNA nucleotide modifications occur in conserved regions involved in translation events or at sites of subunit interaction (Reviewed in Decatur and Fournier, 2002). Ribose methylation and pseudouridinylation have been implicated in refining the rRNA secondary structure, optimizing it for function (Maden, 1990, Ofengand and Bakin, 1997). While rRNA modifications have been thoroughly mapped in many organisms, the functional role of most is currently unknown (Decatur and Fournier, 2002).

The KsgA/Dim1 methyases catalyze a highly conserved 18S rRNA modification

18S adenosine dimethylation (Helix 45)

While overall ribosome structure has been well conserved throughout evolution, only three of the post-transcriptionally modified rRNA nucleotides are present in all branches of life. One is the pseudouridine in domain IV of the large subunit rRNA of cytoplasmic ribosomes (Ofengand, 2002). The other two are the dimethylations of adjacent adenines in the 3'-terminal loop (helix 45) of the small subunit rRNA (Fig. 1.8) (Van Knippenberg *et al.*, 1984). These dimethyladenosines are located at positions A1518 and A1519 in *Escherchia col*i, A1779 and A1780 in *Saccharomyces cerevisiae*, and based on sequence comparisons, putatively at positions A1785 and A1786 in *Arabidopsis thaliana*. Both the modifications and the sequence of the small subunit terminal loop are nearly universally conserved (Van Knippenberg *et al.*, 1984, McCloskey and Rozenski, 2005). The only known exceptions in wild-type organisms are the single dimethyladenosine in *Sulfolobus solfataricus* 16S rRNA, and the single dimethyladenosine or lack of dimethyladenosines in mitochondrial ribosomes from *Euglena gracilis* and *S. cerevisia*e, respectively (van Buul *et al.*, 1984a, Noon *et al.*, 1998, Klootwijk *et al.*, 1975). Research to date in *S. cerevisiae* suggests that in eukaryotes, the methylation event itself is not required for ribosome function, however the dimethylase enzyme that catalyzes the methylation is indispensable due to an indirect role in pre-rRNA processing (Lafontaine *et al.*, 1998, Lafontaine *et al.*, 1995). Interestingly, in prokaryotes neither the methylation nor the methylase enzyme are required for organism survival (Helser *et al.*, 1972, Poldermans *et al.*, 1979c). While the conservation of this nucleotide modification has been known for many years, the functional

significance of this unprecedented level of conservation has yet to be determined.

The KsgA/Dim1 family of dimethylases

The enzymes that carry out the RNA adenine methylation, known as the KsgA/Dim1 family of methylases, represent one of about sixty genes that are conserved in all domains of life (Lafontaine *et al.*, 1994, O'Farrell *et al.*, 2008, Van Buul and Van Knippenberg, 1985, O'Farrell *et al.*, 2006). These enzymes catalyze the transfer of four methyl groups from the cofactor S-adenosyl-L-methionine (SAM) to two adjacent adenosine bases in small subunit rRNA (18s in eukaryotes, 16S in prokaryotes) (Fig. 1.8.) (Helser *et al.*, 1972). The active site, which contains a Rossman-like fold homologous to other SAM-dependent methylases, creates binding pockets for cofactor SAM and the target nucleotide strand (O'Farrell *et al.*, 2008, Fauman *et al.*, 1998, O'Farrell *et al.*, 2004). Additionally, a canonical glycine-rich GXGXG binding motif, two acidic residues (which stabilize SAM binding) and an asparagine residue (shown to interact with SAM) are also present in the active site (Martin and McMillan, 2002).

Despite their common role as rRNA dimethyltransferases, some KsgA/Dim1 family members have gained additional functions during evolution. Eukaryotic Dim1 not only methylates rRNA in yeast, but is also required for pre-rRNA processing events (Lafontaine *et al.*, 1998, Lafontaine *et al.*, 1995). Similarly, the human mitochondrial transcription factors B1 and B2 (mtTFB) double as mitochondrial transcription factors as well as methyltransferases (Seidel-Rogol *et*

al., 2003, Cotney and Shadel, 2006). While the structural basis for their unique functions is currently unknown, alignment of the family members has revealed elements unique to each group (O'Farrell *et al.*, 2008). These proteins not only provide insight into the importance of a highly conserved rRNA nucleotide modification, but also provide an opportunity to study evolution of protein structure and function.

Escherichia coli KsgA

Over thirty years ago, modification of two adjacent adenosines at the 3' end of the 16S rRNA entered the limelight after their role in *E. coli* resistance to the aminoglycoside antibiotic kasugamycin was uncovered (Helser *et al.*, 1971, 1972). Years later, van Buul et al (1985) revealed that the *ksgA* gene disrupted in the resistant mutant encodes a dimethyladenosine transferase. The functional and structural role of both KsgA as well as the conserved dimethyladenosines it generates have been extensively researched since the 1970's.

Other than conferring kasugamycin resistance, lack of the two highly conserved dimethyladenosines only modestly affects *E. coli* fitness. Mutants lacking functional KsgA have reduced translational accuracy (O'Connor *et al.*, 1997, Van Buul *et al.*, 1984b), increased requirement of initiation factor 3 (IF-3) in the absence of initiation factor 1 (IF-1) during translation initiation (Poldermans *et al.*, 1979c), and reduced binding affinity of ribosomal subunits (Poldermans *et al.*, 1980). Recently, Connolly et al (2008) found that Δ*ksgA* mutants are cold sensitive, accumulate more free small ribosomal subunits than wild-type and

have a 16S rRNA maturation defect (seen as increased accumulation of 17S precursor). In addition, the dimethylations have been implicated in ribosome recycling, as the *ksgA* mutation enhances a temperature-sensitive mutant allele of the ribosome recycling factor RRF (Seshadri *et al.*, 2009). These defects are consistent with the localization of the modified residues at the interface between the ribosomal subunits, a region crucial for subunit interaction and translation initiation (O'Farrell *et al.*, 2004, Tu *et al.*, 2009). In support of this, crystallization of a 30S rRNA deficient in the conserved dimethyladenosines revealed a complete lack of hydrogen-bonding interactions between helix 45 (where the dimethyladenosines are located) and helix 44 near the decoding site (Demirci *et al.*, 2010). This loss of interaction perturbs the surrounding rRNA structure in both the A and P sites of the ribosome and may explain the pleiotropic effects seen in the *ksgA* mutation (Demirci *et al.*, 2010). Thus, one role of the conserved dimethylations, and therefore the methylation machinery, may be in establishing a fully active 30S ribosomal subunit.

The structures of KsgA alone and KsgA bound to SAM and 16S rRNA have been solved (O'Farrell *et al.*, 2004, Tu *et al.*, 2009, Xu *et al.*, 2008). KsgA is made up of two domains, a larger N-terminus composed of a mixture of alpha-helices and beta sheets, and a smaller C-terminal domain consisting of four or five alpha helices. The N-terminal domain is highly conserved amongst related methylases, while the C-terminus contains more divergent sequence (O'Farrell *et al.*, 2004, O'Farrell *et al.*, 2008). Biochemical and structural analysis together has unveiled a model of KsgA substrate and cofactor binding. The positively

charged cleft formed by the region spanning the N- and C-terminal domains of KsgA appears to be involved rRNA binding (O'Farrell *et al.*, 2004, Tu *et al.*, 2009, Xu *et al.*, 2008). Additionally, RNA binding is thought to be important for cofactor binding, as free KsgA is unable to bind the cofactor SAM (Poldermans *et al.*, 1979a). Recent crystal structure analysis confirmed this hypothesis by revealing stabilization of two conserved motifs important for SAM binding upon binding of the substrate rRNA (O'Farrell *et al.*, 2004, Tu *et al.*, 2009, Xu *et al.*, 2008). Thus, it appears that KsgA first interacts with the small subunit precursor rRNA and that this triggers a conformation change exposing the SAM binding pocket (O'Farrell *et al.*, 2004, Tu *et al.*, 2009).

KsgA binds to a highly conserved sequence of small subunit rRNA known to be important for translation (O'Farrell *et al.*, 2008, Xu *et al.*, 2008). By overlaying the crystal structures of KsgA and the 30S rRNA, Xu et al (2008) found that KsgA and IF-3 compete for overlapping binding sites. While the point of KsgA binding during ribosome biogenesis is unknown, methylation is known to occurs at a late stage of 30S subunit assembly (Thammana and Held, 1974). KsgA will not methylate naked 16S rRNA (Thammana and Held, 1974), even though it is capable of binding it (Van Gemen *et al.*, 1989). In addition, KsgA can only methylate 30S subunits in a translationally inactive form (Desai and Rife, 2006). In support of this, Connolly et al (2008) found that KsgA is bound only to free small subunits, but not fully assembled 70S ribosomes. Interestingly, presence of a methylation-dead *ksgA* mutant resulted in a more deleterious effect on cell growth and ribosome biogenesis than total lack of KsgA (Connolly *et al.*, 2008).

The methylation-dead protein was found bound in high concentration to precursor 30S rRNA, suggesting that methylation may be required for KsgA release from the maturing small subunit (Connolly *et al.*, 2008). Altogether, it appears KsgA binds to its substrate subsequent to incorporation of almost the full complement of ribosomal proteins, but prior to the establishment of a final active 30S subunit conformation (Desai and Rife, 2006). Thus, KsgA may prevent incompletely assembled 30S subunits from engaging in translation initiation prior to methylation (Xu *et al.*, 2008). In addition, methylation may be a trigger to release the KsgA protein once the 30S subunit has matured to a certain point.

Saccharomyces cerevisiae **Dim1p**

Lafontaine et al (1994) identified the yeast homolog of KsgA, DIM1, by screening for sensitivity to kasugamycin after transformation of the *ksgA* mutant with a yeast genomic library. One kasugamycin-sensitive colony was identified and further analysis found 16S adenine dimethylation to be restored (Lafontaine *et al.*, 1994). Dim1p and KsgA are closely related, sharing 26% amino acid sequence identity and 50% similarity (Lafontaine *et al.*, 1994). One notable difference is the lysine-rich N-terminal extension of Dimlp that is not present in KsgA (Lafontaine *et al.*, 1994). These differences at the sequence level likely result in somewhat divergent function. DIM1 complementation of the *ksgA* mutant was incomplete, resulting in a significant increase in m_6A monomethylation compared to wild-type (Lafontaine *et al.*, 1994, Pulicherla *et al.*, 2009). Additionally, while the *E. coli* Δ*ksgA* mutant is viable, in yeast the *dim1*

knockout is lethal (Lafontaine *et al.*, 1994).

Using a conditional GAL::*dim1* to slowly deplete yeast of Dim1p, Tollervey et al (1995) showed that Dim1p is essential for both 18S rRNA dimethylation as well as pre-rRNA processing. Northern blot analysis with probes designed to hybridize to specific regions of the pre-rRNA identified a novel 22S pre-rRNA species in the GAL::*diml* strain. The specific probe binding pattern revealed that the 22S fragment corresponds to region between sites A_0 and A_3, an results from inhibited processing at sites A_1 and A_2 (Lafontaine *et al.*, 1995). In contrast to the effect on 18S rRNA processing, biogenesis of the 5.8S and 25S rRNA fragments is unaffected by Dim1p depletion (Lafontaine *et al.*, 1995).

Although the dimethylation event occurs late during 40S rRNA maturation (Brand *et al.*, 1977), binding of Dim1p to the 90S pre-ribosomes early during ribosome biogenesis is essential (Fatica and Tollervey, 2002, Lafontaine *et al.*, 1995). Dim1p is thought to be a component of the U3 small nucleolar ribonucleoprotein (snoRNP), a protein-RNA complex that guides processing and modification of the 35S/45S pre-rRNA (Reviewed in Fatica and Tollervey, 2002, Schafer *et al.*, 2003). Binding of the U3 snoRNP within the 5' ETS of the pre-rRNA occurs through U3 snoRNA base pairing (Brown *et al.*, 2003, Brown and Shaw, 1998, Colley *et al.*, 2000). The current body of research, including structural analysis from *E. coli*, suggest that Dim1p binds to the pre-rRNA to ensure proper cleavage but remains enzymatically inactive until a subset of ribosomal proteins have assembled with the rRNA (O'Farrell *et al.*, 2004, Venema and Tollervey, 1999, Connolly *et al.*, 2008, Xu *et al.*, 2008). After

cleavage at sites A_0, A_1 and A_3 many of these factors are thought to dissociate from the pre-RNA (Fig. 1.7) (Fatica and Tollervey, 2002). However, Dim1p and a handful of other proteins remain associated until the 20S pre-rRNA is methylated and processed to 18S (Fatica and Tollervey, 2002).

While the presence of Dim1p is necessary for early nucleolar pre-rRNA processing events (Lafontaine *et al.*, 1995), dimethylation itself is not necessary for processing, ribosome biogenesis or ribosome function in yeast (Lafontaine *et al.*, 1998, Pulicherla *et al.*, 2009). In the *dim1-2* mutant, dimethylation but not pre-rRNA processing is affected, resulting in accumulation of unmethylated 18S rRNA (Lafontaine *et al.*, 1998). In addition, an E85A *dim1* point mutation complements the *dim1* lethality and rRNA processing phenotypes, even though it lacks methylase activity (Pulicherla *et al.*, 2009). While the *dim1-2* mutant, which contains six separate point mutations, reportedly grew slower at higher temperatures (Lafontaine *et al.*, 1998), the E85A mutant did not exhibit reduced growth at any temperature tested (Pulicherla *et al.*, 2009). This not only means that in yeast the dimethylase function of Dim1p can be separated from its role in pre-rRNA processing, but also suggests that methylation is not required for processing of the 20S pre-rRNA to the mature 18S fragment (Lafontaine *et al.*, 1998) or growth (Pulicherla *et al.*, 2009).

In summary, Dim1p catalyzes the dimethylation of A1779 and A1780 at the 3' end of the 18s rRNA in addition to playing an indirect role in pre-rRNA processing. As Dim1p is most likely a component of the U3 snoRNP complex, it has been suggested that Dim1p might directly interact with components required

for rRNA processing and be required for their association with the rest of the complex (Fatica and Tollervey, 2002, Schafer *et al.*, 2003). A second possibility, proposed by Lafontaine et al (1998), is that binding of Dim1p to the pre-ribosomal complex is sensed by a quality control mechanism and that processing at sites A1 and A2 is blocked until this binding has occurred.

Ribosome biogenesis and 18s modification: prokaryotes vs. eukaryotes

Eukaryotic ribosome assembly is more complex than prokaryotic, involving a large number of extra ribosomal factors and temporal and spatial organization (Zemp and Kutay, 2007, Fatica and Tollervey, 2002). In eukaryotes, early processing and assembly occurs in the nucleolus with the final steps taking place in the cytoplasm (Schafer *et al.*, 2003, Udem and Warner, 1973). There are also clear differences in the requirement of the 3' terminal loop dimethyladenosines and the enzymes which catalyze these base modifications. While absence of the KsgA causes minor growth defects in *E. coli*, eukaryotes cannot survive without this conserved methylases (Connolly *et al.*, 2008, Helser *et al.*, 1972, Lafontaine *et al.*, 1994, O'Connor *et al.*, 1997, Poldermans *et al.*, 1979b, Poldermans *et al.*, 1979c).

Furthermore, there is a striking difference in the effect of a methylation-dead methylase between prokaryotes and eukaryotes. In *E. coli,* the methylation-dead E66A *ksgA* was more deleterious to cell growth, rRNA processing and 70S ribosome formation than complete absence of the protein (Connolly *et al.*, 2008). However, two independent reports have shown that methylation-dead *dim1p* has

no to minimal effects on cell growth or ribosome biogenesis (Lafontaine *et al.*, 1998, Pulicherla *et al.*, 2009). Connolly et al (2008) suggested that these discrepancies might be due to differences in the binding affinity of KsgA and Dim1p to precursor SSUs or the ribosome biogenesis components and processes rather than mechanistic or functional differences between the two homologous proteins.

KsgA/Dim1 orthologs from yeast, archaea and the human mitochondria are able to complement for the dimethylation function of *E. coli* KsgA (Lafontaine *et al.*, 1994, O'Farrell *et al.*, 2006, Seidel-Rogol *et al.*, 2003), suggesting that substrate binding has been conserved through evolution. This is supported by a high level of conservation seen in putative binding domains of the KsgA/Dim1 family of enzymes (O'Farrell *et al.*, 2008) as well as within rRNA helix 45 (Van Knippenberg *et al.*, 1984). Presumably, the reason that *E. coli* KsgA and Archael Dim1 (from *M. jannaschii*) cannot complement for eukaryotic Dim1 in *S. cerevisiae* is Dim1's role in the ribosomal small-subunit processosome, an assembly that does not exist in bacteria (O'Farrell *et al.*, 2006, Schafer *et al.*, 2003). It is tempting to suggest that this could be mediated through Dim1p's lysine-rich amino-terminal extension (Lafontaine *et al.*, 1994) or C-terminal domain that is predicted to not make direct contact with rRNA, both poorly conserved in KsgA (O'Farrell *et al.*, 2008, Xu *et al.*, 2008).

Ribosome biogenesis in *Arabidopsis*

Many aspects of ribosomal biogenesis appear to be conserved from yeast

to higher eukaryotes. Ribosomal RNA synthesis and processing is similar, and close homologs of most trans-acting factors involved in yeast ribosome biogenesis have been identified in higher eukaryotes. However, to date research in higher eukaryotes is scarce compared to the wealth of knowledge of *S. cerevisiae* ribosome biogenesis (Zemp and Kutay, 2007). *Arabidopsis* diploid cell nuclei contain four rDNA loci located at the tips of chromosomes 2 and 4. The rDNA gene is transcribed as a 35S unit containing the 18S, 25S and 5.8S transcripts. While the exact protein composition of the *Arabidopsis* cytosolic ribosome is still under debate, the latest report identified 31 SSU and 46 LSU ribosomal proteins (Carroll *et al.*, 2008). The current model of *Arabidopsis* pre-rRNA processing is shown in Figure 1.5.

In plants, as in yeast, ribosome biogenesis occurs largely in the nucleolus, which contains rRNA, ribosomal proteins, and many non-ribosomal proteins. In 2002, the molecular components of the *S. cerevisiae* U3 sno-RNP required for 18S rRNA biogenesis were identified (Dragon *et al.*, 2002). Many of the U3 snoRNP components, including snoRNAs and associated proteins including fibrarillin, identified by Dragon et al have homologs in plants (Barneche *et al.*, 2001, Barneche *et al.*, 2000, Samaha *et al.*, 2010). In addition, a putative U3 snoRNP was purified from cauliflower and shown to specifically cleave 5‘ETS in vivo (Saez-Vasquez *et al.*, 2004). Research to date suggests that in plants, as in yeast, the U3 snoRNP is important in small ribosomal subunit biogenesis.

In addition to the conservation of processing sites and regulators, many of the post-transcriptional modifications are also conserved between plants and

other eukaryotes. Barnache et al (2001) mapped over 86 ribosome methylations, many of which were present in highly conserved regions of rRNA. Interestingly, while three genes encoding KsgA/Dim1-like dimethylase proteins have been identified in the *Arabidopsis* genome (nucleolar protein DIM1A, mitochondrial protein DIM1B, and chloroplastic protein PALEFACE1 (PFC1), the presence of the two highly conserved dimethyladenosines has only been shown in chloroplast and mitochondrial SSU rRNA (Richter *et al.*, 2010, Tokuhisa *et al.*, 1998). Analysis of the DIM1A nucleolar protein as well as the 18S 3'-terminal loop base methylations in *Arabidopsis* would not only provide further insight into the importance of ribosome biogenesis in plants, but also would be the first examination of this highly conserved rRNA modification in cytoplasmic ribosomes of a multicellular organism.

Ribosome biogenesis mutants in *Arabidopsis*

In the past, ribosomes have been perceived as rudimentary components of a cell - simply as non-specific protein synthesis machinery. Recently the developmental role of ribosomal function and regulation has come to light. Interest has been highlighted by specific developmental defects that arise from mutations in ribosomal protein and biogenesis genes, including embryo-lethality; reduced plant size; leaf shape, vascular patterning and cell division defects; reduced fertility; and trichome development defects (Reviewed in Byrne, 2009). While many of these phenotypes can be attributed to lower rates of translation due to reduced production of functional ribosomes, others have been linked to

miss-regulation of specific genes. Much of the insight into the influence of ribosome biogenesis on growth and development in *Arabidopsis* has been through ribosomal protein mutants (Byrne, 2009), however a few studies, which are highlighted below, have focused on the role of non-ribosomal biogenesis factors.

In plants, as in other eukaryotes, ribosome biogenesis occurs largely in the nucleolus, the non-membrane bound structure in the nucleus composed of rRNA, ribosomal proteins, and many non-ribosomal proteins. Five genes encoding non-ribosomal proteins, *AtNUC-L1/PARALLEL1 (NUC-L1/PAR1), OLIGOCELLULA2 (OLI2), SLOW WALKER1 (SWA1), TOMOZ (TOZ)* and *AtEBP1* have been implicated in *Arabidopsis* ribosome biogenesis (Kojima *et al.*, 2007, Petricka and Nelson, 2007, Pontvianne *et al.*, 2007, Fujikura *et al.*, 2009, Griffith *et al.*, 2007, Horváth *et al.*, 2006). *AtNUCL-L1/PAR1* encodes the *Arabidopsis* homolog of nucleolin, a multifunctional protein implicated in rDNA transcription, pre-rRNA processing, pre-ribosome particle assembly, ribosomal subunit and protein nucleo-cytoplasmic transport, DNA unwinding and replication, gene expression regulation, and chromatin remodeling (Mongelard and Bouvet, 2007, Shaw and Jordan, 1995). Unlike other organisms, which have a single copy of nucleolin, *Arabidopsis* has two, *AtNUC-L1/PAR1* and *AtNUC-L2* (Saez-vazquez 2004), the latter of which is not expressed under normal conditions (Kojima et al 2007, Pontvianne et al 2007). Intriguingly, *AtNUCL-L2* is expressed in the *nuc-l1*/*par1* mutant background and is believed to compensate for the lost function of NUC-L1, further supported by the inability to isolate a *nuc-l1*/*par1 nuc-l2* double mutant

(Pontvianne *et al.*, 2007). Loss-of-function *nuc-l1*/*par1* mutants have reduced root growth, reduced overall plant size and growth, pointed leaves, and leaf vascular patterning defects (Kojima *et al.*, 2007, Petricka and Nelson, 2007, Pontvianne *et al.*, 2007). Additionally, the *nuc-l1*/*par1* mutant exhibits defects specific to ribosome biogenesis, including disorganization of nucleolar structure, rDNA chromatin organization defects (Pontvianne *et al.*, 2007), and pre-rRNA processing defects (Kojima *et al.*, 2007, Petricka and Nelson, 2007, Pontvianne *et al.*, 2007)

The *OLI2* gene encodes a putative RNA methyltransferase homologous to the Nop2 protein in *S. cerevisiae* (Fujikura *et al.*, 2009). Yeast Nop2p is a nucleolar localized protein required for 27S pre-rRNA processing into 5.8S and 25S rRNA (de Beus *et al.*, 1994, Hong *et al.*, 1997). Depletion of Nop2p results in reduced processing of 27S pre-rRNA to 25S rRNA coordinately with the reduction of a 2'-O-ribosome methylation within a conserved loop of 27S pre-rRNA, suggesting that processing and methylation events are tightly coupled (Hong *et al.*, 1997). The *Arabidopsis* genome contains three Nop2 related genes, *OLI2* and two *OLI2*-like genes, which may explain why Nop2 is essential in yeast but OLI2 is dispensable in plants (de Beus *et al.*, 1994, Fujikura *et al.*, 2009). While the role of OLI2 in pre-RNA processing of *Arabidopsis* has yet to be investigated, loss-of-function mutations result in pointed-leaves and decreased leaf pallisade mesophyll cells (Fujikura *et al.*, 2009). Together, this suggests that efficient 60S ribosomal subunit synthesis is essential for generating wild-type cell quantity in leaves.

SWA1 and *TOZ* encode WD-40 repeat proteins homologous to U3 snoRNP components identified in yeast (Dragon *et al.*, 2002, Griffith *et al.*, 2007, Shi *et al.*, 2005). Accordingly, SWA1, which was originally identified for its role in female gametophyte progression, is important for pre-rRNA processing at site P (equivalent to yeast site A0 (Fig. 7)) (Shi *et al.*, 2005). Loss of function mutations in TOZ resulted in aberrant planes of division during embryogenesis, but unexpectedly did not have a noticeable effect on rRNA processing (Griffith *et al.*, 2007). A third putative homolog of the yeast pre-ribosomal complex protein, AtEBP1, regulates cell division and organ size, potentially by affecting auxin induction of cell cycle regulators (Horváth *et al.*, 2006). All three proteins localize to the nucleolus in *Arabidopsis* cells (Griffith *et al.*, 2007, Horváth *et al.*, 2006, Shi *et al.*, 2005, Pendle *et al.*, 2005), supporting their conservation as members of the U3 snoRNP. Further analysis of these five proteins is necessary to cement their precise roles in ribosome biogenesis. However, research to date not only implicates them in ribosome biogenesis, but also demonstrates the necessity of efficient ribosome biogenesis in *Arabidopsis* embryogenesis and post-embryonic development.

As revealed recently by molecular and genetic studies, the processes of ribosome biogenesis and translation may participate in specific control of gene expression. One possible mechanism for this involves sensing the rate of ribosome production as a cell cycle checkpoint. Evidence for such a mechanism comes from analysis of induced depletion of ribosomal protein S6 in mice liver which revealed that the rate of ribosome production is sensed and regulates cell

cycle progression (Volarevic *et al.*, 2000). In this study, liver cells were still able to grow and protein synthesis was apparently not affected, however cell division was inhibited and accompanied by a specific reduction in cyclin E mRNA (Volarevic *et al.*, 2000). Another possible mechanism is translational control, possibly mediated through upstream open reading frame (uORF)-mediated regulation. Recently, a mutation in ribosomal protein L24 (RPL24), denoted as *shortvalve 1* (*stv1*) for its apical-basal gynoecium patterning defect, was attributed to defects in uORF-mediated translational regulation of auxin response factor genes *MONOPTEROS* (*MP*) and *ETTIN* (*ETT*) (Nishimura *et al.*, 2005). RPL24, which was previously shown to be important for translation reinitation in *Arabidopsis* (Park *et al.*, 2001), is needed for expression of *ETT* and *MP* as both genes have uORF and efficient translation reinitiation is necessary for read through to the gene ORF. This suggests an interesting possible mechanism of ribosomal protein translational regulation, and may explain the specific phenotypes seen in different ribosomal protein and ribosomal assembly factor mutants.

Taken together, ribosome production and/or function might play a key role in active cell proliferation through the regulation of specific gene expression. Genetic studies have shown that ribosomal proteins and ribosome biogenesis proteins are involved in specific aspects of development. Specific phenotypes resulting from certain ribosomal protein and ribosomal biogenesis protein mutations, including alteration of leaf shape, leaf venation patterns, and responses to auxin and sugars, cannot be explained simply by growth defects

(Ito *et al.*, 2000, Kojima *et al.*, 2007, van Lijsebettens *et al.*, 1994, Petricka and Nelson, 2007, Pinon *et al.*, 2008, Yao *et al.*, 2008). To date, specific connections between individual ribosomal proteins or biogenesis factors and certain aspects of development have been identified. A thorough side-by-side comparison of identified mutants is needed to determine if these specific connections are limited to certain ribosomal factors, or if they pertain to ribosome factors in general. In conclusion, further research is needed to fully understand the connection between ribosome biogenesis and development of multicellular organisms.

Foreshadowing the Thesis

The first chapter of this thesis provides an introduction to development and patterning of the root epidermis, ribosome biogenesis and the importance of a highly conserved ribosomal RNA base modification.

The main focus of my thesis is found in Chapter Two, where I highlight my work on the identification of the *dim1A* patterning mutant and the characterization *DIM1A* and its role in root epidermal patterning and development. In addition, I show that *DIM1A* also plays a role in *Arabidopsis* leaf and trichome development. A handful of ribosomal protein and biogenesis factors have been studied in *Arabidopsis*, however as far as we know this is the first report of the role of ribosome biogenesis in root epidermal patterning. In addition, this is the first report of the importance of the conserved 3'-terminal loop 18S rRNA adenosine dimethylation in eukaryotic cytoplasmic ribosomes.

In Chapter Three, I present my work on using a reverse genetic/genomics

approach to identify additional patterning genes as well as downstream morphology genes involved in root epidermal patterning and hair morphogenesis. Finally, my conclusions and future directions are presented in Chapter Four.

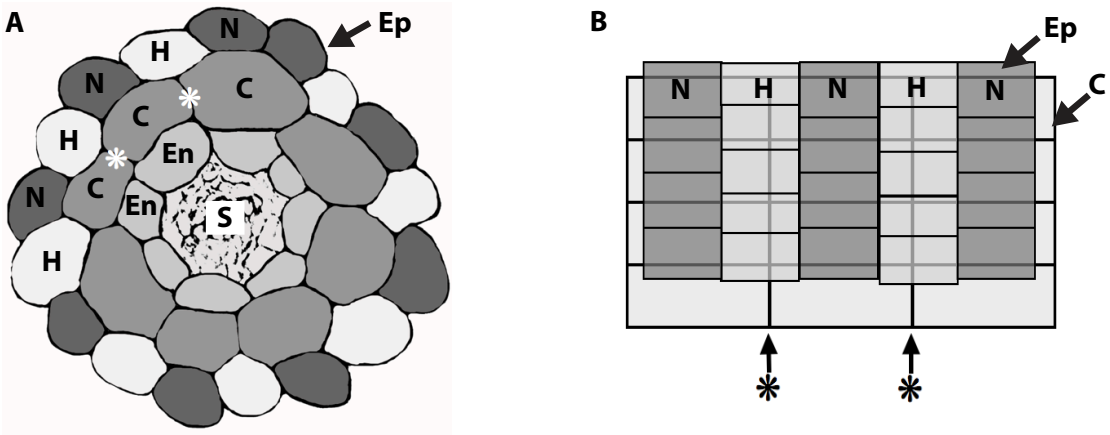

Figure 1.1. Position-dependent cell fate specification in the *Arabidopsis* root epidermis

(A) Diagram of a transverse section of the meristematic region of an *Arabidopsis* root. The primary root is organized in concentric rings of cells including (from outward in) epidermis [Ep], cortex [C], endodermis [En] and stele [S]. Cells that will develop a hair [H] are located over an anticlinal cortical cell wall (ACCW) (denoted as the H position, ⁕), while cells that will develop into non-hair cells [N] are located over a single cortical cell (denoted as the N position). (B) Diagram of a surface view of a section of the root epidermis and underlying cortical cell. Note that the ACCW is visible through the epidermal layer, allowing for determination of cell position.

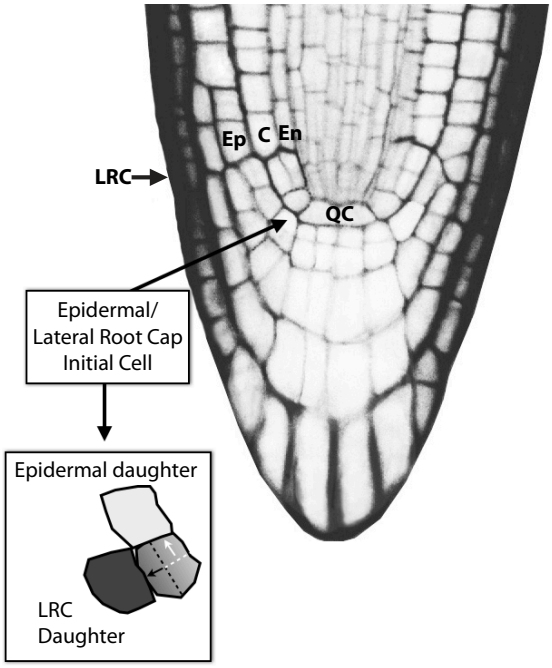

Figure 1.2. Cell types and organization of the *Arabidopsis* root meristem

Longitudinal section of the tip of an *Arabidopsis* root. Notice the organization of cell layers, including the epidermis [Ep], cortex [C], endodermis [En], lateral root cap [LRC]. Epidermal cells are derived from the epidermal/LRC initial cells (inset). The quiescent center [QC] maintains the stem cells required to generate each cell layer.

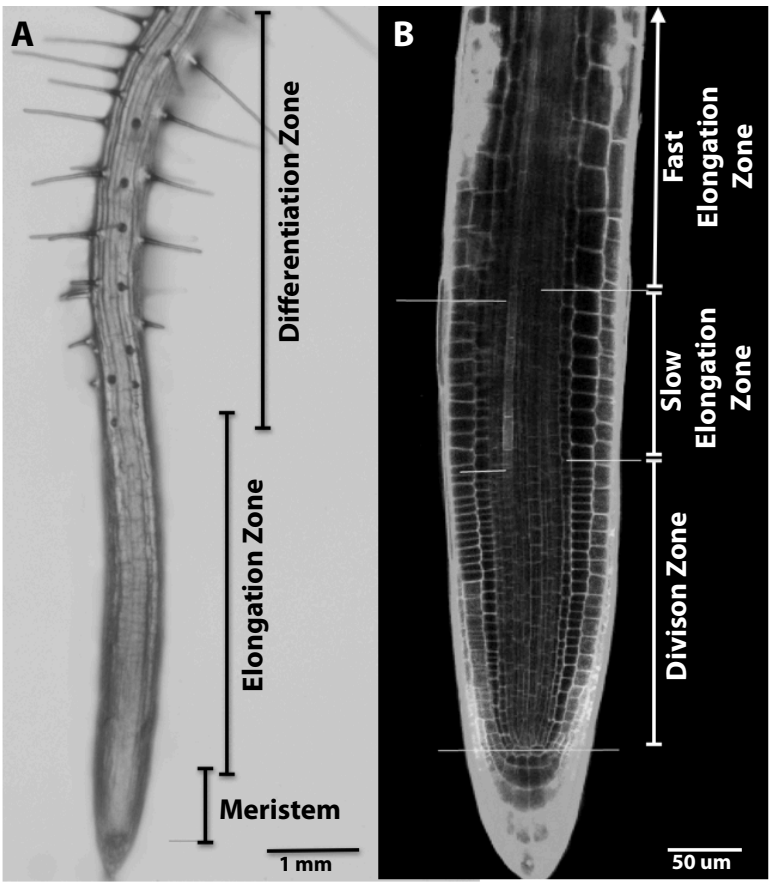

Figure 1.3. Growth zones of the *Arabidopsis* primary root

Developmental zones of the *Arabidopsis* root and root meristem. (A) Dissection-scope image of a root tip showing the progressive development of root hairs. (B) Confocal cross-section of the root meristem depicting specific regions of growth within the root meristem.

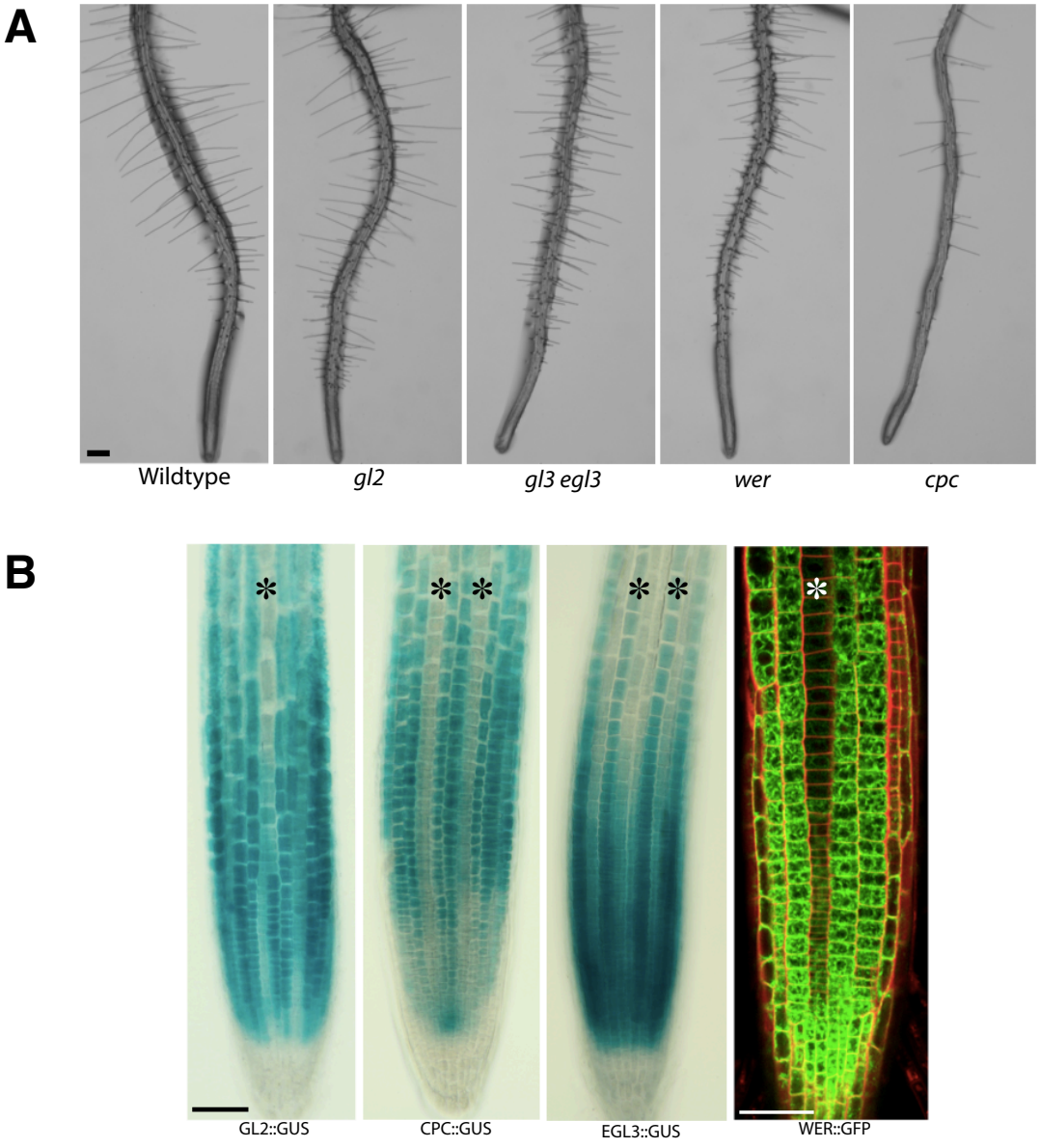

Figure 1.4. Root hair phenotypes and position-dependent expression of epidermal patterning genes

(A) Root hair phenotypes of four-day-old seedlings. Compared to wild-type, the *gl2*, *gl3 egl3* and *wer* mutants have increased root-hair cell frequency, while the *cpc* mutant has reduced hair cell frequency. (B) *GL2*, *CPC* and *WER* expression, as visualized by promoter-reporter construct, are localized mainly to N position cells in the meristem while *EGL3* promoter activity is localized mainly in developing H position cells. H position cell files are indicated by (✻). Scale bars represent 1mm (A) and 50 μm (B).

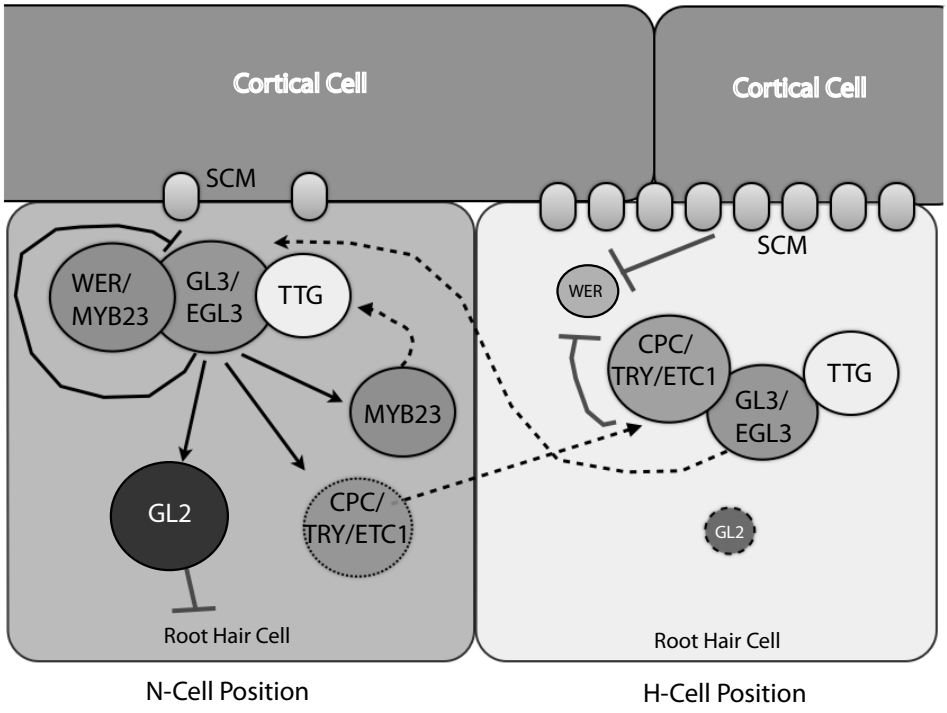

Figure 1.5. Model of position-dependent root epidermal cell-type patterning

The SCM receptor-like-kinase is proposed to influence the downstream patterning network by repressing *WER* expression in H position cells. Preferential accumulation of the activation complex (TTG1-GL3/EGL3-WER) in N position cells leads to *GL2* expression (and subsequent inhibition of hair morphogenesis gene expression) in addition to expression of lateral inhibitor genes *CPC, TRY, and ETC1*. The CPC/TRY/ETC1 proteins preferentially accumulate in H position cells, where they compete with WER for binding to TTG1-GL3/EGL3, therefore preventing *GL2* expression in H position cells. Note: solid lines represent gene regulation, dashed lines indicate protein movement.

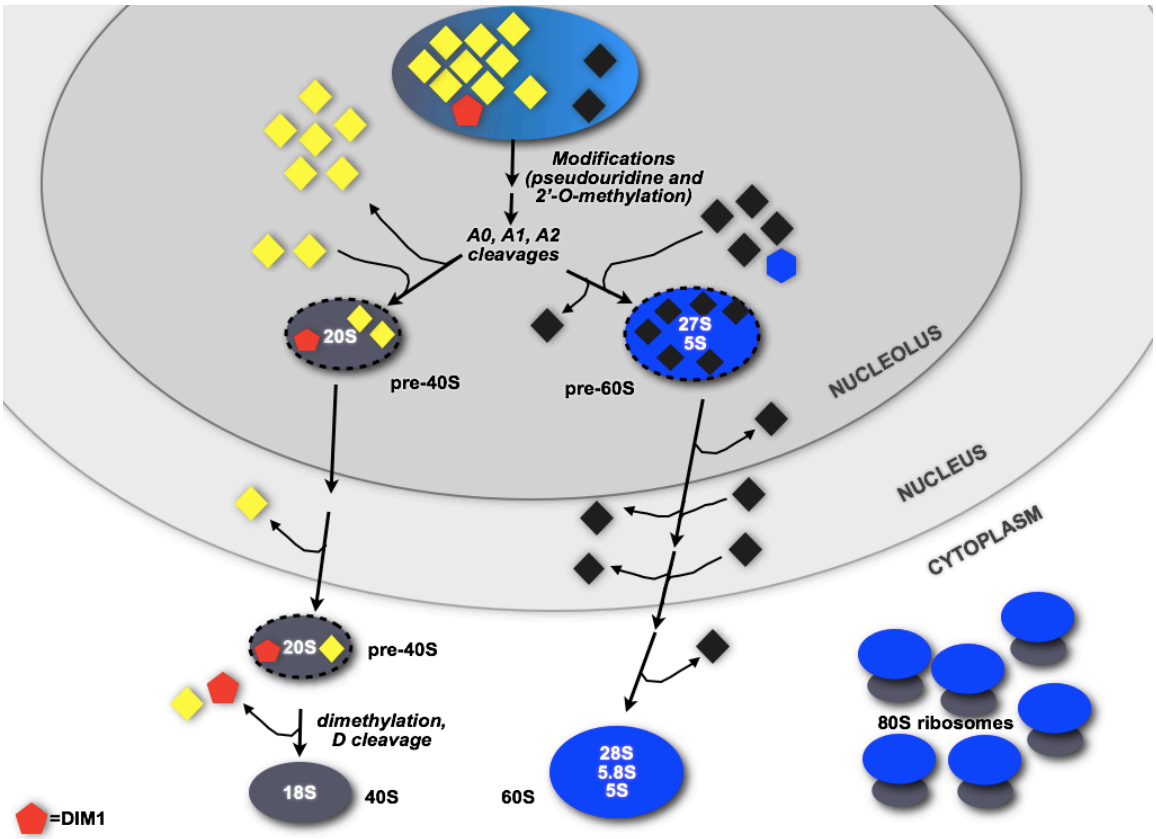

Figure 1.6. Model of eukaryotic ribosome biogenesis

The current model of eukaryotic ribosome biogenesis based on research in *Saccharomyces cerevisiae.* Dim1p (red pentagon) binds to the 90S pre-ribosome in the nucleolus early during ribosome biogenesis. Dim1p remains associated with the immature small subunit until the late cytoplasmic stage, dissociating prior to final processing event that generates the mature 40S ribosomal subunit (adapted from Fatica and Tollervey, 2002).

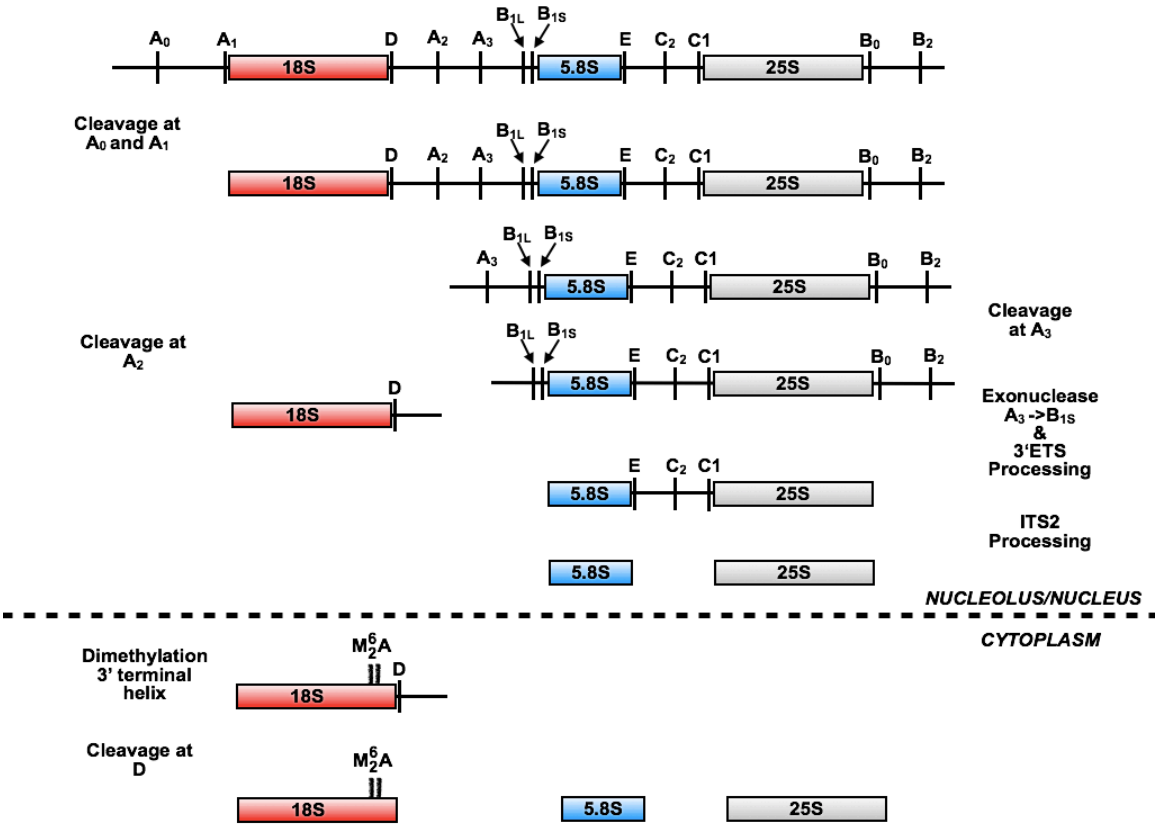

Figure 1.7. Structure and processing of eukaryotic pre-rRNA

Current model of the structure and processing of the 35S pre-rRNA from *Saccharomyces cerevisiae*. What is known about 35S pre-rRNA processing in *Arabidopsis* has shown to be similar to the well-studied yeast 35S pre-rRNA processing pathway. Adapted from (Lafontaine *et al* 1998)

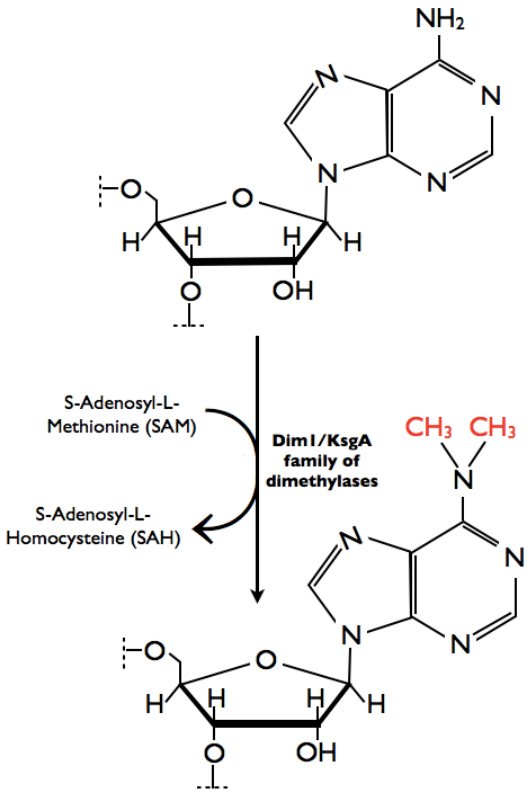

Figure 1.8. The adenosine dimethylation reaction.

The dimethylation reaction catalyzed by the KsgA/Dim1 family of dimethylases. Note, each dimethylation reaction consumes two molecules of cofactor SAM.

Literature Cited

Barneche, F, Gaspin, C, Guyot, R & Echeverria, M (2001) Identification of 66 box C/D snoRNAs in *Arabidopsis thaliana*: extensive gene duplications generated multiple isoforms predicting new ribosomal RNA 2'-O-methylation sites. *J Mol Biol,* 311.

Barneche, F, Steinmetz, F & Echeverria, M (2000) Fibrillarin Genes Encode Both a Conserved Nucleolar Protein and a Novel Small Nucleolar RNA Involved in Ribosomal RNA Methylation in *Arabidopsis thaliana*. *Journal of Biological Chemistry,* 275**,** 27212-27220.

Berger, F, Haseloff, J, Schiefelbein, J & Dolan, L (1998a) Positional information in root epidermis is defined during embryogenesis and acts in domains with strict boundaries. *Curr Biol,* 8**,** 421-30.

Berger, F, Hung, CY, Dolan, L & Schiefelbein, J (1998b) Control of cell division in the root epidermis of *Arabidopsis thaliana*. *Dev. Biol.,* 194**,** 235-45.

Bernhardt, C, Lee, MM, Gonzalez, A, Zhang, F, Lloyd, A & Schiefelbein, J (2003) The bHLH genes *GLABRA3 (GL3)* and *ENHANCER OF GLABRA3 (EGL3)* specify epidermal cell fate in the *Arabidopsis* root. *Development,* 130**,** 6431-6439.

Bernhardt, C, Zhao, M, Gonzalez, A, Lloyd, A & Schiefelbein, J (2005) The bHLH genes *GL3* and *EGL3* participate in an intercellular regulatory circuit that controls cell patterning in the *Arabidopsis* root epidermis. *Development,* 132**,** 291-298.

Brand, RC, Klootwijk, J, Vansteenbergen, TJM, Dekok, AJ & Planta, RJ (1977) Secondary methylation of yeast ribosomal precursor RNA. *European Journal of Biochemistry,* 75**,** 311-318.

Brown, JWS, Echeverria, M & Qu, L-H (2003) Plant snoRNAs: functional evolution and new modes of gene expression. *Trends Plant Sci.,* 8**,** 42-49.

Brown, JWS & Shaw, PJ (1998) Small Nucleolar RNAs and Pre-rRNA Processing in Plants. *Plant Cell,* 10**,** 649-657.

Byrne, M (2009) A role for the ribosome in development. *Trends Plant Sci.,* 14**,** 512-519.

Caro, E, Castellano, MM & Gutierrez, C (2007) A chromatin link that couples cell division to root epidermis patterning in *Arabidopsis*. *Nature,* 447.

Carroll, A, Heazlewood, J, Ito, J & Millar, AH (2008) Analysis of the *Arabidopsis* cytosolic ribosome proteome provides detailed insights into its components and their post-translational modification. *Molecular & Cellular Proteomics,* 7**,** 347-369.

Chevalier, D, Batoux, M, Fulton, L, Pfister, K, Yadav, RK, Schellenberg, M & Schneitz, K (2005) STRUBBELIG defines a receptor kinase-mediated signaling pathway regulating organ development in *Arabidopsis*. *Procl. Natl. Acad. Sci.,* 102**,** 9074-9079.

Clowes, F (2000) Pattern in root meristem development in angiosperms. *New Phytol.*

Colley, A, Beggs, JD, Tollervey, D & Lafontaine, DL (2000) Dhr1p, a putative DEAH-box RNA helicase, is associated with the box C+D snoRNP U3. *Molecular and Cellular Biology,* 20**,** 7238-46.

Connolly, K, Rife, JP & Culver, G (2008) Mechanistic insight into the ribosome biogenesis functions of the ancient protein KsgA. *Mol. Microbiol.,* 70**,** 1062-75.

Cormack, R (1935) Investigations on the development of root hairs. *New Phytol.,* 34**,** 30-54.

Cormack, R (1937) The development of root hairs by *Elodea canadensis*. *New Phytol.,* 36**,** 19-25.

Cormack, R (1947) A comparative study of developing epidermal cells in white mustard and tomato roots. *Am. J. Bot.,* 34**,** 310-314.

Costa, S & Dolan, L (2003) Epidermal patterning genes are active during embryogenesis in *Arabidopsis*. *Development,* 130**,** 2893-901.

Costa, S & Shaw, PJ (2006) Chromatin organization and cell fate switch respond to positional information in *Arabidopsis*. *Nature,* 439**,** 493-496.

Cotney, J & Shadel, GS (2006) Evidence for an early gene duplication event in the evolution of the mitochondrial transcription factor B family and maintenance of rRNA methyltransferase activity in human mtTFB1 and mtTFB2. *J Mol Evol,* 63**,** 707-17.

Cutter, E 1978. The epidermis. *Plant anatomy.* London, UK: Clowes & Sons.

De Beus, E, Brockenbrough, JS, Hong, B & Aris, J (1994) Yeast NOP2 encodes an essential nucleolar protein with homology to a human proliferation marker. *The Journal of Cell Biology,* 127**,** 1799-1813.

Decatur, W & Fournier, M (2002) rRNA modifications and ribosome function. *Trends in Biochemical Sciences,* 27**,** 344-351.

Demirci, H, Murphy, F, Belardinelli, R, Kelley, AC, Ramakrishnan, V, Gregory, ST, . . . Jogl, G (2010) Modification of 16S ribosomal RNA by the KsgA methyltransferase restructures the 30S subunit to optimize ribosome function. *RNA,* 16**,** 2319-2324.

Desai, PM & Rife, JP (2006) The adenosine dimethyltransferase KsgA recognizes a specific conformational state of the 30S ribosomal subunit. *Arch Biochem Biophys,* 449**,** 57-63.

Di Cristina, M, Sessa, G, Dolan, L, Linstead, P, Baima, S, Ruberti, I & Morelli, G (1996) The *Arabidopsis* Athb-10 (GLABRA2) is an HD-Zip protein required for regulation of root hair development. *Plant J.,* 10**,** 393-402.

Dolan, L & Costa, S (2001) Evolution and genetics of root hair stripes in the root epidermis. *J. Exp. Bot.,* 52**,** 413-417.

Dolan, L, Duckett, CM, Grierson, C, Linstead, P, Schneider, K, Lawson, E, . . . Roberts, K (1994) Clonal relationships and cell patterning in the root epidermis of *Arabidopsis*. *Development,* 120**,** 2465-2474.

Dolan, L, Janmaat, K, Willemsen, V, Linstead, P, Poethig, S, Roberts, K & Scheres, B (1993) Cellular organisation of the *Arabidopsis thaliana* root. *Development,* 119**,** 71-84.

Dragon, F, Gallagher, JEG, Compagnone-Post, PA, Mitchell, BM, Porwancher, KA, Wehner, KA, . . . Osheim, Y (2002) A large nucleolar U3 ribonucleoprotein required for 18S ribosomal RNA biogenesis. *Nature,* 417**,** 967-970.

Fatica, A & Tollervey, D (2002) Making ribosomes. *Current Opinion in Cell Biology,* 14**,** 313-318.

Fauman, EB, Blumenthal, RM & Cheng, X 1998. Structure and evolution of AdoMet-dependent methyltransferases. *In:* CHENG, S & BLUMENTHAL, RM (eds.) *S-Adenosylmethionine-Dependent Methyltransferases: Structres and Functions.* Singapore: World Scientific Publishing Co. Pte. Ltd.

Freshour, G, Clay, RP, Fuller, MS, Albersheim, P, Darvill, AG & Hahn, MG (1996) Developmental and Tissue-Specific Structural Alterations of the Cell-Wall Polysaccharides of *Arabidopsis thaliana* Roots. *Plant Physiol,* 110**,** 1413-1429.

Fujikura, U, Horiguchi, G, Ponce, MR, Micol, JL & Tsukaya, H (2009) Coordination of cell proliferation and cell expansion mediated by

ribosome-related processes in the leaves of *Arabidopsis thaliana*. *Plant J,* 59**,** 499-508.

Fulton, L, Batoux, M, Vaddepalli, P, Yadav, RK, Busch, W, Andersen, SU, . . . Schneitz, K (2009) DETORQUEO, QUIRKY, and ZERZAUST represent novel components involved in organ development mediated by the receptor-like kinase STRUBBELIG in *Arabidopsis thaliana*. *PLoS Genet.,* 5.

Galway, ME, Massucci, JD, Lloyd, A, Walbot, V, Davis, RW & Schiefelbein, J (1994) The *TTG* Gene is Required to Specify Epidermal Cell Fate and Cell Patterning in the *Arabidopsis* Root. *Dev. Biol.,* 166**,** 740-754.

Ganot, P, Bortolin, M-L & Kiss, T (1997) Site-specific pseudouridine formation in preribosomal RNA is guided by small nucleolar RNAs. *Cell,* 89**,** 799-809.

Grierson, C & Schiefelbein, J (2002) Root Hairs. *The Arabidopsis Book*.

Griffith, ME, Mayer, U, Capron, A, Ngo, QA, Surendrarao, A, Mcclinton, R, . . . Sundaresan, V (2007) The *TORMOZ* Gene Encodes a Nucleolar Protein Required for Regulated Division Planes and Embryo Development in *Arabidopsis*. *Plant Cell,* 19**,** 2246-2263.

Guimil, S & Dunand, C (2006) Patterning of *Arabidopsis* epidermal cells: epigenetic factors regulate the complex epidermal cell fate pathway. *Trends Plant Sci.,* 11**,** 601-609.

Helser, TL, Davies, JE & Dahlberg, JE (1971) Change in methylation of 16S ribosomal RNA associated with mutation to kasugamycin resistance in Escherichia coli. *Nature New Biol,* 233**,** 12-14.

Helser, TL, Davies, JE & Dahlberg, JE (1972) Mechanism of kasugamycin resistance in *Escherichia coli*. *Nature New Biol,* 235**,** 6-9.

Hofer, R-M 1991. Root hairs. *In:* WAISEL Y., EA, KAFKAFI U. (ed.) *Plant Roots: The Hidden Half.* 1 ed.

Hong, B, Brockenbrough, J, Wu, P & Aris, JP (1997) Nop2p is required for pre-rRNA processing and 60S ribosome subunit synthesis in yeast. *Mol Cell Biol,* 17**,** 378-388.

Horváth, B, Magyar, Z, Zhang, Y, Hamburger, AW, Bako, L, Visser, RGF, . . . Bogre, L (2006) *EBP1* regulates organ size through cell growth and proliferation in plants. *EMBO J.,* 25**,** 4909-4920.

Ito, T, Kim, GT & Shinozaki, K (2000) Disruption of an *Arabidopsis* cytoplasmic ribosomal protein S13-homologous gene by transposon-mediated

mutagenesis causes aberrant growth and development. *Plant J,* 22**,** 257-64.

Kang, YH, Kirik, V, Hulskamp, M, Nam, K, Hagely, K, Lee, MM & Schiefelbein, J (2009) The *MYB23* gene provides a positive feedback loop for cell fate specification in the *Arabidopsis* root epidermis. *Plant Cell,* 21**,** 1080-1094.

Kirik, V, Simon, M, Huelskamp, M & Schiefelbein, J (2004) The *ENHANCER OF TRY AND CPC1* gene acts redundantly with *TRIPTYCHON* and *CAPRICE* in trichome and root hair cell patterning in *Arabidopsis*. *Dev. Biol.,* 268**,** 506-513.

Kiss-Laszlo, Z, Henry, Y, Bachellerie, J-P, Caizergues-Ferrer, ML & Kiss, T (1996) Site-specific ribose methylation of preribosomal RNA: a novel function for small nucleolar RNAs. *Cell,* 85**,** 1077-1088.

Klootwijk, J, Klein, I & Grivell, LA (1975) Minimal post-transcriptional modification of yeast mitochondrial ribosomal RNA. *J Mol Biol,* 97**,** 337-50.

Kojima, H, Suzuki, T, Kato, T & Enomoto, K (2007) Sugar-inducible expression of the nucleolin-1 gene of *Arabidopsis thaliana* and its role in ribosome synthesis, growth and development. *Plant J.,* 49**,** 1053-1063.

Koornneef, M (1981) The complex syndrome of *ttg* mutants. *Arabid. Inf. Serv.*, 45-51.

Koornneef, M (1990) Mutations affecting the testa color in *Arabidopsis*. *Arabid. Inf. Serv.,* 27**,** 94-97.

Kos, M & Tollervey, D (2010) Yeast pre-rRNA processing and modification occur cotranscriptionally. *Molecular Cell,* 37**,** 809-20.

Koshino-Kimura, Y, Wada, T, Tachibana, T, Tsugeki, R, Ishiguro, S & Okada, K (2005) Regulation of *CAPRICE* Transcription by MYB Proteins for Root Epidermis Differentiation in *Arabidopsis*. *Plant Cell Physiol.,* 46**,** 817-826.

Kurata, T, Ishida, T, Kawabata-Awai, C, Noguchi, M, Hattori, S, Sano, R, . . . Wada, T (2005) Cell-to-cell movement of the CAPRICE protein in *Arabidopsis* root epidermal cell differentiation. *Development,* 132**,** 5387-5398.

Kwak, S-H & Schiefelbein, J (2007) The role of the SCRAMBLED receptor-like kinase in patterning the *Arabidopsis* root epidermis. *Dev. Biol.,* 302**,** 118-131.

Kwak, S-H & Schiefelbein, J (2008) A feedback mechanism controlling SCRAMBLED receptor accumulation and cell-type pattern in *Arabidopsis*. *Curr Biol,* 18**,** 1949-1954.

Kwak, S-H, Shen, R & Schiefelbein, J (2005) Positional signaling mediated by a receptor-like kinase in *Arabidopsis*. *Science,* 307**,** 1111-1113.

Lafontaine, D, Delcour, J, Glasser, AL, Desgres, J & Vandenhaute, J (1994) The *DIM1* Gene Responsible for the Conserved m62Am62A Dimethylation in the 3'-Terminal Loop of 18S rRNA is Essential in Yeast. *J Mol Biol,* 241**,** 492-497.

Lafontaine, D, Preiss, T & Tollervey, D (1998) Yeast 18S rRNA dimethylase Dim1p: a quality control mechanism in ribosome synthesis? *Mol Cell Biol,* 18**,** 2360-70.

Lafontaine, D, Vandenhaute, J & Tollervey, D (1995) The 18S rRNA dimethylase Dim1p is required for pre-ribosomal RNA processing in yeast. *Genes Dev.,* 9**,** 2470-2481.

Larkin, JC, Brown, ML & Schiefelbein, J (2003) How do cells know what they want to be when they grow up? *Annu. Rev. Plant Biol.,* 54**,** 403-430.

Lee, MM & Schiefelbein, J (1999) WEREWOLF, a MYB-Related Protein in *Arabidopsis*, Is a Position-Dependent Regulator of Epidermal Cell Patterning. *Cell,* 99**,** 473-483.

Lee, MM & Schiefelbein, J (2002) Cell Pattern in the *Arabidopsis* Root Epidermis Determined by Lateral Inhibition with Feedback. *Plant Cell,* 14**,** 611-618.

Lin, Y & Schiefelbein, J (2001) Embryonic control of epidermal cell patterning in the root and hypocotyl of *Arabidopsis*. *Development,* 128**,** 3697-3705.

Maden, B (1990) The numerous modified nucleotides in eukaryotic ribosomal RNA. *Progress in nucleic acid research and molecular biology,* 39**,** 241-303.

Martin, J & Mcmillan, F (2002) SAM (dependent) I AM: the S-adenosylmethionine-dependent methyltransferase fold. *Current Opinion in Structural Biology,* 12**,** 783-793.

Massucci, JD, Rerie, WG, Foreman, DR, Zhang, M, Galway, ME, David Marks, M & Schiefelbein, J (1996) The homeobox gene *GLABRA2* is required for position-dependent cell differentiation in the root epidermis of *Arabidopsis thaliana*. *Development,* 122**,** 1253-1260.

Mccloskey, JA & Rozenski, J (2005) The Small Subunit rRNA Modification Database. *Nuc. Acids Res.,* 33**,** D135-8.

Menand, B, Yi, K, Jouannic, S, Hoffmann, L, Ryan, E, Linstead, P, . . . Dolan, L (2007) An ancient mechanism controls the development of cells with a rooting function in land plants. *Science,* 316**,** 1477-80.

Mongelard, F & Bouvet, P (2007) Nucleolin: a multiFACeTed protein. *Trends in cell biology,* 17**,** 80-86.

Nishimura, T, Wada, T, Yamamoto, KT & Okada, K (2005) The *Arabidopsis* STV1 protein, responsible for translation reinitiation, is required for auxin-mediated gynoecium patterning. *Plant Cell,* 17**,** 2940-53.

Noon, KR, Bruenger, E & Mccloskey, JA (1998) Posttranscriptional modifications in 16S and 23S rRNAs of the archaeal hyperthermophile Sulfolobus solfataricus. *J Bacteriol,* 180**,** 2883-8.

O'connor, M, Thomas, CL, Zimmermann, RA & Dahlberg, AE (1997) Decoding fidelity at the ribosomal A and P sites: influence of mutations in three different regions of the decoding domain in 16S rRNA. *Nuc. Acids Res.,* 25**,** 1185-1193.

O'farrell, H, Pulicherla, N, Desai, P & Rife, JP (2006) Recognition of a complex substrate by the KsgA/Dim1 family of enzymes has been conserved throughout evolution. *RNA,* 12**,** 725-732.

O'farrell, H, Scarsdale, J & Rife, JP (2004) Crystal Structure of KsgA, a Universally Conserved rRNA Adenine Dimethyltransferase in Escherichia coli. *J Mol Biol,* 339**,** 337-353.

O'farrell, H, Xu, Z, Culver, G & Rife, JP (2008) Sequence and structural evolution of the KsgA/Dim1 methyltransferase family. *BMC Research Notes,* 1**,** 108.

Ofengand, J (2002) Ribosomal RNA pseudouridines and pseudouridine synthases. *FEBS letters,* 514**,** 17-25.

Ofengand, J & Bakin, A (1997) Mapping to nucleotide resolution of pseudouridine residues in large subunit ribosomal RNAs from representative eukaryotes, prokaryotes, archaebacteria, mitochondria and chloroplasts. *J Mol Biol,* 266**,** 246-268.

Ohashi, Y, Oka, A, Rodrigues-Pousada, R, Possenti, M, Ruberti, I, Morelli, G & Aoyama, T (2003) Modulation of Phospholipid Signaling by *GLABRA2* in Root-Hair Pattern Formation. *Science,* 300**,** 1427-1430.

Park, HS, Himmelbach, A, Browning, KS, Hohn, T & Ryabova, LA (2001) A plant viral "reinitiation" factor interacts with the host translational machinery. *Cell,* 106**,** 723-33.

Payne, C, Zhang, F & Lloyd, AM (2000) *GL3* encodes a bHLH protein that regulates trichome development in *Arabidopsis* through interaction with GL1 and TTG1. *Genetics,* 156**,** 1349-1362.

Pemberton, LMS, Tsai, S, Lovell, PH & Harris, PJ (2001) Epidermal patterning in seedling roots of eudicotyledons. *Ann. Bot.,* 87**,** 649-654.

Pendle, AF, Clark, GP, Boon, R, Lewandowska, D, Lam, YW, Andersen, J, . . . Shaw, PJ (2005) Proteomic analysis of the Arabidopsis nucleolus suggests novel nucleolar functions. *Mol Biol Cell,* 16**,** 260-269.

Pesch, M & Hulskamp, M (2004) Creating a two-dimensional pattern de novo during Arabidopsis trichome and root hair initiation. *Curr Opin Genet Dev,* 14**,** 422-7.

Petricka, J & Nelson, T (2007) *Arabidopsis* nucleolin affects plant development and patterning. *Plant Physiol.,* 144**,** 173-186.

Pinon, V, Etchells, J, Rossignol, P, Collier, S, Arroyo, JM, Martienssen, RA & Byrne, ME (2008) Three *PIGGYBACK* genes that specifically influence leaf patterning encode ribosomal proteins. *Development,* 135**,** 1315-1324.

Poldermans, B, Bakker, H & Van Knippenberg, PH (1980) Studies on the function of two adjacent N6, N6-dimethyladenosines near the 3' end of 16 S ribosomal RNA of Escherichia coli. IV . The effect of the methylgroups on ribosomal subunit interaction. *Nuc. Acids Res.,* 8**,** 143-151.

Poldermans, B, Goosen, N & Van Knippenberg, PH (1979a) Studies on the Function of Two Adjacent N",N"-Dimethyladenosines Near the 3' End of 16 S Ribosomal RNA of *Escherichia coli* I.THE EFFECT OF KASUGAMYCIN ON INITIATION OF PROTEIN SYNTHESIS. *The Journal of Biological Chemistry,* 254**,** 9085-9089.

Poldermans, B, Roza, L & Van Knippenberg, PH (1979b) Studies on the Function of Two Adjacent iV,W-Dimethyladenosines Near the 3' End of 16 S Ribosomal RNA of *Escherichia coli* III. PURIFICATION AND PROPERTIES OF THE METHYLATING ENZYME AND METHYLASE-30S INTERACTIONS. *The Journal of Biological Chemistry,* 254**,** 9094-9100.

Poldermans, B, Van Buul, CPJJ & Van Knippenberg, PH (1979c) Studies on the Function of Two Adjacent N6,N6-Dimethyladenosines Near the 3' End of 16 S Ribosomal RNA of *Escherichia coli*. *The Journal of Biological Chemistry,* 254**,** 9090-9094.

Pontvianne, F, Matia, I, Douet, J, Tourmente, S, Medina, FJ, Echeverria, M & Saez-Vasquez, J (2007) Characterization of *AtNUC-L1* Reveals a Central Role of Nucleolin in Nucleolus Organization and Silencing of *AtNUC-L2* Gene in *Arabidopsis*. *Mol Biol Cell,* 18**,** 369-379.

Pulicherla, N, Pogorzala, L, Xu, Z, O'farrell, H, Musayev, FN, Scarsdale, JN, . . . Rife, JP (2009) Structural and Functional Divergence within the Dim1/KsgA Family of rRNA Methyltransferases. *J Mol Biol,* 391**,** 884-893.

Rerie, W, Feldmann, K & David Marks, M (1994) The *GLABRA2* gene encodes a homeo domain protein required for normal trichome development in *Arabidopsis*. *Genes Dev.,* 8**,** 1388-1399.

Richter, U, Kühn, K, Okada, S, Brennicke, A, Weihe, A & Börner, T (2010) A mitochondrial rRNA dimethyladenosine methyltransferase in *Arabidopsis*. *Plant J,* 61**,** 558-69.

Ryu, KH, Kang, YH, Park, Y-H, Hwang, I, Schiefelbein, J & Lee, MM (2005) The WEREWOLF MYB protein directly regulates CAPRICE transcription during cell fate specification in the Arabidopsis root epidermis. *Development,* 132**,** 4765-4775.

Saez-Vasquez, J, Caparros-Ruiz, D, Barneche, F & Echeverria, M (2004) A plant snoRNP complex containing snoRNAs, fibrillarin, and nucleolin-like proteins is competent for both rRNA gene binding and pre-rRNA processing in vitro. *Molecular and Cellular Biology,* 24**,** 7284-97.

Samaha, H, Delorme, VR, Pontvianne, F, Cooke, R, Delalande, F, Dorsselaer, AV, . . . Saez-Vasquez, J (2010) Identification of protein factors and U3 snoRNAs from a *Brassica oleracea* RNP complex involved in the processing of pre-rRNA. *Plant J.,* 61**,** 383-398.

Schafer, T, Strauss, D, Petfalski, E, Tollervey, D & Hurt, E (2003) The path from nucleolar 90S to cytoplasmic 40S pre-ribosomes. *EMBO J.,* 22**,** 1370-80.

Schellmann, S, Hulskamp, M & Uhrig, J (2007) Epidermal pattern formation in the root and shoot of *Arabidopsis*. *Biochem. Soc. Trans.,* 35**,** 146-148.

Schellmann, S, Schnittger, A, Kirik, V, Wada, T, Okada, K, Beermann, A, . . . Hülskamp, M (2002) TRIPTYCHON and CAPRICE mediate lateral inhibition during trichome and root hair patterning in *Arabidopsis*. *EMBO J.,* 21**,** 5036-5046.

Scheres, B, Wolkenfelt, H, Willemsen, V, Terlouw, M, Lawson, E, Dean, C & Weisbeek, P (1994) Embryonic origin of the *Arabidopsis* primary root and root meristem initials. *Development,* 120**,** 2475-2475.

Schiefelbein, J, Kwak, S-H, Wieckowski, Y, Barron, C & Bruex, A (2009) The gene regulatory network for root epidermal cell-type pattern formation in *Arabidopsis*. *J. Exp. Bot.,* 60**,** 1515-1521.

Seidel-Rogol, BL, Shadel, V & Mcculloch, GS (2003) Human mitochondrial transcription factor B1 methylates ribosomal RNA at a conserved stem-loop. *Nature genetics*.

Seshadri, A, Dubey, B, Weber, MHW & Varshney, U (2009) Impact of rRNA methylations on ribosome recycling and fidelity of initiation in Escherichia coli. *Mol. Microbiol.,* 72**,** 795-808.

Shaw, PJ & Jordan, EG (1995) The nucleolus. *Annual Review of Cell and Developmental Biology,* 11**,** 93-121.

Shi, D-Q, Liu, J, Xiang, Y-H, Ye, D, Sundaresan, V & Yang, W-C (2005) *SLOW WALKER1*, essential for gametogenesis in *Arabidopsis*, encodes a WD40 protein involved in 18S ribosomal RNA biogenesis. *Plant Cell,* 17**,** 2340-54.

Simon, M, Lee, MM, Lin, Y, Gish, L & Schiefelbein, J (2007) Distinct and overlapping roles of single-repeat MYB genes in root epidermal patterning. *Dev. Biol.,* 311**,** 566-578.

Thammana, P & Held, WA (1974) Methylation of 16S RNA during ribosome assembly in vitro. *Nature,* 251**,** 682-686.

Tokuhisa, J, Vijayan, P, Feldmann, K & Browse, J (1998) Chloroplast Development at Low Temperatures Requires a Homolog of *DIM1*, a Yeast Gene Encoding the 18S rRNA Dimethylase. *Plant Cell,* 10**,** 699-711.

Tominaga, R, Iwata, M, Okada, K & Wada, T (2007) Functional analysis of the epidermal-specific MYB genes *CAPRICE* and *WEREWOLF* in *Arabidopsis*. *Plant Cell,* 19**,** 2264-77.

Tu, C, Tropea, JE, Austin, BP, Court, DL, Waugh, DS & Ji, X (2009) Structural Basis for Binding of RNA and Cofactor by a KsgA Methyltransferase. *Structure/Folding and Design,* 17**,** 374-385.

Udem, SA & Warner, JR (1973) The cytoplasmic maturation of a ribosomal precursor ribonucleic acid in yeast. *Journal of Biological Chemistry,* 248**,** 1412-1416.

Ueda, M, Koshino-Kimura, Y & Okada, K (2005) Stepwise understanding of root development. *Curr. Opin. Plant Biol.,* 8**,** 71-76.

Van Buul, CP, Hamersma, M, Visser, W & Van Knippenberg, PH (1984a) Partial methylation of two adjacent adenosines in ribosomes from *Euglena gracilis* chloroplasts suggests evolutionary loss of an intermediate stage in the methyltransfer reaction. *Nuc. Acids Res.,* 12**,** 9205-9208.

Van Buul, CPJJ & Van Knippenberg, PH (1985) Nucleotide sequence of the *ksgA* gene of *Escherichia coli*: comparison of methyitransferases effecting dimethylation of adenosine in ribosomal RNA. *Gene,* 38**,** 65-72.

Van Buul, CPJJ, Visser, W & Can Knippenberg, PH (1984b) Increased translational fidelity caused by the antibiotic kasugamycin and ribosomal ambiguity in mutants harbouring the *ksgA* gene. *FEBS letters,* 177**,** 119-124.

Van Den Berg, C, Willemsen, V, Hendriks, G, Weisbeek, P & Scheres, B (1997) Short-range control of cell differentiation in the *Arabidopsis* root meristem. *NATURE,* 390**,** 287-289.

Van Gemen, B, Twisk, J & Van Knippenberg, PH (1989) Autogenous regulation of the *Escherichia coli ksgA* gene at the level of translation. *J Bacteriology,* 171**,** 4002-4008.

Van Knippenberg, PH, Van Kimmenade, JMA & Heus, HA (1984) Phylogeny of tbe conserved 3' terminal structure of the RNA of small ribosomal subunits. *Nuc. Acids Res.,* 12**,** 2595-2604.

Van Lijsebettens, M, Vanderhaeghen, R, Block, MD, Bauw, G, Villarroel, R & Van Montagu, M (1994) An S18 ribosomal protein gene copy at the *Arabidopsis PFL* locus affects plant development by its specific expression in meristems. *EMBO J.,* 13**,** 3378-3388.

Venema, J & Tollervey, D (1999) Ribosome synthesis in *Saccharomyces cerevisiae*. *Annual review of genetics,* 33**,** 261-311.

Volarevic, S, Stewart, MJ, Ledermann, B, Zilberman, F, Terracciano, L, Montini, E, . . . Thomas, G (2000) Proliferation, but not growth, blocked by conditional deletion of 40S ribosomal protein S6. *Science,* 288**,** 2045-2047.

Wada, T, Kurata, T, Tominaga, R, Koshino-Kimura, Y, Tachibana, T, Goto, K, . . . Okada, K (2002) Role of a positive regulator of root hair development, *CAPRICE*, in *Arabidopsis* root epidermal cell differentiation. *Development,* 129**,** 5409-5419.

Wada, T, Tachibana, T, Shimura, Y & Okada, K (1997) Epidermal Cell Differentiation in *Arabidopsis* Determined by a Myb Homolog, *CPC*. *Science,* 277**,** 1113-1116.

Walker, AR, Davison, PA, Bolognesis-Winfield, AC, James, CM, Srinivasan, N, Blundell, TL, . . . Gray, JC (1999) The *TRANSPARENT TESTA GLABRA1* Locus, Which Regulates Trichome Differentiation and Anthocyanin Biosynthesis in *Arabidopsis*, Encodes a WD40 Repeat Protein. *Plant Cell,* 11**,** 1337-1349.

Xu, C, Liu, C, Wang, Y, Li, L-C, Chen, W-Q, Xu, Z-H & Bai, S-N (2005) Histone acetylation affects expression of cellular patterning genes in the *Arabidopsis* root epidermis. *Procl. Natl. Acad. Sci.,* 102**,** 14469-14474.

Xu, Z, O'farrell, H, Rife, JP & Culver, G (2008) A conserved rRNA methyltransferase regulates ribosome biogenesis. *Nature Structural and Molecular Biology,* 15**,** 534-536.

Yao, Y, Ling, Q, Wang, H & Huang, H (2008) Ribosomal proteins promote leaf adaxial identity. *Development,* 135**,** 1325-1334.

Zemp, I & Kutay, U (2007) Nuclear export and cytoplasmic maturation of ribosomal subunits. *FEBS letters,* 581**,** 2783-2793.

Zhang, F, Gonzalez, A, Zhao, M, Payne, C & Lloyd, A (2003) A network of redundant bHLH proteins functions in all TTG1-dependent pathways of *Arabidopsis*. *Development,* 130**,** 4859-4869.

CHAPTER 2

The Role of DIM1A, a Highly Conserved rRNA Dimethylase, in *Arabidopsis thaliana* Root Development and Epidermal Patterning

Abstract

Differentiation of specialized cell types during development requires precise regulatory networks to generate distinct patterns of gene expression. The establishment of a position-dependent pattern of hair and non-hair cells in the *Arabidopsis* root epidermis provides a powerful system to research the regulatory networks involved in cell fate specification. The *Arabidopsis DIM1A* gene is required for position-dependent expression of the epidermal patterning genes *GLABRA2*, *CAPRICE* and *WEREWOLF*. DIM1A belongs to the highly conserved Dim1/KsgA family of dimethylases that are involved in post-transcriptional modification of ribosomal RNA and pre-rRNA processing. While the two small subunit RNA nucleotide modifications they catalyze are present in almost every known organism, the functional significance of these modifications is currently unknown. In this study, we provide the first characterization of a Dim1/KsgA

homolog in a multicellular organism. In addition to defects in root epidermal patterning, the *dim1A* mutant displays reduced root meristem cell division rate and defects in leaf size, shape, vascular patterning and trichome branching. The *Dim1A* gene is expressed in rapidly dividing tissues throughout the plant, and the protein is localized in the nucleus with enrichment in the nucleolus. Here we show that the *dim1A* mutant lacks the two 18S rRNA dimethyladenosines, however the mutation does not affect pre-rRNA processing. Thus, it is likely that the developmental defects seen in the *Arabidopsis dim1A* mutant are a result of the lack of these two highly conserved rRNA base modifications.

Introduction

Development of multicellular organisms from a single cell involves strict regulation of cell fate specification. The differential expression of many genes in different cell types implies that transcription factors play crucial roles in this process. Defining regulatory events responsible for generating distinct patterns of gene expression during development is essential for understanding how specialized cell types form.

Over the last twenty years, the *Arabidopsis* root epidermis has emerged at the forefront of research on transcriptional regulation during development. The *Arabidopsis* root epidermis contains two types of cells, hair cells and non-hair cells, which arise in a stereotyped pattern influenced by cell position. Genetic analysis has defined a regulatory network involved in specifying the two distinct cell fates. Five genes, *WEREWOLF (WER)*, *GLABRA3 (GL3)*, *ENHANCER OF*

GLABRA3 (EGL3), *TRANSPARENT TESTA GLABRA1 (TTG1)* and *GLABRA2 (GL2)* are required to specify the non-hair fate (Bernhardt *et al.*, 2003, Galway *et al.*, 1994, Lee and Schiefelbein, 1999, Massucci *et al.*, 1996). Current models suggest that WER (an R2R3-MYB protein), GL3/EGL3 (related bHLH proteins) and TTG1 (a WD40-repeat protein), which preferentially accumulate in N position cells, work together as a core transcriptional activation complex to influence non-hair cell fate (Lee and Schiefelbein, 2002, Pesch and Hulskamp, 2004, Schiefelbein *et al.*, 2009, Ueda *et al.*, 2005) by directly regulating expression of the homeodomain transcription factor *GL2* (Di Cristina *et al.*, 1996, Rerie *et al.*, 1994). GL2 is necessary for non-hair cell specification (Massucci *et al.*, 1996) and has been shown to negatively regulate root-hair-specific genes and positively regulate non-hair-specific genes (Lee and Schiefelbein, 1999, 2002, Massucci *et al.*, 1996, Ohashi *et al.*, 2003). In addition, the activation complex promotes lateral inhibition by regulating transcription of three genes *CAPRICE (CPC), TRIPTYCHON (TRY)* and *ENHANCER OF CPC AND TRY (ETC1)* which act semi-redundantly to promote the hair cell fate (Kirik *et al.*, 2004, Schellmann *et al.*, 2002, Wada *et al.*, 1997). In developing hair cells, the lateral inhibitors CPC, TRY, and ETC1 promote hair cell fate by competing with WER for binding to other activation complex members (Lee and Schiefelbein, 1999, 2002, Tominaga *et al.*, 2007). As an additional feedback look, *GL3* and *EGL3* are preferentially transcribed in H-position cells while the GL3 (and likely EGL3) proteins preferentially accumulate in N position cells (Bernhardt *et al.*, 2005).

SCRAMBLED (SCM), a leucine-rich repeat receptor-like kinase (LRR-RLK),

is necessary for the position-dependence of root epidermal cell fate specification. Loss of function mutations in SCM make a similar frequency of hair cells as wild-type, however there is a remarkable disconnect between cell fate and position (Kwak *et al.*, 2005). Detailed genetic analysis has determined that SCM likely influences the molecular network within epidermal cells by repressing *WER* transcription in H position cells (Kwak and Schiefelbein, 2007).

Furthermore, an extensive body of research has characterized the development of *Arabidopsis* root epidermal cells from origin to maturity (Dolan *et al.*, 1994, Dolan *et al.*, 1993, Scheres *et al.*, 1994), providing a solid foundation for the study of cell fate specification. Root epidermal cells are formed continuously in cell files, which means that a complete developmental timeline may be observed along the axis of growth at any point in time.

Recent studies have implicated ribosomal protein and ribosome assembly factors in regulation of gene expression during development (reviewed in Byrne, 2009). However, the connection between ribosome biogenesis and root cell-type patterning has, to date, has not been investigated.

The ribosome, a large RNA-protein complex composed of two subunits, is essential for protein synthesis. The large subunit (60S; LSU), which catalyzes the formation of the polypeptide, consists of three ribosomal RNAs (rRNAs) (25S-28S, 5.8S and 5S). The small ribosomal subunit (40S; SSU) functions in the process of decoding, or discriminating against aminoacyl transfer RNAs that do not match the codon of messenger RNA, and translocation, which involves coordination with the large ribosomal subunit to move the tRNAs and associated

mRNA one codon at a time. Together, these actions ensure accuracy in translation of the genetic message encoded in the genome.

Ribosome biogenesis is a complex process requiring coordinated transcription, RNA processing, RNA modification, folding and complexing of ribosomal RNA and proteins. In eukaryotes, transcription of the rDNA genes and the majority of rRNA processing occur in the nucleolus. The rDNA gene is transcribed as a single 35S/45S pre-rRNA and is then processed to yield the individual subunits. During rRNA processing, the rRNA goes through extensive modification guided by trans-acting factors and small nucleolar RNAs (Brown and Shaw, 1998, Ganot *et al.*, 1997, Kiss-Laszlo *et al.*, 1996). While rRNA modifications have been thoroughly research and mapped and are known to occur in conserved regions of the ribosome, for the most part their functional significances are currently unknown (Decatur and Fournier, 2002).

Only three post-transcriptional rRNA modifications identified to date are conserved in all three domains of life (Van Knippenberg *et al.*, 1984, Decatur and Fournier, 2002, Ofengand, 2002, McCloskey and Rozenski, 2005). Two are the dimethylations of adjacent adenosines in the 3'-terminal loop (helix 45) of the small subunit rRNA (Van Knippenberg *et al.*, 1984). Research to date in *S. cerevisiae* suggests that in eukaryotes, the methylation events themselves are not required for ribosome function, however the dimethylase enzyme that catalyzes the methylation, Dim1p, is indispensable due to an indirect role in pre-rRNA processing (Lafontaine *et al.*, 1994, Lafontaine *et al.*, 1995, Lafontaine *et al.*, 1998, Pulicherla *et al.*, 2009). Interestingly, in prokaryotes, lack of the

methylations and/or the methylase enzyme only modestly affect ribosome function and organism fitness (Helser *et al.*, 1972, Poldermans *et al.*, 1979a, Poldermans *et al.*, 1979c, Van Buul *et al.*, 1984, O'Connor *et al.*, 1997).

Here we report the characterization and cloning of the *Arabidopsis* gene *DIM1A*, which encodes a homolog of the KsgA/Dim1 family of highly conserved rRNA dimethylases. We isolated a unique mutant version of DIM1A gene in which the encoded enzyme lacks methylase activity without affecting its role in pre-rRNA processing, allowing us to not only study the role of DIM1A but also of the highly conserved rRNA methylations. The *dim1A* mutant was isolated for its effect on position-dependent expression of *GL2*, and after further analysis was found to affect the expression patterns and expression levels of additional patterning genes. In addition, we found the *dim1A* mutant to have defects in root meristem cell division, leaf morphogenesis and trichome branching. Taken together, we propose that the post-transcriptional modification catalyzed by DIM1A is important for generating stable and spatially well-defined patterns of gene expression necessary for generating two distinct cell fates in the *Arabidopsis* root epidermis.

Materials and Methods

Plant material and growth conditions

Seeds were surface-sterilized using a 30% sodium hypochlorite/1% tritonX-100 solution, stratified for two days in water at 4°C and subsequently germinated

and grown in petri dishes on agarose-solidified mineral nutrient media under 24 hour light (Schiefelbein and Somerville, 1990). Plants in pots were transferred at seven to ten days post-germination from plates and grown in soil supplemented with Osmocote (Scotts). Unless otherwise specified, *Arabidopsis* plants were grown at 22°C under long-day conditions in growth chambers.

The following lines were previously described: *wer-1* (Lee and Schiefelbein, 1999), *gl3-1* (Koorneef et al, 1982), *egl3-1* (Zhang et al, 2003), *gl2-1* (Koornneef, 1981), *ttg1-1(Galway et al., 1994)*, *scm-2* (Kwak *et al.*, 2005), *pWER::green fluorescent protein (GFP)* (Lee and Schiefelbein, 1999), *pGL2::β-glucuronidase (GUS)* (Massucci *et al.*, 1996), *pEGL3::GUS* (Zhang *et al.*, 2003), *pCPC::GUS* (Wada *et al.*, 2002). Reporter genes and mutations were introduced into each line by crossing and subsequently verified to be homozygous by phenotypic analysis (reporters) or molecular genotyping (mutant lines)

DNA extraction from plant tissue

DNA was extracted from individual plants or pools of seedlings by grinding tissue with a pestle in a micro-centrifuge tube containing DNA extraction buffer (200 mM Tris-HCl pH 7.5, 250 mM NaCl, 25 mM EDTA, 0.5% SDS). After centrifugation to remove debris, DNA was precipitated with an equal volume of 100% isopropanol and resuspended in water.

Patterning mutant identification and positional cloning

Seed mutagenesis of the *GL2::GUS* reporter line (WS ecotype) with ethyl

methanesulfonate (EMS) was performed as described (Lee and Schiefelbein, 1999). The *45-137* mutant was identified by screening M3 seedlings stained for GUS for defects in *GL2* promoter activity in the root apical meristem. *45-137 GL2::GUS* plants were crossed to *Ler* wild-type to generate F2 and F3 offspring for genetic mapping. Approximately 30 F3 pools were taken for bulk-segregant analysis using sixteen SSLP primers spread over the five *Arabidopsis* chromosomes to rough map the mutation to a single chromosome (Table 2.3) (Lukowitz *et al.*, 2000). Subsequently, DNA from 618 individual mutants identified phenotypically from F2 seed populations were analyzed using novel primers to further narrow down the region containing the mutation (Table 2.4).

Cloning and construction of transgenic plant lines

Complementation

Using Pfu Turbo (Strategene), 3.2 Kb genomic fragment of *Arabidopsis Dim1A* (At2g47420) was amplified from DNA isolated from BAC clone T30B22 (ABRC) using the primers 45137COMP-LP and 45137COMP-RP (Table 2.5). The 3.2 Kb fragment spanned the entire length of the *DIM1A* gene and also included the 5' and 3' intergenic spaces as well as the 3'UTR, one exon and one intron of both the 5' and 3' neighboring genes. The amplified fragment was ligated into the Gateway® pENTR/SD/TOPO vector (Invitrogen, Carlsbad, CA) following the manufacturer's instructions and transformed into TOP10 competent cells. Resultant clones were selected on LB plates containing kanamycin (50

μg/ml) and screened for size after plasmid linearization with the restriction enzyme NotI. Putative positives were sequenced using the M13F and M13R primers before proceeding. LR clonase^{TM} recombination reactions (Invitrogen, Carlsbad, CA) were performed to transfer the *DIM1A* genomic fragment into the pMDC99 Gateway binary vector. Due to both the pENTR and binary vectors containing the kanamycin resistant gene, pENTR/DIM1A plasmid DNA was linearized and subsequently purified using the Qiagen PCR purification kit prior to recombination. The clonase reaction was performed according to manufacturers specification and the reaction mixture was transformed into DB3.1 cells. Resultant clones were sequenced, and plasmid DNA was isolated from positives using a Qiagen miniprep kit (Qiagen). Plasmid DNA was transformed into *Agrobacterium tumefacians strain* GV301 for plant transformation.

C-terminal GFP fusion protein

To make the GFP-tagged protein construct, a 2.4 Kb fragment containing the same upstream and genomic region of the complementation construct but stopping before the TAA stop codon was amplified using primers 45137GFP-LP and 45137GFP-RP (Table 2.5). Amplification and cloning were performed as mentioned above for the complementation construct, except the final recipient vector was pMDC117, a native promoter driven c-terminal GFP tag GATEWAY vector.

Dim1A::GUS promoter-reporter

A 1.3 Kb region upstream of the *DIM1A* start codon was amplified using the primers 45137PRO-LP and 45137GFP-RP (Table 2.5). Amplification and cloning were performed as described above, except the final recipient vector was pMDC43, a native promoter driven GUS gene GATEWAY vector.

Overexpression constructs

A 1.2 Kb genomic region of *DIM1A* from the start codon through the stop codon, which was replaced with an alanine (TAA ➔ GCG) was amplified using the primers 45137PRO-LP and 45137GFP-RP (Table 2.5). Amplification and cloning were performed as mentioned above for the complementation construct, except the final recipient vector was pMDC43, a 35S:GFP-tagged plant overexpression GATEWAY vector.

Generation of transgenic plant lines

Three-week-old *Arabidopsis* plants were transformed using a modified version of the *Agrobacterium*-mediated floral dip transformation protocol (Clough and Bent, 1998). T1 plants were grown on mineral media with hygromycin (50 µg/ml) according to and positives were selected and grown up on soil. T2 pools were screened for transgene segregation and subsequently T3 pool homozygosity was tested by hygromycin selection.

Microscopy and image analysis

All cell-type pattern analysis was conducted with four-day-old seedlings

grown vertically on agar-solidified media containing mineral nutrients unless otherwise indicated (Schiefelbein and Somerville, 1990). All images captured using a dissection or compound scope were taken with a Canon Powershot with attached MM series adapter (www.martinmicroscope.com/).

GUS analysis

For histochemical analysis of plants containing the *GUS* reporter gene, seedlings were staining in GUS staining solution (0.1M NaPO4 pH 7.0, 10 mM EDTA pH 7.0, 0.75 mM KFerricyanide, 0.75 mM KFerrocyanide, 1% Triton X-100, 0.4 mM X-Glucoronide) (Massucci *et al.*, 1996). Seedlings containing the following transgenes were stained for the specified amounts of time: *GL2::GUS,* 25 minutes; *CPC::GUS,* 2.5 hours; *EGL3::GUS,* 30 minutes; *DIM1A::GUS,* 2.5 hours. For quantitative analysis of reporter-expressing cells, epidermal cell location was determined relative to an anticlinal cortical cell wall (ACCW) and cells within one hair file (bordering and underlying ACCW) and one non-hair file (not bordering and underlying ACCW) were counted from the meristem initial up to the elongation zone.

Root hair counting

The pattern of epidermal cell types was determined by staining seedling roots with toluidine blue, followed by examination at 160X magnification to determine locations of epidermal cells relative to the underlying ACCW. The pattern of hair and non-hair cell types in the root epidermis was determined by

examining at least 20 seedlings from each strain. Ten cells in each the hair position (H position) and non-hair position (N position) were counted for each seedling root. An epidermal cell was scored as a root-hair cell if any protrusion was visible, regardless of its length.

Epidermal clone analysis

The relative cell division rate in H and N position cells was determined by counting the number of cells in each position derived from a rare longitudinal division in a H position cell in the meristem division zone as previously described (Berger *et al.*, 1998).

Confocal microscopy

All fluorescent imaging was performed with a TCS SP5 DM6000B broadband confocal microscope using a HCX PL APO CS 20x dry lens or HCX PL APO CS 100.0x1.40 oil lens. Image capture and analysis was done using LAS AF software (Leica microsystems). GFP and propidium iodide (PI) were observed sequentially on separate channels. The GFP signal was excited using the argon 488-nm laser set to 25% power and captured using PMT2 between bandwidth 493nm and 557nm. The PI signal was excited using DPSS 561-nm laser and captured using PMT3 between 591nm and 765nm. Image capture was performed with a pinhole of 60.8 nm, a line and frame average both of two, and a scan speed of 200 hz. Just prior to imagining, seedlings were counterstained for two minutes with light shaking in 10 µg/ml PI in water. After washing twice in

ddH_20, roots were mounted on slides, with cotyledons removed, in ddH_20.

WER::GFP quantification

WER::GFP intensity was quantified with LAS AF software using the ROI tool to measure total pixels from individual cells (cell boundaries identified by PI staining). Meristem length was measured from the first visible epidermal cell (in the cell file of interest) at the tip of the root up to the cell previous to the first that was longer than wider (indicating entry into rapid elongation zone and exit from the meristematic region). Pixel sum analysis was performed on cells within a region one-third the length of the meristem measured towards the root tip from the last meristematic cell. For each file, averaged pixel sum was calculated from the specific aforementioned measured cells. Analysis was completed on one N file and one H file of five different roots for three biological repeats (for a total of fifteen wild-type and fifteen *dim1A* roots).

Meristem cell size and number analysis

Analysis of meristem cell size and cell number was measured from longitudinal sections collected using confocal microscopy. Cells that were significantly wider than longer, indicating rapid division without expansion, were considered to lie within the Division Zone (DZ) while cells with relatively equal width and length were considered to be within the Slow Elongation Zone (SEZ). All measurements were done using Adobe Photoshop CS3.

Mature cell size measurements

The length of mature epidermal cell was determined by staining seedling roots with toluidine blue, imaging at 160X magnification, and subsequently measuring individual cells using Adobe Photoshop.

Root length measurements

Root length was measured from seedlings grown vertically on minimal media plates (as described above). Individual seedlings were tracked and imaged every day for six days after germination. Roots were measured using Adobe Photoshop.

Leaf surface area measurements and trichome analysis

The surface area and trichome characteristics were determined for the first pair and second pair of wild-type and *dim1A* plants using fully expanded leaves from twenty one-month-old soil-grown plants. Leaf surface area was measured using the image analysis software Macnification (Orbicle). Trichome counts and branching were analyzed for individual leaves using a dissection scope. Trichome density (trichomes/area) was determined by dividing the total number of trichomes on a leaf by its surface area.

Leaf venation and stomatal pattern

Leaf venation and stomatal pattern were analyzed on leaves cleared overnight in 70% ethanol. Venation was analyzed and imaged using a dissection

scope. Stomatal pattern on the abaxial leaf surface was analyzed at 160X magnification using a compound scope.

Microarray expression analysis of root epidermal cells

For this analysis, six independent samples were used i.e. three from wild-type *WER::GFP* and three from *dim1A WER::GFP*. The procedure leading to the acquisition of epidermal cells was adapted from the Benfey Lab (Birnbaum *et al.*, 2003). For each sample, approximately 100 µl of seeds were surface sterilized and then sown at high density on MS plates (0.433% MS salts, 1% sucrose, 0.02 % MES, 0.6% agarose, pH 5.8) covered with a 100-gauge NYTEX mesh (Sefar). After vernalization at 4° C, plates were incubated vertically under constant light for five days. Root tips were excised using a razor blade and transferred to a 70 micron filter submerged in enzyme solution B (600 mM mannitol, 2mM MgCl2, 0.1% BSA, 2mM CaCl2, 2mM MES, 10 mM KCL, 1.5% cellulysin, 0.1% pectolyase) contained within a petri dish. Root tips were incubated for one hour with gentle shaking, after which the strainer was gently shaken and removed. Solution B containing the protoplasted cells was then centrifuged at 200Xg at room temperature for six minutes. The supernatant was aspirated and the pellet was resuspended in solution A (600 mM mannitol, 2mM MgCl2, 0.1% BSA, 2mM CaCl2, 2mM MES, 10 mM KCL), then strained through a 70 um and subsequently a 40 um filter to remove unprotoplasted debris. Isolated protoplasts were taken immediately for fluorescently activated cell sorting (FACS) and sorted as described (Birnbaum *et al.*, 2003). Sorted cells were collected in

RLT Buffer (Qiagen) containing beta-mercaptoethanol (BME). RNA was subsequently extracted from cells using the Qiagen Rneasy Micro kit (Qiagen) and RNA quality and concentration was analyzed using a Nanodrop. RNA was amplified, labeled and hybridized to an Affymetrix ATH1 GeneChip.

Poisoned primer extension, RNA sequencing and RT-PCR

Isolation of RNA from plant tissue

Total cellular RNA was extracted from whole five-day-old *Arabidopsis* seedlings (grown on nutrient plates as described above) using TRIZOL (Invitrogen, Inc.) as described (Weigel and Glazebrook, 2002). RNA was treated with TURBO-Free^{TM} DNAse (Ambion, Inc.) following manufacturers protocol.

Primer extension

Poisoned primer extension procedure was adapted from (Richter et al 2010). A total of 50 pmol of PAGE-purified DNA oligonucleotide primer 18SPE (Table 2.5) was end-labeled with 150 µCi $^{32}P\gamma$-ATP using T4-polynucleotide kinase (Fermentas, Inc.) and then subsequently separated from unincorporated nucleotides by running through G-50 sephadex column (GE Healthcare). Two pmol of end-labeled primer was annealed to 4 µg RNA in the presence of 1 mM nucleotides (ddATP, dCTP, dGTP, dTTP) by incubating at 95°C for one minute, 65°C for five minutes followed by immediate transfer to ice for fifteen minutes. The extension reaction were performed using AMV reverse transcriptase

(Promega) in the presence of 10 mM sodium pyrophosphate (pre-warmed to 42°C) at 42°C for 90 minutes. The extension reaction was stopped by addition of an equal volume of stop buffer (95% formamide, 20 mM EDTA, 0.05% bromophenol blue, 0.05 xylene cyanol). Four RNA sequencing reactions were set up identically to the primer extension reaction, except with 2 µg of RNA and a nucleotide mixture containing four dNTPs and one of each ddNTP. Resulting products were analyzed on a 10% acrylamide/6 M urea sequencing gel.

Processing assay and RT-PCR

DNASE-treated total RNA was used to make cDNA using random hexamer primers with a First-Strand cDNA Synthesis Kit (GE Healthcare) according to manufacturers instructions. cDNA was diluted to a final concentration of 1/10,00 for the processing assay and 1/200 for *DIM1A* expression analysis and subjected to PCR using specific primers (Table 2.3).

Multiple alignment and target signal analysis

DIM1A homologs were identified using Blastp from NCBI (http://blast.ncbi.nlm.nih.gov/) with the entire DIM1A protein sequence. Resulting amino acid sequences were aligned using Multalin (Corpet 1998) then exported and edited in Pages (iWork v9.0, Apple, Inc.).

Results

Patterning mutant identification

A mutant, preliminarily designated *45-137*, was identified in a forward genetic screen for root epidermal patterning defects in EMS-mutagenized plants expressing the non-hair-specific reporter *GL2::GUS*. The *45-137* mutant was initially characterized as expressing *GL2::GUS* in a pattern that is no longer strictly associated with epidermal cell position relative to the underlying cortical cells. In wild-type roots, approximately 95% of epidermal cells in the H position (bordering an underlying anticlinal cortical cell wall (ACCW)) lack *GL2::GUS* expression, and 100% of cells in the N position (not bordering an ACCW) express *GL2::GUS* (Fig. 2.1). In *45-137* roots, only 80% of cells in the H position lack *GL2::GUS*, and 94% of cells in the N position express *GL2::GUS* (Fig. 2.1). Additionally, in the mature portion of the root, *45-137* has a statistically significant increase in the frequency of non-hair cells in H cell files (20%, compared to 5% in wild-type) and a small increase in the frequency of hair cells in N cell files (1.6% compared to 0% in wild-type) (Table 2.1).

The *45-137* mutant phenotype is caused by a recessive allele, as F1 offspring from a cross between *45-137* and wild-type plants produced roots with normal phenotype. Additionally, F1 offspring from a cross of *45-137* and *scm-2* were all phenotypically normal, indicating that *45-137* is not a new mutant allele of *SCM* but rather a novel patterning mutant (data not shown). Thus, *45-137* represents a novel mutation affecting epidermal cell fate specification.

Positional cloning and complementation

Bulk-segregant analysis of F3 pools, generated by crossing *45-137* (WS ecotype) to wild-type (Ler ecotype), with sixteen SSLP-markers (Table 2.3) spread over the five *Arabidopsis* chromosomes located the mutation to the bottom arm of chromosome two (Jander *et al.*, 2002, Lukowitz *et al.*, 2000). Based on recombination frequencies we determined that the *45-137* mutation was below marker PLS4 at 9.0 Mb, in the vicinity of marker CER459187 at 17.01 Mb (Fig. 2.2).

To obtain a high-resolution map position, over 600 homozygous mutant plants were selected from F2 progeny. Mapping analysis with primer CER460253 (19.55Mb), located close to the telomere, resulted in a very low rate of recombination (2/1232), suggesting that the mutation was between marker CER459187 and the bottom end of chromosome two rather than between PLS4 and CER459187 (Fig. 2.3). Analysis with SSLP, CAPS and dCAPS primers between 17.01 and 19.55 Mb (Table 2.4) narrowed the mutation to an 83 Kb region (19.407 - 19.490) containing 41 genes (Fig. 2.3).

Due to the infrequency of recombination events at the bottom of chromosome two, the 41 genes between 19.407 and 19.490 Mb were systematically sequenced in order to identify the mutation. Sequence analysis of the *45-137* mutant identified a G->A change in locus At2g47420 at position 19, 457,770 which causes a predicted GLY to GLU missense at position 66 in the gene product (Fig. 2.3).

To verify that the mutation in gene At2g47420 was the cause of the *45-137* mutant phenotype, a construct containing a full-length genomic fragment of At2g47420 was stably transformed into *45-137* plants (Fig. 2.3). This construct fully complemented the *GL2::GUS* cell-type expression defect of the *45-137* mutant (Fig. 2.1), indicating that the phenotypic defects seen in *45-137* result from the single base change identified in locus At2g47420. As At2g47420 was previously designated *DIM1A* (Richter et al., 2010), from here on out we refer to the *45-137* mutant as *dim1A*.

DIM1A is predicted to encode the nuclear 18S rRNA dimethylase

At2g47420 encodes a putative 18S ribosomal RNA S-adenosyl-L-methionine (SAM)-dependent adenosine dimethylase. A BLAST search revealed two other predicted rRNA dimethylase genes in *Arabidopsis*, encoded by At1g01860 and At5g66360. At1g01860 corresponds to previously characterized *PALEFACE1*, necessary for methylation of plastid rRNA and important for cold tolerance (Tokuhisa *et al.*, 1998). At5g66360, designated as *DIM1B*, was recently shown to be a mitochondrial 18S rRNA dimethylase, with homology to mitochondrial transcription factors B, but with no apparent function as a transcription factor (Richter *et al.*, 2010). A BLASTp search (National Centre for Biotechnology Information (NCBI)) revealed that DIM1A is closely related to two well-studied dimethylases, Dim1p in *S. cerevisiae* and KsgA in *E. coli*. These two enzymes have been shown to carry out a conserved methylation of two adjacent adenosines at the 3' end of 18S/16S rRNA (Lafontaine *et al.*, 1995,

Helser *et al.*, 1972). In addition, yeast Dim1p plays an indirect role in processing of the precursor 35S rRNA at two sites, A_1 and A_2, which are necessary for proper formation of the 18S rRNA species during ribosome biogenesis (Lafontaine *et al.*, 1995). While *Arabidopsis* DIM1A is most similar to the predicted 18S rRNA dimethylases in other plant species (Fig. 2.4), it shares 45.6% and 21.8% amino acid sequence identity (and 59.7% and 31.1% sequence similarity) with yeast Dim1p and *E. coli* KsgA, respectively.

DIM1A is expressed in regions of rapid cell division and development

To investigate the *DIM1A* expression pattern in *Arabidopsis thaliana*, a *DIM1A* promoter β-glucuronidase (*GUS)* fusion construct, *DIM1A::GUS*, was generated and characterized. This construct utilized the same promoter region (Fig. 2.3) shown to complement the *dim1A* mutation when driving expression of the *DIM1A* coding region (Fig. 2.1). *DIM1A::GUS* expression was enriched in the root epidermis and vasculature of two-day-old roots (Fig. 2.5), while in older roots expression was restricted to the vasculature and lateral root primordia (Fig. 2.5b,c). In developing cotyledons and leaves, *DIM1A::GUS* expression was observed in zones of development and cell division at the tip of the leaves as well as in the vascular tissue (Fig. 2.5d, g). *DIM1A::GUS* was expressed throughout floral tissue, particularly in vasculature of petals, anther and pollen (Fig. 2.5e,f). *DIM1A::GUS* expression was also enriched in stem vasculature and the abscission zone at the bottom of siliques (Fig. 2.5e). The RNA accumulation pattern of *DIM1A* reported in the Genevestigator ((Zimmermann *et al.*, 2004);

www.genevestigator.ethz.ch) and the eFP database ((Winter *et al.*, 2007); www.bar.utoronto.ca/efp) indicate that *DIM1A* is expressed in rapidly dividing tissues, largely confirming our expression data. Taken together, this demonstrates that *DIM1A* is expressed in many tissues throughout the plant and enriched in regions of rapid cell division and vascular tissue.

DIM1A is localized in cell nucleus and nucleolus of dividing tissues

DIM1A was expected to be a nucleolar protein based on the known location of rRNA processing as well as what was gleaned from analysis with targeting prediction software (data not shown). To examine the sub-cellular and organism-wide localization of the DIM1A protein in *Arabidopsis*, we constructed a carboxy-terminal GFP fusion of the DIM1A protein, *DIM1A::DIM1A-GFP*. This construct was created using the same 5' genomic fragment used for complementation (Fig. 2.3) with the stop codon and 3' untranslated region removed and replaced with the GFP coding region and a NOS terminator. *DIM1A::DIM1A-GFP* transformed into *dim1A* plants was able to fully complement the *dim1A* mutant phenotypes (Fig. 2.1), suggesting that the DIM1A-GFP fusion protein is functional. Simultaneous imaging using DIC and UV illumination revealed that DIM1A-GFP is localized primarily in nuclei of root cells with little to no enrichment in the cytoplasm (Fig. 2.6a,b). Nuclear fluorescence most strongly localized to a subnuclear region, presumably the nucleolus (Fig. 2.6a,b). As a control, free GFP was imaged and was found to exhibit diffuse fluorescence in the cytoplasm and nucleoplasm of root tissue (Fig. 2.6a). This result is consistent

with work recently published showing that DIM1A-GFP transiently expressed in *Arabidopsis* protoplasts is localized to the nucleolus (Richter *et al.*, 2010). Additionally, it is consistent with work done in yeast showing primarily nucleolar localization of Dim1p (Lafontaine *et al.*, 1998).

At an organ-wide level, DIM1A-GFP was observed throughout developing root tissue in the root tip, and persisted in differentiating cells until just after the beginning of the fast elongation zone (Fig. 2.6c). Interestingly, DIM1A-GFP appears to be more abundant in epidermal cells in the H position than in the N position (Fig 2.6c). Localization in rapidly dividing and differentiating cells of the root meristem supports its importance in root patterning and development.

dim1A lacks a highly conserved small subunit rRNA base modification

The missense mutation in the *dim1A* mutant lies between beta sheet 1 and alpha helix A within the putative N terminal SAM binding domain (O'Farrell *et al.*, 2004, Tu *et al.*, 2009) (Fig. 2.4). Specifically, the mutation disrupts a highly conserved glycine within the canonical SAM binding sequence (Martin and McMillan, 2002), which has been shown in bacterial KsgA to form part of the cofactor binding pocket (Tu *et al.*, 2009). Thus, the *dim1A* may cause a defect in SAM binding by the G66A *dim1A* mutant protein. In support of this, RT-PCR of *DIM1A* from RNA isolated from wild-type and *dim1A* seedlings revealed that the *dim1A* mutation does not significantly affect *DIM1A* transcript abundance (Fig. 2.7). Thus, the *dim1A* mutation does not appear affect *DIM1A* gene expression

but rather may result from reduced catalytic efficiency due to inadequate SAM binding.

Primer extension was used to assess the methylation status of 18S rRNA nucleotides A1785 and A1786 in wild-type and *dim1A*. It has previously been shown that adenosines dimethylated in the N-6 position disrupt base pairing during transcription and prevents reverse transcriptase from extending a DNA oligonucleotide past such a modification (Hagenbuchle *et al.*, 1978). In wild-type, primer extension was inhibited at the rRNA bases A1785 and A1786, indicating that these adenosines possess the N-6 dimethylations (Fig. 2.8). In *dim1A*, the primer extension reaction proceeded beyond A1785 and A1786 and was terminated at U1783 as a result of inclusion of ddATP instead of dATP in the nucleotide mixture to force the reaction to stop at a measurable distance (Fig. 2.8). This indicates that *DIM1A* is necessary for the N-6 dimethylation of adenosines at position 1785 and 1786 at the 3' end of the 18S rRNA and that disruption of a single conserved glycine within the SAM binding domain is sufficient to abolish this methylation.

We evaluated whether the lack of the conserved 18S rRNA dimethyladenosines resulted in a structural defect of fully assembled ribosomes or deficient accumulation of ribosomes by analyzing *dim1A* responses against an array of antibiotics with known ribosomal targeting locations. We observed growth of wild-type and *dim1A* mutant seedlings on plates containing nine different antibiotics and found a moderate resistance to streptomycin, characterized by larger, greener cotyledons and slightly longer and more robust

roots (Fig. 2.9). The lack of general hypersensitivity to antibiotics in *dim1A* suggests that the total number of ribosomes was similar to that in the wild type. The resistance specifically to known small ribosomal subunit target streptomycin (Carter *et al.*, 2000, Poehlsgaard and Douthwaite, 2005) may be a consequence of the absence of the 18S rRNA methylations and therefore and indication of an aberrant population of ribosomes in the *dim1a* mutant.

Processing of precursor 35S rRNA is not disrupted in *dim1a*

In eukaryotic cells, mature 18S, 5.8S and 25S-28S rRNA are formed by coordinated cleavage of an rRNA precursor (35S in yeast and plants, 45S in higher eukaryotes) transcribed from rDNA (Fig. 2.10a). It has been reported that yeast Dim1p is necessary not only for 18S adenosine dimethylation, but also plays an indirect role in 35S rRNA precursor processing at sites A_1, which gives rise to the mature 5' end of the 18S rRNA, and A_2, which separates the 18S precursor from that of the 5.8S and 25S (Lafontaine *et al.*, 1995). The *dim1* mutant accumulates an aberrant 22S species in place of the 18S subunit, resulting in lethality (Lafontaine *et al.*, 1995). As it has been shown in yeast that the dimethylation function of Dim1p can be separated from its role in rRNA processing (Lafontaine *et al.*, 1998), we were interested to know if the *dim1A* mutation affects rRNA processing as well as dimethylation. While little is known about processing of 35S rRNA in *Arabidopsis*, based on the role of Dim1p in yeast, we hypothesize that DIM1A is involved in processing at site A_1 (5' border of 18S; position +1838) and A_2 (ITS1; position +3665) (Zakrzewska-Placzek *et*

al., 2010). An RT-PCR-based assay, using previously designed primers (Huang *et al.*, 2010, Shi *et al.*, 2005) designed to flank the putative processing sites, was performed and we found similar levels of unprocessed 5‘ ETS, at both site P and A_1, as well as ITS1, in wild-type and *dim1A* (Fig. 2.10b). Primers specific for 18S rRNA, which amplify sequences from both processed and unprocessed species, and elongation factor four alpha (EF14a) were used as controls. This result suggests that the *dim1A* mutation affects 18S rRNA dimethylation, but not 35S rRNA processing.

dim1A affects expression of known patterning genes *GL2*, *CPC* and *WER*

Preliminary analysis found that the *dim1A* mutant affects proper position dependent expression, but not expression level, of *GL2::GUS* (Fig. 2.1). To further define the role of the *DIM1A* in root epidermal cell fate specification, we analyzed the effect of the *dim1A* mutant on expression level and cell-type expression location of several transcription factor genes in the specification pathway. The hair-cell-expressing *EGL3::GUS* and the non-hair cell expressing *CPC::GUS* and *WER::GFP* promoter-reporter transgenes were independently introduced into the *dim1A* by crossing. The *EGL3::GUS* expression level did not appear to be significantly altered in *dim1A*, however we observed a reduction in the frequency of H file cells that express *EGL3::GUS* (Fig. 2.11b). This suggests that the cell-position-dependent expression, but not expression level, of *EGL3* requires functional *DIM1A*. Root epidermal cell expression of *CPC::GUS* is reduced significantly in the *dim1A* mutant compared to wild-type, with very faint

GUS visible only upon staining overnight (Fig. 2.11a). *CPC* promoter activity is still visible in the vascular tissue, as seen in wild-type as well, and which has been shown previously to not play a role in epidermal cell fate specification (Koshino-Kimura *et al.*, 2005, Wada *et al.*, 2002). This shows that *DIM1A* is necessary for epidermal cell expression of *CPC*.

In the *dim1A WER::GFP* line, the most striking feature is the similarity of *WER::GFP* expression in H file and N file cells. In the wild-type *WER::GFP* root, especially in the later division zone just before elongation begins, there is a striking difference in *WER::GFP* levels in cells in the N and H file (Fig. 2.11c,d). Quantification of the level of *WER::GFP* expression was undertaken by measuring total pixels in cells in the upper one-third of the root meristem using Leica LAS AF software. The N/H cell ratio of *WER::GFP* in *dim1*A is significantly reduced as compared to wild-type (1.5 vs. 3.2) (Fig. 2.11e). To determine the cause of the reduced N/H *WER::GFP* expression in *dim1A* we compared total pixel sum for each file to wild-type roots. While there is a small decrease in N file *WER::GFP* expression (4.3%) in *dim1A*, the major factor is the almost two-fold increase in *WER::GFP* expression in H file cells. While overall *WER::GFP* expression level is altered in *dim1A*, we did not notice a cell-type *WER::GFP* patterning defect (*i.e*. N position cells expressing *WER::GFP* at levels comparable to expression in H position cells and H position cells with *WER::GFP* expressed at N position cell levels). Together, these results suggest that *DIM1A* is important establishing or maintaining a high N/H ratio of *WER* expression.

Genetic interaction of *dim1A* with epidermal patterning mutants

The results described above suggest that *DIM1A* may play a role in specifying the hair cell fate through maintenance of epidermal *CPC* expression and restriction of *WER* expression to cells in the N position. To further investigate the role of *DIM1A* in epidermal cell fate specification we introduced the *dim1A* mutation into the *wer-1*, *scm-2*, *gl2*, *ttg1* single mutant and *egl3 gl3* double mutant backgrounds, in the presence of the *GL2::GUS* reporter, to investigate possible genetic interactions.

WER has previously been shown to be necessary for non-hair cell fate as well as *GL2* expression (Lee and Schiefelbein, 1999). *GL2::GUS* expression is nearly completely abolished in the *wer-1* mutant background (Lee and Schiefelbein, 1999, 2002) and is limited to a variable number of H or N position cells in the upper meristem. The *wer-1 dim1A* double mutant possessed a significant increase in *GL2::GUS* expression compared to the *wer-1* mutant alone (Fig. 2.12a). While 75% of wild-type roots (n=44) compared to only 4% of *wer-1 dim1A* roots (n=83) completely lacked *GL2::GUS* expressing cells, 16% of wild-type compared to 24% of *wer-1 dim1A* show between one and four *GL2::GUS* expressing cells and 9% of wild-type compared to 72% of *wer-1 dim1A* roots show more than five *GL2::GUS* expressing cells. Since *GL2* is expressed in cells that adopt the non-hair fate, we examined the root epidermal cell types to see if the increase in *GL2* promoter activity in the root meristem translated to change in frequency of root hairs. We found that, compared to *wer-1* in which 94.5% of epidermal cells develop root hairs, there was a statistically significant decrease in

hair cells in the *wer-1 dim1A* double mutant with only 83.5% of epidermal cells being specified as root hair cells (Table 2.1). Hair cell specification in the H position was similar in *wer-1* and *wer-1 dim1A*, with 96.5% and 94.5% of H file cells possessing root hairs, respectively. However, while 92.5% of N position cells develop root hairs in *wer-1* only 72.6% of N position cells become hair cells in *wer-1 dim1A*.

While *dim1A* was able to restore some *GL2::GUS* expression in the *wer-1* double mutant background, *dim1A* did not alter the *ttg1* and *gl3 egl3 GL2::GUS* expression phenotypes. Consistent with prior reports, we observed that *ttg1* and *gl3 egl3* have significantly reduced root epidermal cell *GL2::GUS* expression (Bernhardt *et al.*, 2003, Galway *et al.*, 1994). The *ttg1* and *gl3 egl3 GL2::GUS* expression patterns did not deviate from the single mutant phenotypes when the *dim1A* mutation was present in their respective backgrounds (Fig. 2.12a), suggesting that *TTG1* and *GL3/EGL3* are essential for any *GL2* expression in the *dim1A* mutant. Additionally, it appears that *GL2* is not involved with *DIM1A* in epidermal patterning as the *dim1A gl2* double mutant exhibits the same *GL2::GUS* cell-type expression pattern as the *dim1A* single mutant (Fig. 2.12a)

The SCM LRR-RLK is required for proper position-dependent cell-type patterning, evident in loss-of-function mutations in *SCM* which exhibit a disconnect between epidermal cell-type specification and patterning gene expression (Kwak and Schiefelbein, 2007, Kwak *et al.*, 2005). Interestingly, introducing *dim1A* into the *scm-2* mutant background partially rescued the *scm-2* epidermal cell-type patterning phenotype (Fig. 2.12a,b). While the double mutant

showed a slight reduction in *GL2::GUS* expressing cells in H file, from 40.6% in *scm-2* to 32.2% in *scm-2 dim1A*, the most significant difference was in *GL2::GUS* lacking N file cells, with 30.6% in *scm-2* compared to only 9.2% in *scm-2 dim1A* double mutant (Fig. 2.12b). Altogether, these genetic experiments suggest that the *dim1A* mutation promotes the non-hair specification pathway.

"Hair genes" are preferentially downregulated in the *dim1A* mutant

To obtain information about the importance of *DIM1A* for transcription, we performed microarray analysis by using root epidermal RNA from wild-type and *dim1A* mutants and the Affymetrix ATH1 chip. We identified 975 genes that were differentially expressed by at least two-fold (P value <0.1). According to the Gene Ontology (GO) enrichment analysis, the categories of genes that were most affected in the *dim1A* mutant were those involved in catalytic activity and cation binding. In addition, the biological processes most affected were response to different stimuli and stresses, including chemical stimuli, oxidative stress, endogenous stimuli and hormone stimuli.

To better understand the effect of *dim1A* on transcription of genes involved in epidermal cell-type patterning we compared the 975 genes differentially expressed in the *dim1A* mutant to a list of 208 "root epidermal patterning" genes identified by our lab through extensive transcriptome analysis (J. Schiefelbein, unpublished). Interestingly, *dim1A* affects transcription of 39 of the 154 genes "hair genes." Out of these 39 "hair genes", 90% (35/39) were downregulated and 10% (4/39) were upregulated in the *dim1A* mutant (Table

2.2). This supports our earlier suggesting that the *dim1A* mutation promotes the non-hair specification pathway.

While only a handful of ribosomal protein ribosomal assembly genes were part of the 975 genes differentially expressed in *dim1A*, an interesting factor that did show up on the list was *AtNUC-L2*. The *Arabidopsis* genome contains two nucleolin genes, *AtNUC-L1/PAR1* and *AtNUC-L2* (Kojima *et al.*, 2007, Pontvianne *et al.*, 2007). Under normal conditions *AtNUC-L2* is not expressed, however it is upregulated in and can partially rescue the *atnuc-L1* mutant (Pontvianne *et al.*, 2007). Our microarray data shows *AtNUC-L2* to be upregulated by 13.5 fold (albeit not statistically significantly; P =0.26) in the *dim1A* mutant background, while expression of the primary nucleolin is slightly downregulated (-1.28 fold, P=0.20). Interestingly, a similar result was reported in the mutant of *APUM23*, which encodes a pumilio-protein involved in ribosome biogenesis, in which *AtNUC-L2* transcription was significantly up-regulated (120-fold as measured by microarray analysis, 20-fold measured by RT-PCR) (Abbasi *et al.*, 2010).

Overexpression of *DIM1A* or G66E-*dim1A* does not significantly affect epidermal patterning

Research in *E.coli* has demonstrated that excess cellular concentration of wild-type KsgA or the catalytically inactive E66A *ksgA* mutant inhibits translation initiation (Connolly *et al.*, 2008). These and other results led Connolly et al (2008) to hypothesize that methylation is required for KsgA to be released from

the small subunit rRNA (Connolly *et al.*, 2008). Interestingly, this result contradicts what was observed in yeast, where the growth of the catalytically inactive E85A *dim1* mutant does not differ from wild-type (Pulicherla *et al.*, 2009). In order to investigate the effect of *DIM1A* overexpression and the potential deleterious effect of the methylation-dead G66E *dim1A* mutant, we constructed a carboxy-terminal GFP fusion of the DIM1A protein driven by the constitutive CaMV35S promoter. A genomic fragment (Fig. 2.3) was amplified from both wild-type and the *dim1A* mutant and inserted between the 35S promoter and *GFP* to create *35S::DIM1A-GFP* and 35S::dim1A-GFP. Each construct was transformed into both wild-type and *dim1A* plants and multiple homozygous lines were analyzed. In the *dim1A* mutant background, overexpressing the mutant G66E *dim1A* did not alter epidermal patterning, while overexpressing the wild-type DIM1A essentially complemented the *dim1A* mutant phenotype (Fig . 2.13). In the wild-type background, overexpressing either the wild-type or G66E *dim1A* mutant *DIM1A* gene did not significantly affect epidermal patterning (Fig. 2.13) or overall plant growth and development (data not shown). Overall, the results from our overexpression experiment suggest that, in plants, overabundance of DIM1A protein does not affect epidermal patterning or meristem development. Also, unlike *E. coli* where the addition of catalytically inactive KsgA into wild-type cells negatively affects growth, in *Arabidopsis*, catalytically inactive G66E *dim1A* did not affect root meristem cell-type patterning or growth.

The role of *DIM1A* in root cell division and growth

Initial observations revealed that the roots of *dim1A* seedlings were shorter than observed in wild-type (Fig. 2.14a). Measurements of root length revealed that *dim1A* root growth rate is reduced by 50% on average during the first four days of growth after germination (Fig. 2.14b). Root length is determined by the rate of cell division and the final cell size (reviewed in Ivanov *et al.*, 2002), therefore we investigated the cellular basis for this reduction in root growth rate. Detailed measurements did not reveal a difference in the length of wild-type and *dim1A* mature hair and non-hair epidermal cells (Fig 2.14c). Thus, we concluded that reduced cell production, rather than reduced cell size, is the cause of the reduced root length and growth rate of the *dim1A* mutant.

To determine the cause of reduced cell production, we examined characteristics of *dim1A* and wild-type root meristems. For this analysis, we defined the meristem as the region of the root tip containing actively dividing cells (Division Zone (DZ) and Slow Elongation Zone (SEZ)), before they enter a zone of rapid elongation without division (the Fast Elongation Zone (FEZ)) (Fig. 2.15a). The meristem size/height was measured from the first cortical cell visible at the base of the root up to the last cell before the FEZ. The *dim1A* mutant exhibited a slight reduction in overall meristem size, to 77.6% of wild-type meristem height (Fig. 2.15b), however the most noticeable phenotype was the reduction in number of meristematic cells. Meristem cell number was determined by counting the number of cortical cells as well as N position and H position epidermal cells (as determined by cell position relative to the underlying anticlinal cortical cell wall) in single cell file in the meristem. Compared to wild-type roots, we

observed a reduction of 60.5% of H file cells, 67.9% of N file cells and 49.9% of cortical cells (Fig. 2.15b). Interestingly, the cell types observed were much larger in size; we calculated a ~155% increase in cortical cell size compared to wild-type (Fig. 2.15b), a fact that appears to explain the discrepancy between the cell number and meristem size reductions.

It is known that in wild-type root meristems H files contain more cells than N files (Berger *et al.*, 1998). The H/N cell ratio, ~1.3 in wild-type roots, is a marker of relative fate specification between cells in H files and those in N files and is reduced in mutants affecting early fate specification, such as *ttg*, *we*r and *gl3 egl3* (Berger *et al.*, 1998, Bernhardt *et al.*, 2003, Galway *et al.*, 1994, Lee and Schiefelbein, 1999) but not *gl2*, which is involved in later aspects of fate specification (Massucci *et al.*, 1996). The H/N ratio is significantly reduced in *dim1A* to 1.21 compared to our measured wild-type (WS) value of 1.35 (Fig. 2.16a) suggesting that *DIM1A* is needed to specify the earlier aspects of fate specification and position-dependent pattern formation.

Epidermal clones arise from rare longitudinal divisions of root epidermal cells followed by additional transverse divisions (Fig. 2.16b) (Berger *et al.*, 1998). The rare longitudinal division may occur at any point within the division zone of the meristem and the number of resulting cells in each file is a consequence of the rounds of cell division that occur before division ceases upon entering the elongation zone. Thus, by examining the number of cells in epidermal clones in wild-type and *dim1A* roots, we can assess the relative rate of cell division within the meristem. More than 100 clones derived from developing hair cells of wild-

type and *dim1A* lines were examined and classified based on the maximum number of cells in the H position according to (Berger *et al.*, 1998). For example a class-two clone (two divisions) will have two cells, while a class-four clone (four divisions) will have between five and eight cells. Epidermal clone class distribution is significantly different in wild-type and *dim1A* roots. Wild-type root meristems contain mainly class five clones (44.1%), while *dim1A* roots contain mostly class three clones (29.6%). Interestingly, while 18.9% of wild-type clones were class six, we only observed a single class-six clone in *dim1A* roots. Also to note, *dim1A* contains significantly fewer epidermal clones; 40.8% of total files observed in *dim1A* roots contained epidermal clones compared to 79.9% in wild-type. Overall these results support the view that cell division is reduced in the *dim1A* root meristem.

To determine if there was a connection between the reduced cell division rate and epidermal cell-type patterning we observed the *GL2::GUS* expression pattern of wild-type roots exposed to treatment conditions that caused decreased epidermal cell number comparable to the *dim1A* mutant. We identified five different treatment conditions that reduced wild-type epidermal cell number to an extent similar to that of the *dim1A* mutant (Fig. 2.17a), however none of these conditions caused a significant effect on the *GL2::GUS* expression pattern (Fig. 2.17b,c). This result suggests that the epidermal cell-type patterning defect in the *dim1A* mutant is not connected to the defect in meristem cell division rate and cell size.

The role of *DIM1A* in leaf development and epidermal cell-type specification

Morphological defects associated with *dim1A* were also observed in plant organs and tissues other than the root. The *dim1A* shows a pointed-leaf phenotype (pfl) (Fig. 2.18a) characteristic of *Arabidopsis* ribosomal protein mutants including *rpl4a*, *rps13a/pfl2*, *rps18a/pfl1*, *rps23a* (Rosado *et al.*, 2010, van Lijsebettens *et al.*, 1994, Ito *et al.*, 2000, Degenhardt and Bonham-Smith, 2008) and other ribosome assembly factor mutants *nuc-l1/par1* (Kojima *et al.*, 2007, Petricka and Nelson, 2007, Pontvianne *et al.*, 2007), *oligocellula 2 (oli 2)* (Fujikura *et al.*, 2009) and *apum23-1* (Abbasi *et al.*, 2010). Leaves in the *dim1A* mutant were also reduced in size; the first set of true leaves in *dim1A* were 47% and the second 61% of the size of wild-type first and second set of true leaves, respectively (Fig. 2.18b). Additionally, defects in cotyledon venation and additional true leaf defects were observed in *dim1A*. In wild-type cotyledons, a primary midvein forms and is followed by secondary veins, which are connected relatively symmetrically to the midvein (Fig. 2.18c). Most of the *dim1A* cotyledons observed had unsymmetrical secondary veins, many ending erratically without connecting back to the midvein (Fig. 2.18c). In true leaves, reduced higher order tertiary and quaternary veins were observed (Fig. 2.18c). These defects suggest *DIM1A* influences plant growth and patterning in organs in addition to the root.

As the *dim1A* phenotypic defects resemble those seen in characterized ribosomal protein and ribosome biogenesis gene mutants, we also looked briefly at leaf cell size and shape and size as well as stomatal development, as

ribosomal protein mutants *rpl4a*, *rps13a/pfl2*, *oli5* and *oli7* (Fujikura *et al.*, 2009, Ito *et al.*, 2000, Rosado *et al.*, 2010) were found to have defects in these processes. Interestingly, we did not observe a noticeable difference in abaxial or adaxial (not shown) leaf cell characteristics or stomatal patterning and development (Fig. 2.19a). Thus, some but not all phenotypes of characterized ribosomal protein and ribosome biogenesis mutants overlap with the phenotypic defects seen in *dim1A*.

We did, however, observe a reduction in higher-order trichome branching in the *dim1A* mutant (Fig. 2.19b). Compared to wild-type where 35.9% of trichomes on first true leaves and 59.9% of trichomes on second true leaves contained three branches, the dim1A had only 12.1% and 21.4% three-branched trichomes, respectively. These results indicate that functional *DIM1A* may be essential for normal trichome development.

Discussion

This work explored the function of *Arabidopsis* DIM1A, a highly conserved ribosome biogenesis factor, and its connection to the development and patterning of the root epidermis. The *DIM1A* gene was identified in a genetic screen for mutants affecting position-dependent expression of root epidermal non-hair fate regulator *GLABRA2*. Further investigation revealed a role for *DIM1A* in *CAPRICE* gene expression and restricting *WEREWOLF* expression to non-hair cells. In addition, *DIM1A* is generally important for adequate root cell

division, leaf development and trichome branching. The *DIM1A* gene encodes a nucleolar protein which our data suggests is necessary for the methylation of the adenosines at position 1785 and 1786 in the 3' terminal loop of 18S ribosomal RNA. We propose that DIM1A, and the post-transcriptional rRNA modification it catalyzes, are important for root epidermal cell-type patterning, root cell division control, leaf development and trichome branching. Our work is not only the first examination of the connection between ribosome biogenesis and root epidermal patterning, but it is also the first analysis of the role of the conserved small subunit rRNA adenosine methylations in nuclear ribosomes of a multicellular organism.

The *dim1A* mutation affects epidermal cell fate specification

Analysis of cell-fate specification in five-day-old seedlings revealed that one of the major effects of the *dim1A* mutant is a decrease in root-hair cells compared, due to an increase in non-hair cells specified in the H position (Table 2.1). This suggests that *DIM1A* is normally involved in ensuring cells in the H position are specified as root-hair cells. In support of this, analysis of *GL2::GUS* expression in the root meristem of *dim1A* seedlings revealed a significant increase in *GL2::GUS*-expressing cells in the H position. *GL2* expression in epidermal cells in the H position is known to result in differentiation as a non-hair cell despite position relative to the underlying anticlinal cortical cell wall (Lee and Schiefelbein, 2002, Wada *et al.*, 2002). Therefore, ectopic *GL2* expression in H position cells is the likely cause of the decrease in specification of hair cells in the

dim1A mutant.

The current model of cell fate specification in the root epidermis suggests that *GL2* is the target of an upstream molecular network involved in generating cell-type specific patterns of gene expression necessary to generate distinct hair and non-hair cells (Lee and Schiefelbein, 2002, Pesch and Hulskamp, 2004, Schellmann *et al.*, 2007, Schiefelbein *et al.*, 2009, Ueda *et al.*, 2005). To uncover the reason for increased non-hair/*GL2*::GUS-expressing cells we analyzed the effect of *dim1A* on upstream patterning genes.

Formation of two distinct cell types in the *Arabidopsis* root epidermis has been shown to rely heavily on the balance between expression of R2R3 MYB-domain proteins (WER and MYB23) and R3 MYB-domain proteins (CPC, TRY and ETC1) (Lee and Schiefelbein, 1999, 2002). *WER* is needed to specify the non-hair cell fate and *CPC* is needed to specify the hair cell fate, however there is abundant root hair production in the *wer* mutant, which lacks *CPC* expression (Lee and Schiefelbein, 1999, 2002, Wada *et al.*, 1997). This result, together with other findings, suggests that in wild-type roots, *CPC* (and *TRY* and *ETC1*) promote the hair cell fate in H position cells by preventing WER-directed non-hair cell specification (Lee and Schiefelbein, 2002, Simon *et al.*, 2007, Wada *et al.*, 2002). The *dim1A* mutation reduces the N cell to H cell ratio of *WER* gene expression from 3.2 in wild-type to 1.5 (Fig 2.11c-e) and causes deficient epidermal *CPC* gene expression (Fig. 2.11a). Together, this may disrupt the balance between protein levels of WER and CPC and cause the *dim1A*-patterning defect. Current research suggests that CPC inhibits WER action in H

position cells by competing for binding to TTG1-GL3/EGL3 and subsequent formation of the core transcriptional activation complex (Lee and Schiefelbein, 2002, Tominaga *et al.*, 2007). In N position cells the core complex (TTG1-GL3/EGL3-WER) is able to promote expression of *GL2*, while the inactive complex (TTG1-GL3/EGL3-CPC) cannot do so (Lee and Schiefelbein, 2002, Wada *et al.*, 2002). Therefore, we hypothesize that the increase in *GL2::GUS*-expressing cells in H position cells results from a relatively high level of WER in the H position, which reduces the ability of CPC to compete with WER for binding to TTG-GL3/EGL3 and increases the likelihood of the functional core transcriptional complex in H position cells.

However, the above hypothesis does not account for the small increase in N position cells lacking *GL2::GUS* expression seen in *dim1A* roots. We suggest that, due to the plethora of feedback loops in the root epidermal patterning network (Bernhardt *et al.*, 2005, Kwak and Schiefelbein, 2008, Wada *et al.*, 2002), having a functional transcriptional activation complex (TTG-GL3/EGL3-WER) in some H position cells generates CPC lateral inhibition directed against the N cells, which confuses the system and results in the small number of N position cells lacking *GL2::GUS* expression and developing as hair cells. In support of this hypothesis, expression of *WER* equally in N and H position cells in a *wer* mutant results in a scrambled pattern of *GL2::GUS* expression, with *GL2::GUS*-expressing and non-expressing cells found in both N position and H position cells (Lee and Schiefelbein, 2002, Ryu *et al.*, 2005). Additionally, the LRR-receptor like kinase SCRAMBLED is thought to translate positional

information to epidermal cells by down-regulating expression of *WER* in H position cells (Kwak and Schiefelbein, 2008). Prior research clearly demonstrates the importance of the regulation of WER gene expression in the two cell positions. Thus, during root epidermal cell-type patterning, *DIM1A* might be involved restricting *WER* expression to cells in the N-position.

In addition to investigating the effect of *dim1A* on the expression of patterning genes, we set out to determine if there was a genetic interaction between *dim1A* and the patterning mutants *wer*, *ttg1*, *gl3 egl3*, *gl2* and *scm-2*. We observed that the *dim1A* mutation partially rescues the hairy-root phenotype of the *wer* mutation (Table 2.1). WER has been shown to activate *GL2* gene expression by binding to two MYB-binding domains in the *GL2* promoter (Koshino-Kimura *et al.*, 2005, Ryu *et al.*, 2005) and lack of functional *WER* results in almost complete absence of *GL2* promoter activity (Lee and Schiefelbein, 1999). Unexpectedly, the addition of the *dim1A* mutation to the *wer* background resulted in increase in *GL2::GUS*-expressing cells and non-hair cell specification (Fig. 2.12a; Table 2.1). Interestingly, a similar phenomena is seen when you add the *cpc* or *cpc* and *try* mutations into the *wer GL2::GUS* background (Lee and Schiefelbein, 2002, Simon *et al.*, 2007). As mentioned previously, CPC down regulates *GL2* expression by competing with WER for binding to TTG-GL3/EGL3 (reviewed in Schiefelbein *et al.*, 2009). This is evident in the *cpc* mutant, where *GL2* promoter activity is extended beyond N position cells to also include cells in the H position (Lee and Schiefelbein, 2002, Wada *et al.*, 2002). Increased GL2::GUS-expressing cells in the *wer cpc* and *wer cpc try*

mutants may indicate an alternative pathway involved in *GL2* gene regulation that is differentially regulated in the absence of *CPC* and *TRY*. Since *CPC* expression is down regulated in the *dim1A* mutant (Fig. 2.12a), this putative pathway may be affected similarly as in the *wer cpc* and *wer cpc try* mutants.

Furthermore, we found that addition of *dim1A* affected the *scm-2* pattern of *GL2::GUS* expression (Fig. 2.12a,b). Compared to the *scm-2* single mutant, the *dim1A scm-2* double mutant had slightly fewer *GL2::GUS*-expressing cells in the H position and significantly fewer non-*GL2::GUS*-expressing cells in the N position (Fig. 2.12a,b). Together, the net effect of introducing the *dim1A* mutation into the *scm-2* background is an increase in *GL2::GUS* expressing cells. Since *GL2* promotes specification of the non-hair fate, it is likely that the *scm-2 dim1A* double mutant would have fewer hairs than the *scm-2* single mutant, however this was not determined in the present study.

Altogether, increased *GL2::GUS* expression in the *dim1A* single mutant as well as the *dim1A wer* and *dim1A scm-2* double mutants, suggests that the role of *DIM1A* is preventing *GL2* expression and subsequent adoption of the non-hair cell fate. By comparing specification of cell fates in *dim1A* single mutant and *wer dim1A* double mutant backgrounds (Table 2.1) we can conclude that the increase in non-hair cells in the H position seen in the *dim1A* single mutant is WER-dependent. While about 20% of H position cells adopt the non-hair fate in *dim1A* roots (compared to 5% in wild-type), only about 5% of H position cells become non-hair cells in the *dim1A wer* double mutant. This further supports our hypothesis suggesting that the *dim1A*-patterning defect results from increased

WER in developing cells in the H position.

In conclusion, the *dim1A* G66E putative methylation-dead mutation appears to affect root epidermal patterning by disrupting establishment of distinct gene expression patterns in developing root-hair and non-hair cells. Specifically, the *dim1A* mutation disrupts the tightly regulated cell-type-specific expression of *WER,* resulting in a disruption of position-dependent cell fate specification in the root epidermis. Previous genetic analysis of *Arabidopsis* root epidermis has revealed the importance of generating cell-type specific gene expression patterns in establishing two distinct cell types. While further analysis is necessary to uncover the exact mechanism of *dim1A*s effect on epidermal cell fate specification, the current analysis strengthens the notion of the importance of precise regulation of gene regulatory networks in developing two distinct cell types.

Arabidopsis **ribosome biogenesis and** ***DIM1A***

Processing of the RNA product of rDNA transcription involves a large collection of non-ribosomal factors collectively referred to as the 90S pre-ribosome complex (Dragon *et al.*, 2002, Fatica and Tollervey, 2002, Venema and Tollervey, 1999). *Arabidopsis* DIM1A is homologous to a family of highly conserved small ribosomal subunit rRNA adenosine methylases, referred to as the KsgA/Dim1 family (O'Farrell *et al.*, 2008). The KsgA/Dim1 family of methylases catalyzes the almost universally conserved dimethylation at the N-6 position of two adjacent adenosines in the small subunit rRNA (Helser *et al.*,

1972, Lafontaine *et al.*, 1994, Van Knippenberg *et al.*, 1984). The *Arabidopsis* genome encodes three KsgA/Dim1 homologs, DIM1A, DIM1B and PFC1. DIM1B and PFC1 are essential for dimethylation of mitochondrial 18S and plastidial 16S rRNA, respectively (Richter *et al.*, 2010, Tokuhisa *et al.*, 1998), while our data supports the role of DIM1A in modification of nuclear 18S rRNA. The ability of reverse transcriptase to extend a primer specific to the 3' end of the small subunit rRNA by using an RNA template from *dim1A* mutants but not from wild-type plants indicates that the *dim1A* mutation disrupts rRNA methylation activity. Dim1 in yeast and potentially KsgA in bacteria have two functions - rRNA methylation and pre-rRNA processing (Connolly *et al.*, 2008, Lafontaine *et al.*, 1995). Results from our primer extension experiment (Fig. 2.8) and RT-PCR rRNA processing assay (Fig. 2.19) suggest that the *dim1A* G66E mutant is likely only deficient in rRNA methylation.

A similar catalytically inactive methylase mutant was identified in *E. coli* and found to result in severe growth defects when expressed in wild-type cells. Interestingly, lack of the 16S dimethyladenosines in the *ksgA* mutant only mildly affects organism fitness (Helser *et al.*, 1972, O'Connor *et al.*, 1997, Poldermans *et al.*, 1979a, Poldermans *et al.*, 1979b, Poldermans *et al.*, 1979c). This suggests that the KsgA enzyme and the dimethyladenosines are not essential for ribosome function, but that in the case where the enzyme is present, methylation activity is crucial for ribosome biogenesis. Interestingly, two independent methylation-dead alleles of yeast DIM1 were reported to result in mild (*dim1-2*) (Lafontaine *et al.*, 1998) or no (*dim1* E85A) (Pulicherla *et al.*, 2009) growth

defects. The mild growth defects in *dim1-2* have been suggested to result from additional mutations in the *DIM1* gene (six in total), suggesting that catalytically inactive Dim1p does not affect yeast growth (Pulicherla *et al.*, 2009). Results presented here suggest that the *dim1A* phenotype is due to the presence of a catalytically inactive DIM1A protein and subsequent lack of the highly conserved rRNA dimethyladenosines. In addition, by expressing the catalytically inactive *dim1a* in the wild-type background my results suggest that, unlike in *E. coli* and similar to yeast, methylation may not be required for ribosome biogenesis (Fig. 2.13). Connolly and colleagues speculated that the severe ribosome biogenesis and growth defects observed upon overexpression of catalytically inactive *ksgA* was due to the dimethylase enzyme remaining bound to the ribosomal small subunit and preventing mature ribosome formation. Structural analysis in *E. coli* has shown that KsgA binds to the decoding center of the ribosome, preventing initiation factor 3 (IF-3) from binding and likely preventing translation initiation (Xu *et al.*, 2008). Therefore, we conclude that due to the limited effects of *dim1A* on overall translation and plant growth, it is unlikely that the catalytically inactive DIM1A encoded by the dim1A allele remains bound to rRNA.

Additionally, we found the *dim1A* mutation to confer partial resistance to streptomycin. Although most antibiotics target organellar ribosomes in eukaryotic cells, streptomycin has been shown to target cytoplasmic ribosomes in *Chlamydomonas reinhardtii* (Boschetti and Bogdanov, 1973). This and other work suggests that cytoplasmic ribosomes, while far less sensitive to antibiotics, are not resistant to their effects. Recently, mutations in large subunit ribosomal

protein 4 (RPL4) (Rosado *et al.*, 2010) and ribosomal rRNA processing factor APUM23 (Abbasi *et al.*, 2010), were reported to confer mild resistance to streptomycin. Partial resistance in the *rpl4* mutant may result from structural changes to the ribosome which preventing streptomycin from binding efficiently (Apirion and Saltzman, 1974, Gabashvili *et al.*, 2001, Rosado *et al.*, 2010). The mechanism of streptomycin resistance in the *apum23-1* mutant remains unknown, but is thought to result from an aberrant ribosome population resulting from imbalanced ribosomal protein accumulation or misprocessed rRNA species (Abbasi *et al.*, 2010). Analysis of the crystal structure of *E. coli* and *T. thermophilus* ribosomal small subunits suggest that KsgA binds to and methylates the 16S rRNA near the decoding region of the ribosome (Demirci *et al.*, 2010, Schluenzen *et al.*, 2006, Xu *et al.*, 2008), the same region where streptomycin is known to bind (Poehlsgaard and Douthwaite, 2005). Additionally, crystal structure of the small subunit (30S) RNA from *Thermus thermophilus* lacking the two dimethylations showed significant conformation change in the ribosome structure (Demirci *et al.*, 2010). Thus, we postulate that the partial streptomycin resistance of *dim1A* mutant seedlings may result from a conformational change in the structure of the ribosome resulting from the lack of the 18S adenosine dimethylations.

The *Arabidopsis* DIM1A protein is predominantly localized to the nucleus and is enriched in a subnuclear structure presumed to be the nucleolus. This is consistent with localization of Dim1p in yeast (Lafontaine *et al.*, 1998), hsDim1 in humans (Ahmad *et al.*, 2009) and DIM1A in *Arabidopsis* protoplasts (Richter *et*

al., 2010). Interestingly, eukaryotic Dim1p has been implicated in both pre-rRNA processing and methylation (Lafontaine *et al.*, 1995, Pulicherla *et al.*, 2009). Studies from yeast suggest that the final methylation of the 20S pre-rRNA as well as its final processing into the 18S mature rRNA both occur in the cytoplasm of eukaryotic cells (Udem and Warner, 1973). Interestingly, localization of in both Dim1p in yeast (Lafontaine *et al.*, 1998) and DIM1A in plants (our study) is limited to the nucleus with nucleolar enrichment. This suggests either the predicted site of processing has been incorrectly identified, or possibly that methylation occurs immediately following 20S pre-rRNA translocation to the cytoplasm and that the Dim1p/DIM1A proteins are rapidly transported back to the nucleolus.

The role of conserved dimethylations during plant development.

We found that *DIM1A* is expressed throughout the plant in regions of rapid cell division as well as in vascular tissue. This expression pattern is largely consistent with the that of other ribosomal proteins, including *RPL24b/STV1* (Nishimura *et al.*, 2005), *RPL4A*, (Rosado *et al.*, 2010) and ribosome biogenesis factor *atNUC-L1/PAR1* (Petricka and Nelson, 2007). Consistent with a role in cell division, the *dim1A* mutation results in reduced root cell division and leaf shape, size and vascular patterning defects. The absence of a defect in cotyledon length (data not shown), an organ shown to rely solely on elongation rather than division for growth (Gendreau *et al.*, 1997), further supports the role of *DIM1A* in cell division.

Maintaining cell size homeostasis during proliferation requires balance

between cell growth and division. In the root meristem, all of the cells are actively dividing (Beemster and Baskin, 1998, Ivanov *et al.*, 2002). If some cells were not dividing, they would be larger than their neighbors due to the fact that these cells grow symplastically. Therefore, meristem cell length depends on elongation rate and cell division. Upon exit from the meristem, root cells cease dividing and rapidly elongate in the direction of root growth until they reach their mature size. Thus, final root length reflects the balance between meristem cell production and cell elongation. In the *dim1A* mutant, root length and growth rate were significantly reduced (Fig. 2.14). However, we did not detect a measurable difference in the size of mature epidermal cells (Fig. 2.14c). This suggested that meristem cell production, not cell elongation, may cause the root growth defect, prompting us to further investigate the meristem cell characteristics. Previously, mutations in ribosomal protein and ribosome assembly factor genes have also been shown to affect root length. Mutations in *SWA1*, RPL24b/*STV1*, *RID2*, *RPS6a* and *RPS6b* all have reduced root length, even though mature epidermal cells in the *stv1*, *rps6a* and *rps6b* mutants, were observed to be the same length as wild-type (Creff *et al.*, 2010, Nishimura *et al.*, 2005, Ohbayashi *et al.*, 2011). Careful measurements of meristem size, cell size and cell division rate confirmed that cell production is deficient in the meristem of *dim1A* mutants (Fig. 2.15). Creff et al (2010) measured the cell index in *rps6*a and *rps6b* mutant backgrounds and found that, similar to *dim1A*, the meristem of *rps6a* and *rps6b* contained about half the number of cells as in wild-type. This suggests the possibility of a common mechanism for ribosome biogenesis in maintenance of

root meristem cell division rate. It will be interesting to determine if reduced meristem cell production is responsible for the short-root phenotype observed in the *swa1*, *stv1* and *rid2* mutants.

Interestingly, a study in mammals linked ribosome protein accumulation to cell cycle progression. Depletion of the RPS6 homolog in mice liver revealed that the rate of ribosome production is sensed and regulates cell cycle progression (Volarevic *et al.*, 2000). In this study, liver cells were still able to grow and protein synthesis was apparently not affected, however cell division was inhibited and accompanied by a specific reduction in cyclin E mRNA (Volarevic *et al.*, 2000). Thus, it is tempting to speculate that the reduced root length phenotype of *dim1A* and the other ribosomal protein and ribosomal assembly factor mutants may result from root meristem cells sensing a defect in the rate of ribosome biogenesis and thus slowing cell cycle progression. An interesting possible connection between DIM1A and cell cycle progression came out of a recent genome-wide search for targets of the retinoblastoma (RB)/E2F/DP pathway. In this study, *DIM1A* was identified as being a bona fide target of the E2F transcription factor (Ramirez-Parra *et al.*, 2003). In higher eukaryotes, the RB/E2F/DP pathway is crucial because E2F/DP transcription factors regulate the expression of genes required for G1/S transition and S-phase progression (Trimarchi and Lees, 2002). Therefore, it is possible that *DIM1A* expression may specifically up-regulated during cell division.

In addition to defects in root cell division and patterning, we observed leaf development defects in the *dim1A* mutant, many of which are common to

ribosomal protein and biogenesis factor mutants. Leaf shape results from the coordination of cell growth and differentiation. To date, twelve of the seventeen ribosomal protein mutants that have been examined display altered leaf shape, in particular the "pointed first leaf (pfl)" phenotype (Creff *et al.*, 2010). Many ribosomal protein and biogenesis factor mutants show defects in vascular patterning (Byrne, 2009), which have often been attributed to defects in auxin signaling (Degenhardt and Bonham-Smith, 2008, Petricka and Nelson, 2007, Rosado *et al.*, 2010). Vascular development in wild-type cotyledons is highly reproducible, resulting in a recognizable pattern (Berleth *et al.*, 2000 and references within). Petricka and Nelson (2007) suggested that the pointed-leaf and disrupted leaf venation phenotypes result from a lack of marginal auxin sources or response factors. Subsequently, decreased lateral expansion of the leaf and reduced vasculature result from reduced auxin-mediated cell division at leaf margins. In support of this notion, Weijers et al (2001) observed the vascular patterning defect in the *rps5a* mutant to result from a defect in cell division rather than differentiation of the vascular tissue. While further analysis is needed to determine the exact mechanism of ribosome protein and biogenesis factor involvement, it is clear that these components are needed for proper leaf development.

The overlapping phenotype of *dim1A* and characterized ribosomal protein and ribosome biogenesis mutants in *Arabidopsis* supports the role of the dimethylation in ribosome biogenesis and/or function, and our hypothesis that lack of the two dimethylations results an aberrant ribosome population. While

crystal structure analysis has shown that the two small subunit rRNA adenosine dimethylations are essential for optimal conformation for translation, we cannot conclude for sure that this structural change also occurs in the *Arabidopsis* ribosome. In addition, we cannot say for sure that the lack of these methylations alone causes the developmental defects observed in the *dim1A* mutant background. It remains a possibility that lack of the methylations disrupts binding of a ribosomal protein, and that depletion of this protein from the mature ribosome affects it's function and results in the *dim1A* mutant phenotypes. However, the position 1785 and 1786 dimethylations occur at helix 45 of the 18S rRNA which, like many other heavily-modified rRNA regions, are found in the interior of the ribosome which is devoid of ribosomal proteins (Decatur and Fournier, 2002). Thus, it seems more likely that the *dim1A* mutant phenotypes result from structural changes to the small subunit rather than depletion of a ribosomal protein.

An interesting possibility is the role of the conserved dimethyladenosines in uORF-mediated translational control. Translational control plays a key role in numerous developmental and physiological processes. In plants, translational regulation contributes to the regulation of specific genes in response to environmental cues, sugar homeostasis, and light–dark transitions (Kawaguchi and Bailey-Serres, 2002). If the uORF upstream of an ORF encoding a gene product is recognized by a ribosome, translation will be terminated at the stop codon of the uORF and will not translate the primary ORF downstream. Translation of the downstream ORF requires translational

reinitiation, which requires the assembly of a new initiation complex. The conserved dimethyladenosines have previously discussed as being important for translational fine-tuning (Lafontaine *et al.*, 1998, Demirci *et al.*, 2010, Van Buul *et al.*, 1984) and recently have been implicated in ribosome recycling and translational re-initiation (Seshadri *et al.*, 2009). Interestingly, ribosomal proteins have also been implicated in translation re-initiation. STV1/RPL24b is important for translational reinitiation, and the *stv1/rpl24b* mutant results in decreased expression of genes with uORF (Nishimura *et al.*, 2005). Further analysis will be needed to determine if uORF translational regulation is affected in the *dim1A* mutant and if so, to determine if epidermal cell-type patterning is influenced by such a mechanism.

ACKNOWLEDGEMENTS

I would like to thank Dr. Su-Hwan Kwak, Dr. Angela Bruex and Dr. Myeong Min Lee for helpful comments throughout this project. The primer extension experiment would not have been possible without the guidance of Dr. Janine Maddock and technical assistance of Dr. Ryszard Zielke. In addition, Aaron Sluis provided technical assistance with protoplasting and FACS for the microarray analysis and Gregg Soboccinski provided invaluable assistance with confocal microscopy. Also, the 35S::GFP plant line was a kind gift from Dr. Jennifer Gagne. Finally, this research was partially supported by the NIH-funded Cellular Biotechnology Training Program at the University of Michigan.

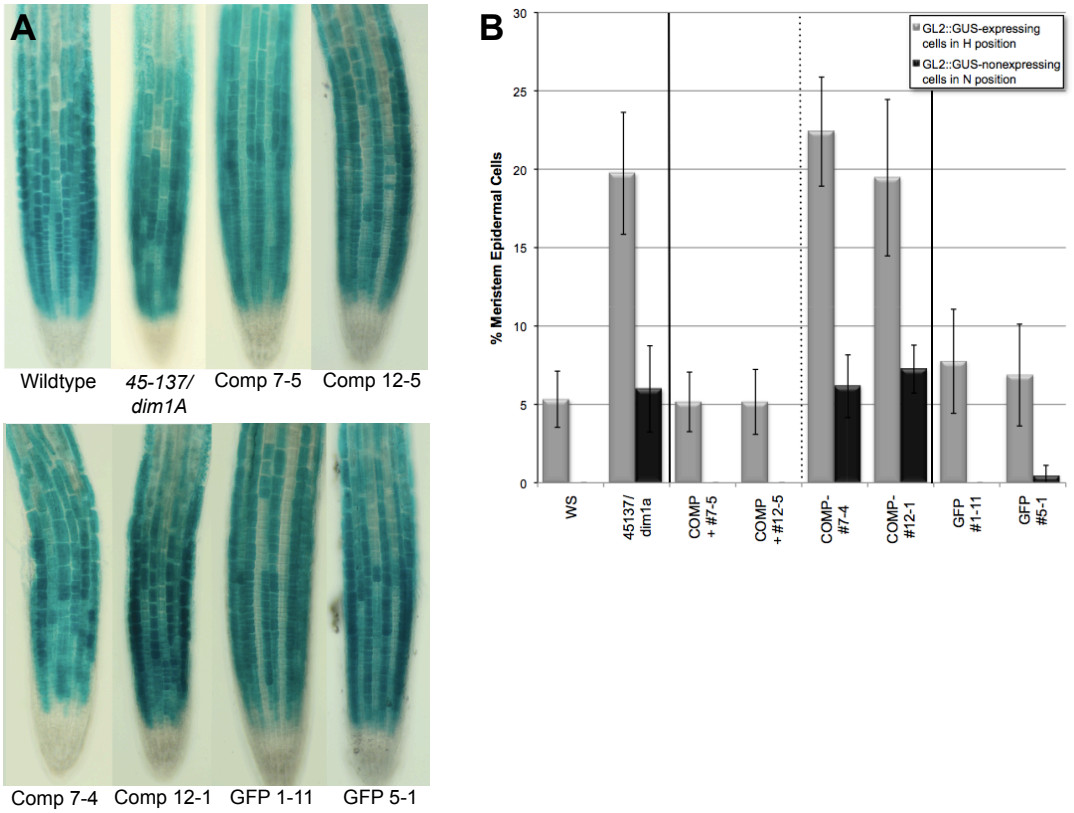

Figure 2.1. Cell-type expression of *GL2::GUS* is altered in *45-137/dim1A*

Analysis of position-dependent expression of *GL2* using promoter-reporter transgene *GL2::GUS* in wild-type (WS), the *45-137*/*dim1A* mutant, the *dim1A* complementation lines (#7-5 and #12-5), and *DIM1A::DIM1A-GFP* lines (#1-11 and #5-1. Lines #7-4 and #12-1 are included as negative controls for complementation lines #7-5 and #12-5, respectively. (A) Expression pattern of *GL2:GUS* in the root meristem of four-day-old seedlings. (B) Quantification of the epidermal cell-type pattern, showing frequencies of ectopic *GL2::GUS*-expressing cells in the H-cell position (gray bars) and ectopic non-*GL2::GUS*-expressing cells in the N-cell position (black bars), for each line. Scale bars: 50 μm.

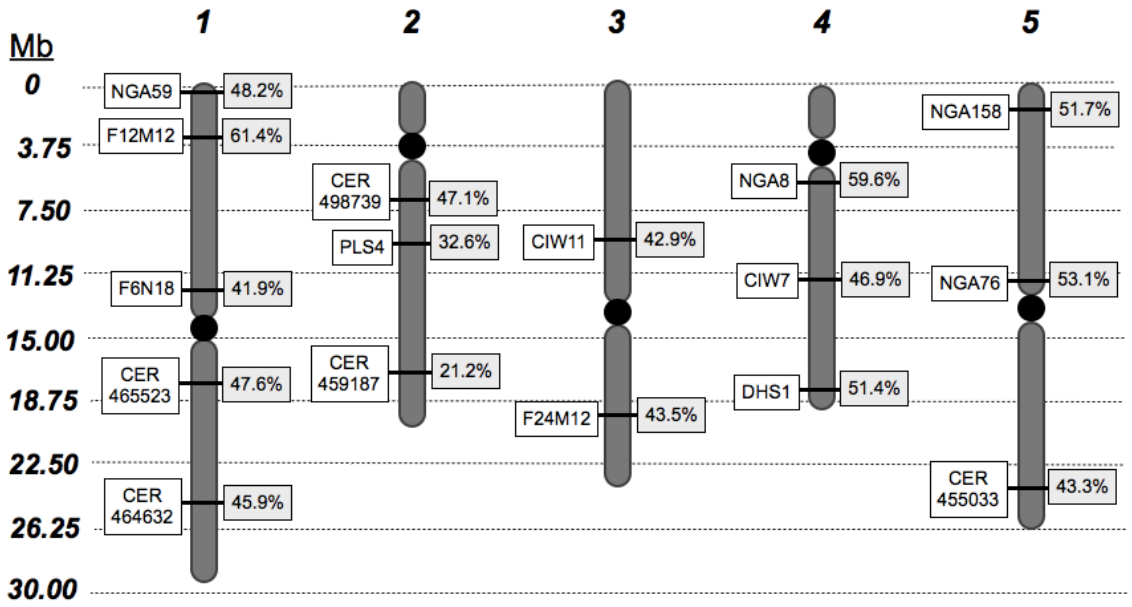

Figure 2.2. Rough mapping the mutation in the *45-137* mutant background

Bulk-segregant analysis using pools of F3 seedlings from a mapping population were analyzed for meiotic recombination events using SSLP markers that identify polymorphisms between Ws (mutant) and Ler (WT) revealed that the mutation causing the *45-137* mutant phenotype was linked to the bottom of chromosome two near marker CER459187.

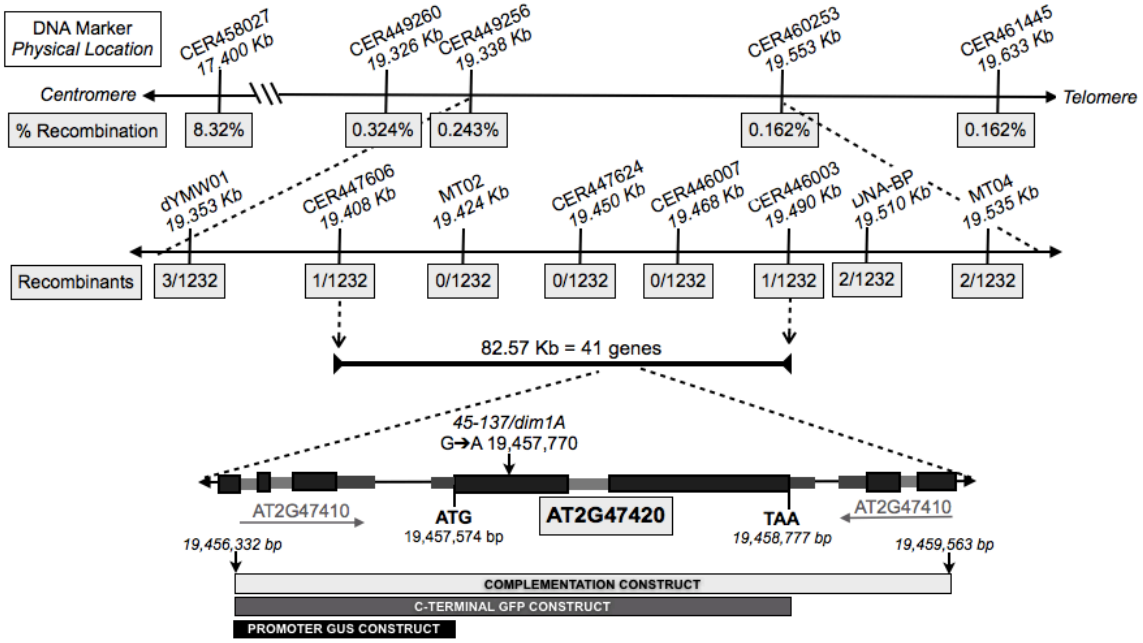

Figure 2.3. Fine mapping revealed the *45-137* mutation in locus At2g47420

Individual F2 plants from a mapping population were analyzed used to fine map the *45-137* mutation. The gene was delimitated to a 82 Kb region on the lower arm of chromosome 2 between marker CER447606 and CER446003 The 41 genes within this region were systematically sequenced until the mutation, a single base substitution in loci At2g47420, was identified. At2g47420, which contains two exons (black bars) and one intron (grey bar), encodes DIM1A, a putative rRNA dimethyladenosine transferase. Genomic regions used for construction of complementation, GFP-protein fusion and promoter-reporter constructs are also indicated.

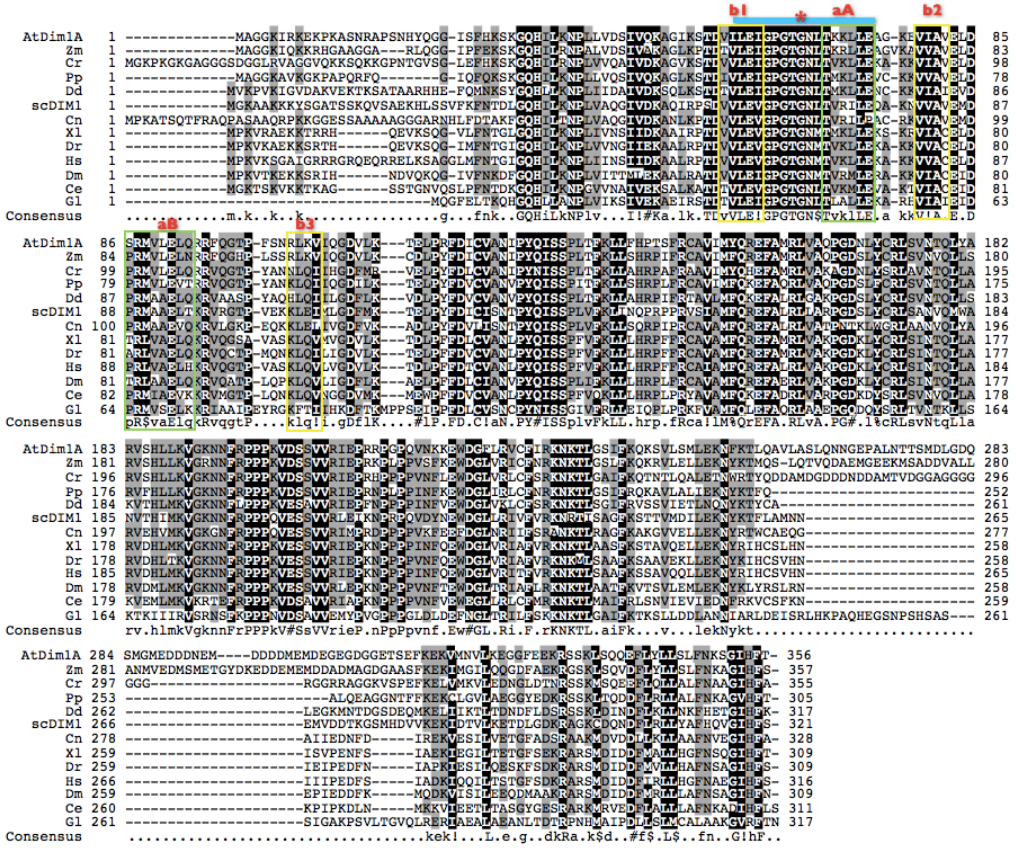

Figure 2.4. Protein sequence alignment of DIM1A homologs

Multiple alignment of the amino acid sequences from eukaryotic DIM1A homologs. The blue bar indicates the position of "motif I," which contains the canonical GXGXG SAM-binding sequence. Red letters indicate the location of highly conserved β sheets (yellow boxes) and α helices (green boxes) important for SAM binding. The asterisk within motif I indicates the position of the mutation in *dim1A*. Abbreviations: *Arabidopsis thaliana* (At), *Chlamydomonas reinhardtii* (Cr), *Physcomitrella patens* (Pp), *Dictyostelium dictoideim* (Dd), *Saccharomyces cerevisiae* (Sc), *Cryptococcus neoformans* (Cn), *Xenopus laevis* (Xl), *Danio rerio* (Dr), *Homo sapian* (Hs), *Drosophila melanogaster* (Dm), *Caenorhabditus elegans* (Ce), *Giardia lambia* (Gl). Black shading indicates 90% consensus, grey shading indicates 50% consensus, ! is anyone of IV, $ is anyone of LM, % is anyone of FY, # is anyone of NDQEBZ.

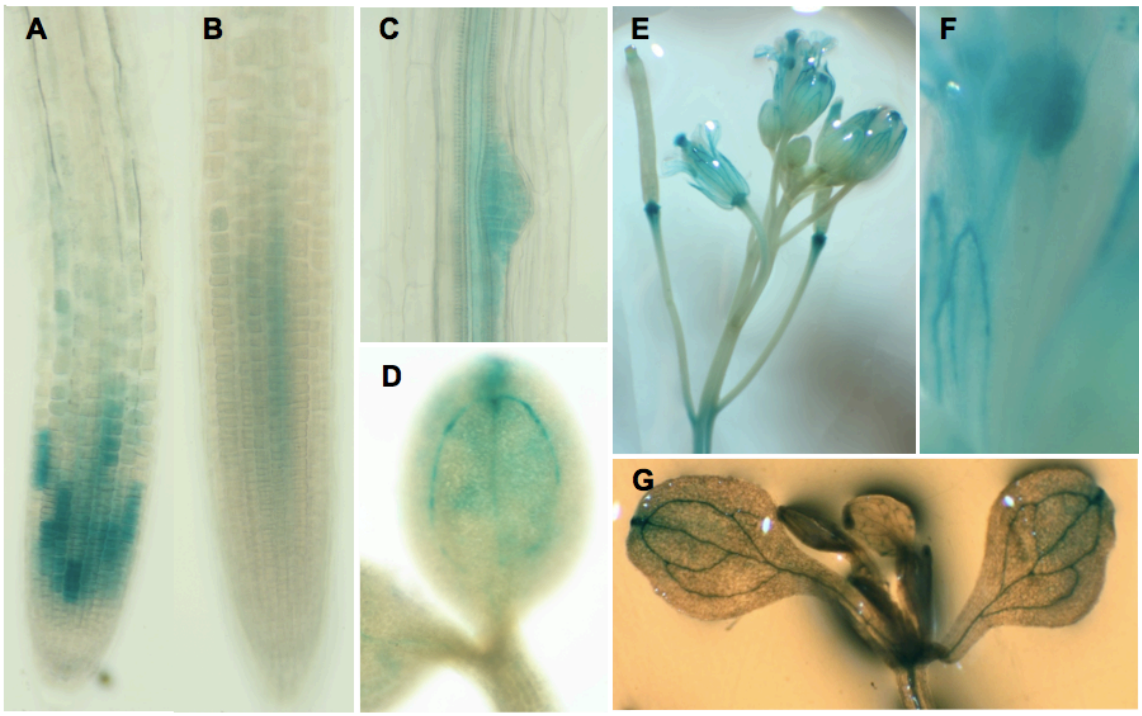

Figure 2.5. *DIM1A* is expressed in developing tissues

Histochemical GUS staining pattern of transgenic plants carrying the *DIM1A::GUS* transgene. T3 plants identified as homozygous for *DIM1A::GUS* were observed: (A) Two-day-old root tip; (B) four-day-old root tip; (C) root vasculature and lateral root emergence site of a four-day-old seedling; (D) two-day-old cotyledon; (E) floral tissue (stigma, petals); (F) anther, pollen grains and sepal vasculature; (G) developing leaves and cotyledon of ten-day-old plant.

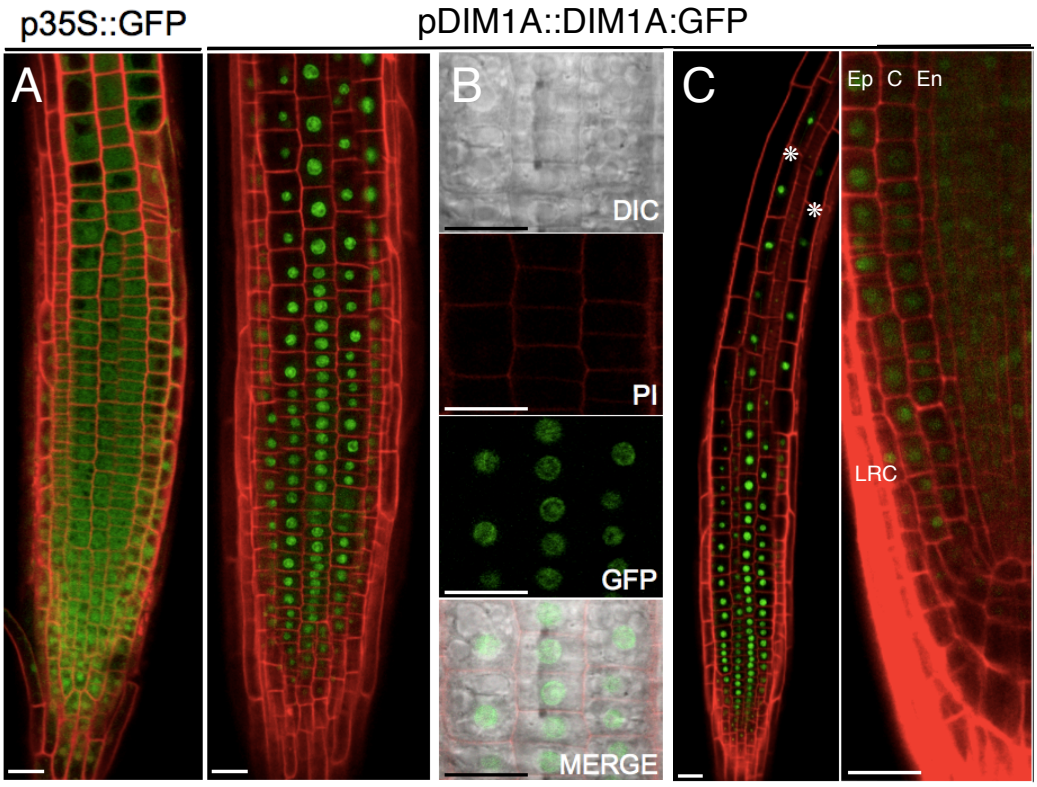

Figure 2.6. DIM1A:GFP localizes to the nucleus and nucleolus of root cells

Sub-cellular and root tissue localization of DIM1A:GFP expressed from the DIM1A promoter of four-day-old seedlings. Seedlings were stained with propidium iodide (red) for visualizing the cell wall and DIM1A:GFP accumulation (green). (A) Root meristem localization of free GFP (left) and DIM1A:GFP (right). Panels in (B) show overlay of fluorescence image and differential interference contrast optics. (C) DIM1A:GFP persists longer in developing hair cells(⁕) than non-hair cells (left) and is present in all meristematic tissues (left). Abbreviations: Epidermis (Ep), cortex (C), endodermis (En), lateral root cap (LRC). Scale bars represent 20 μm

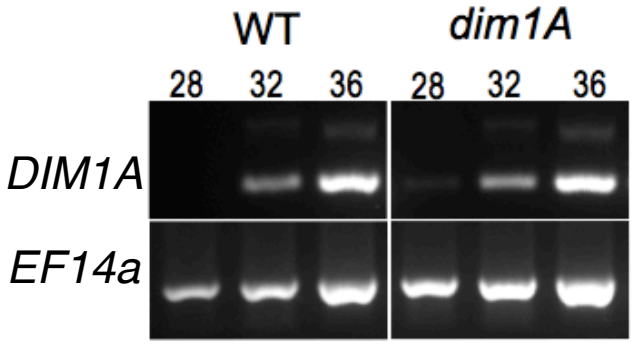

Figure 2.7. Expression of *DIM1A* is not altered in the *dim1A* mutant

RT-PCR of *DIM1A* from mRNA isolated from five-day-old wild-type and *dim1A* seedlings. No difference is seen between wild-type and *dim1A* at 28, 32 or 36 PCR cycles. Translation elongation factor EF1αA4 (EF14a) was used as a control.

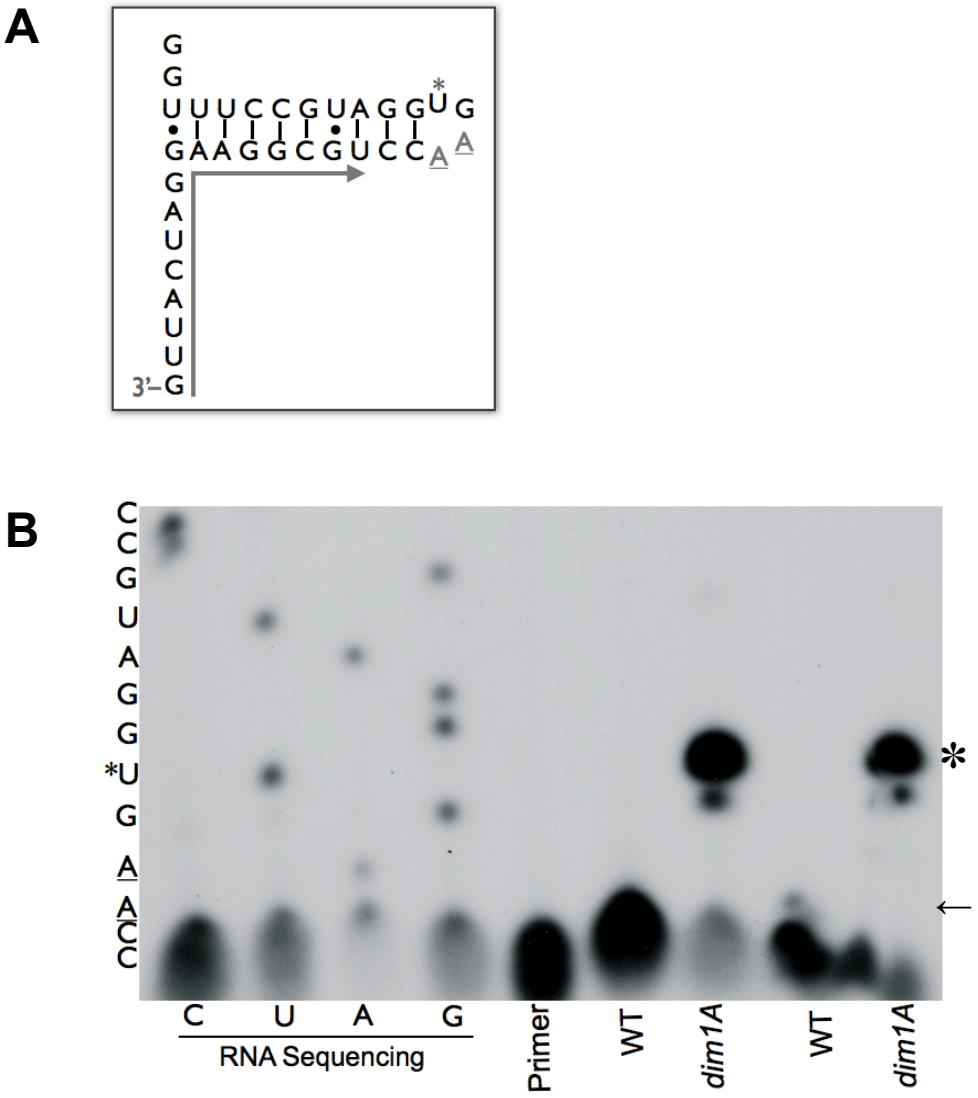

Figure 2.8. d*im1A* lacks two conserved 18S rRNA adenosine dimethylations

(A) Predicted sequence and structure of the 3'-end of the *Arabidopsis thaliana* 18S rRNA. The arrow represents the reverse complement of the16 bp primer used in the poisoned primer extension experiment. (B) Poisoned primer extension products using RNA isolated from wild-type and *dim1A*. The left side of the gel shows the RNA sequencing reaction for reference. Primer extension yields a signal at the adenosine doublet in wild-type (←). In the *dim1A* mutant there is no indication of a reverse transcriptase stop at either of the adenosines, but rather termination is seen at the next uridine in the 18S rRNA sequence (✻). In both (A) and (B) "A" represent the adenosines that are putatively dimethylated and U* indicates the uridine at which the reaction was forced to stop due to the presence of ddATP in place of dATP in the nucleotide mixture.

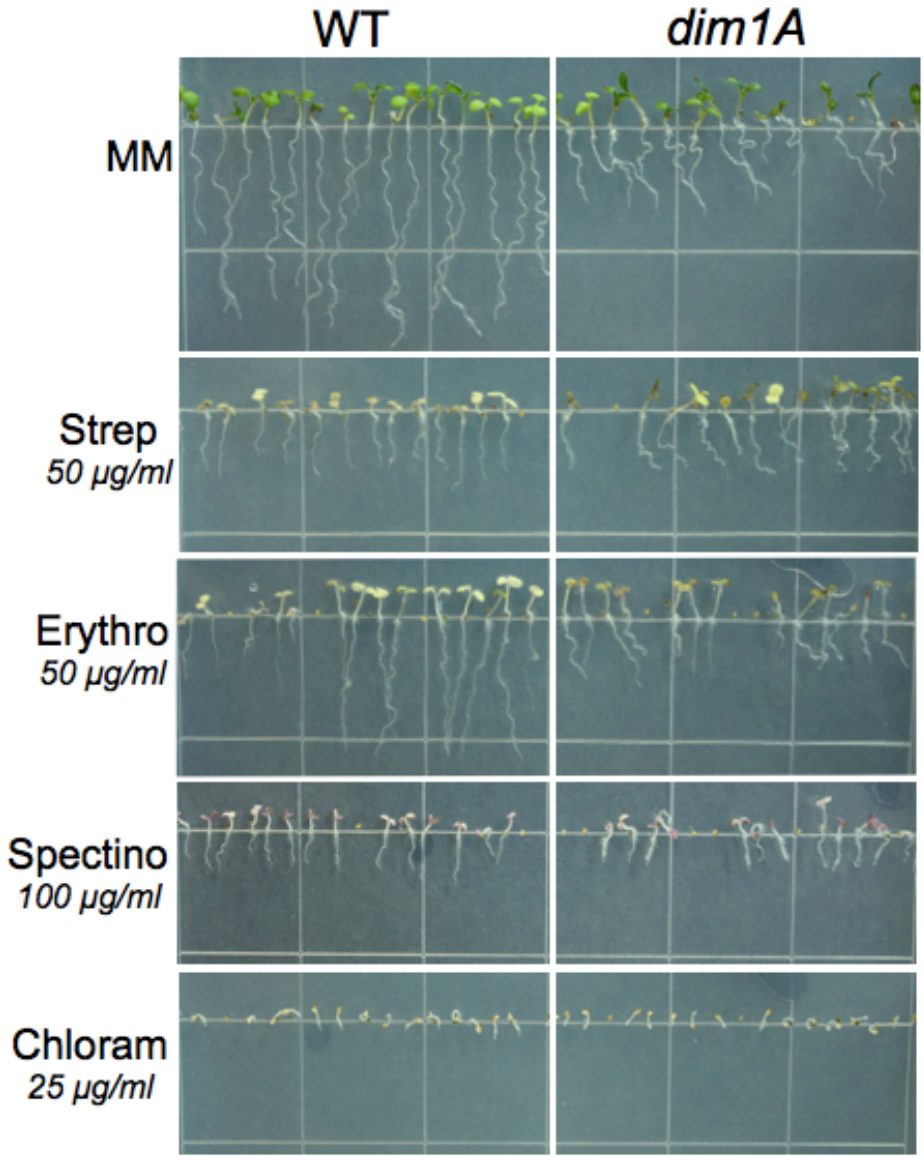

Figure 2.9. The *dim1A* mutation confers partial resistance to streptomycin

Compared to wild-type seedlings (left), *dim1A* mutant seedlings (right) display mild resistance to streptomycin, characterized by larger, greener hypocotyls and slightly longer roots. The *dim1A* mutant exhibited similar sensitivity as wild-type to erythromycin, spectinomycin, chloramphenicol (above) as well as puromycin, tetracycline, gentamycin, hygromycin and carbenicillin (not shown). Seedlings were directly germinated on media containing various antibiotics and photographed at six-days post-germination..

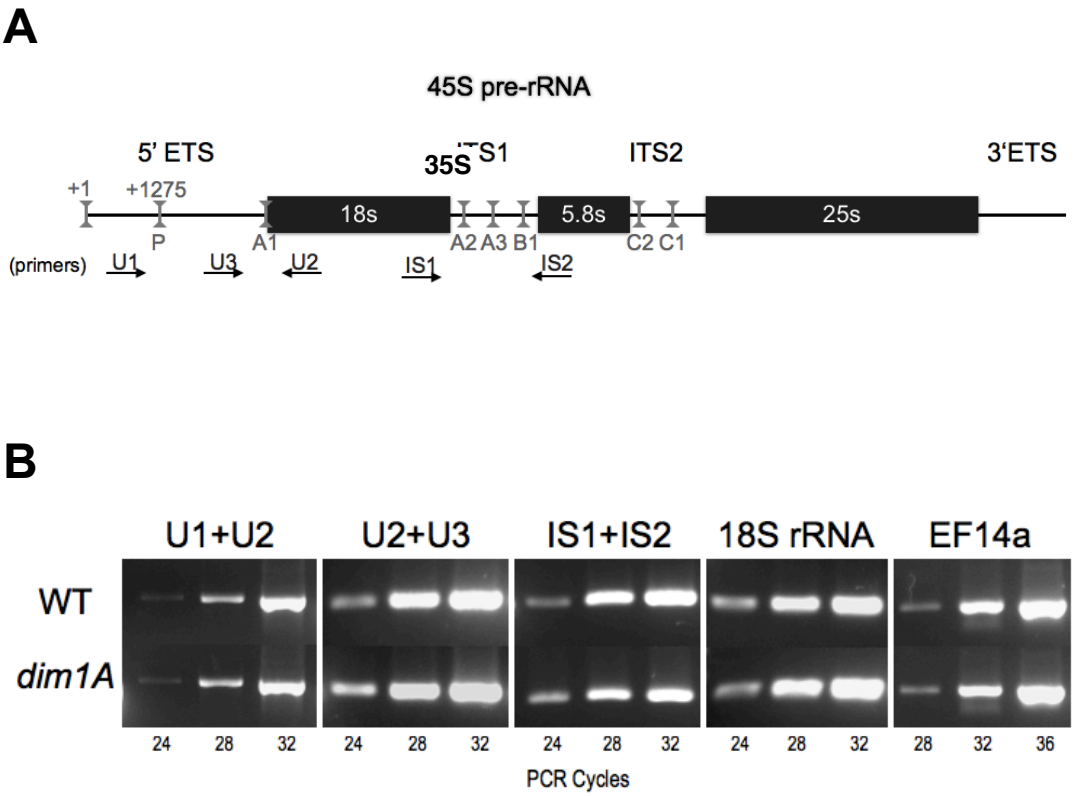

Figure 2.10 The *dim1A* mutation does not affect 35S pre-rRNA processing

(A) Structure of *Arabidopsis* pre-rRNA transcript and predicted processing sites. The 35S pre-rRNA is composed of the 5′ ETS, 18S rRNA (18S), ITS1, 5.8S rRNA (5.8S), ITS2, 25S rRNA (25S) and 3′ ETS. The primers U1 and U2 were designed to detect processing at site P, primers U2 and U3 to detect the 5′ ETS, and primers IS1 and IS2 to detect ITS1. (B) Total RNA was purified from five-day-old wild-type and *dim1A* plants and subjected to RT–PCR using primers specific for 5′ ETS, ITS1, 18S and translation elongation factor EF1αA4 (EF14a) as a control. No significant difference in product accumulation between wild-type and *dim1A* was observed at 24, 28 or 32 PCR cycles. Based on knowledge of Dim1-dependent processing in yeast, DIM1A is putatively required for processing at sites A1 and A2, which were detected using primer sets U2+U3 and IS1+IS2, respectively.

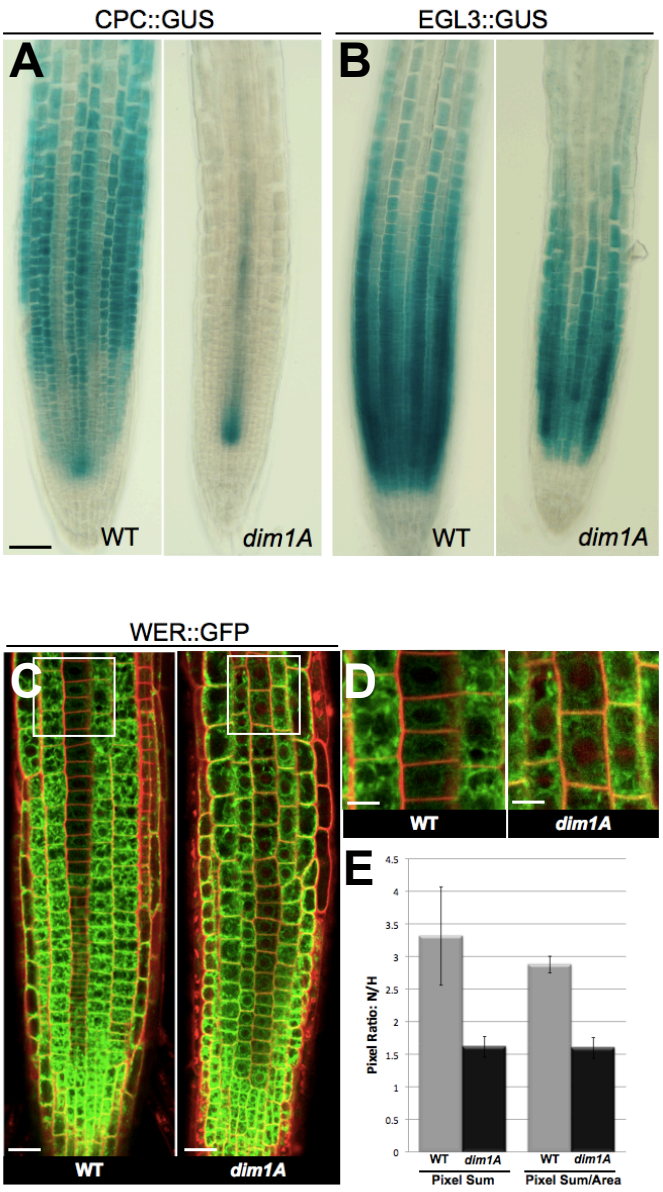

Figure 2.11. Effect of *dim1A* on expression of *CPC*, *EGL3* and *WER*

Expression pattern of the following transcription factor reporter genes in roots of wild-type and *dim1A* four-day-old seedlings: (A) *CPC::GUS*, (B) *EGL3::GUS*, (C,D) *WER::GFP*. Images in (D) represent magnification of region within boxes diagrammed in (C). (E) Graphical representation of the ratio of the amount of WER::GFP measured in cells in the N position to the amount measured in cells in the H position in wild-type (grey bars) and *dim1A* roots (black bars). GFP pixel quantification was done in cells in the uppermost (shootward) one-third of the meristem (Measurements are expressed in terms of total pixels (left) and pixels/ area (right). Scale bars represent 50 μm (A,B,D), 25 μm (C)

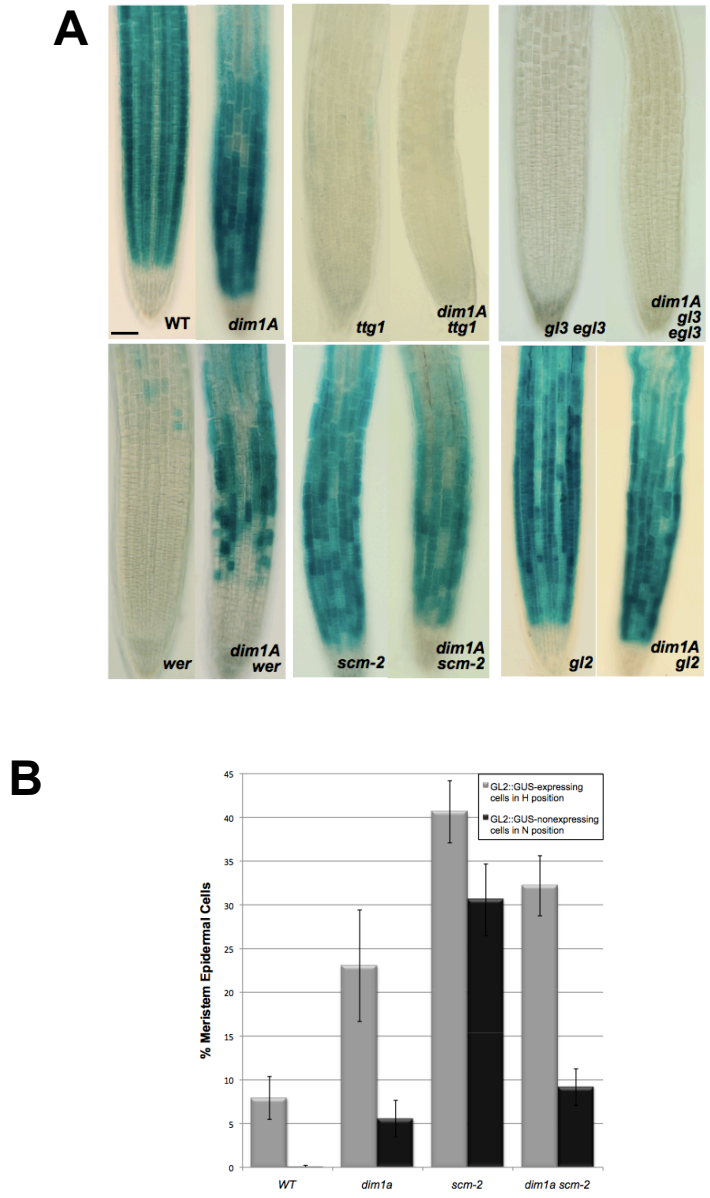

Figure 2.12. Genetic interaction of *dim1A* with epidermal patterning mutants

(A) Expression of the *GL2::GUS* transcriptional reporter in the following lines: wild-type and *dim1A*; *ttg1* and *dim1A ttg1*; *gl3 egl3* and *dim1A gl3 egl3*; *wer* and *dim1A wer*; *scm-2* and *dim1A scm-2*; *gl2* and *dim1A gl2*. (B) Quantification of the epidermal cell-type pattern, showing frequencies of ectopic *GL2::GUS*-expressing cells in the H cell position (gray bars) and ectopic non-*GL2::GUS*-expressing cells in the N cell position (black bars) in wild-type, *dim1A*, *scm-2* and *dim1A scm-2* lines. The mean and standard deviation are indicated for each line. Scale bars represent 50 μm

		H Cell Position		N Cell Position	
Genotype	Hair Cells in the Epidermis (%)	Hair Cells (%)	Non-hair Cells (%)	Hair Cells (%)	Non-hair Cells (%)
Wild type	47.5 ± 3.0	95.0 ± 6.1	5.0 ± 6.1	0 ± 0	100 ± 0
dim1A	40.8 ± 10.1	80.3 ± 15.1[a]	19.7 ± 15.1[a]	1.6 ± 3.9	98.4 ± 3.9
wer-1	94.5 ± 5.5	96.5 ± 6.7	3.5 ± 6.7	92.5 ± 11.2[a]	7.5 ± 11.2[a]
wer-1 dim1A	83.5 ± 9.6	94.5 ± 6.9	5.5 ± 6.9	72.6 ± 18.5[b]	27.4 ± 18.5[b]

At least 20 5-day-old seedlings were examined for each line. Values represent mean +/- SD.

[a]Differs significantly from the wild-type (P<0.01; Student's t-test)

[b]Differs significantly from the wer (P<0.01; Student's t-test)

Table 2.1. Cell-type patterning in the root epidermis

Analysis of cell types specified in epidermal cells in the N and H position. Roots of *dim1A* mutant seedlings specify fewer hair cells, due mainly to a significant increase in non-hair cells specified in the H-position. Analysis of the *wer* mutant roots revealed a “hairy” root phenotype, due to specification of about 90% of epidermal cells as hair cells (as previously reported (Lee and Schiefelbein, 1999). Roots of *wer dim1A* double mutants were less hairy than *wer* single mutant roots.

Figure 2.13. The effect of overexpression of *DIM1A* or G66E *dim1A* on root epidermal patterning and meristem cell division

(A) Confocal images of *35S::DIM1A:GFP* and *35S::dim1A:GFP* lines comparing expression levels (as determined by GFP intensity) in the overexpression lines to the DIM1A::DIM1A:GFP line, in which *DIM1A:GFP* expression is driven by the native promoter. (B) *GL2::GUS* cell-type expression pattern in the overexpression lines. The *dim1A DIM1A::DIM1A:GFP* line is included as a control to illustrate the wild-type pattern of *GL2::GUS* expression. (C) Quantification of the epidermal cell-type pattern, showing frequencies of ectopic *GL2::GUS*-expressing cells in the H cell position (gray bars) and ectopic non-*GL2::GUS*-expressing cells in the N cell position (black bars) in wild-type, *dim1A*, *dim1A DIM1A::DIM1A:GFP* and the seven overexpression lines. The mean and standard deviation are indicated for each line. (C) Quantification of meristematic epidermal cell number. Averages counted from at least fifteen seedlings are represented here relative to averages from wild-type. Scale bars represent 20 μm (A), 50 μm (B).

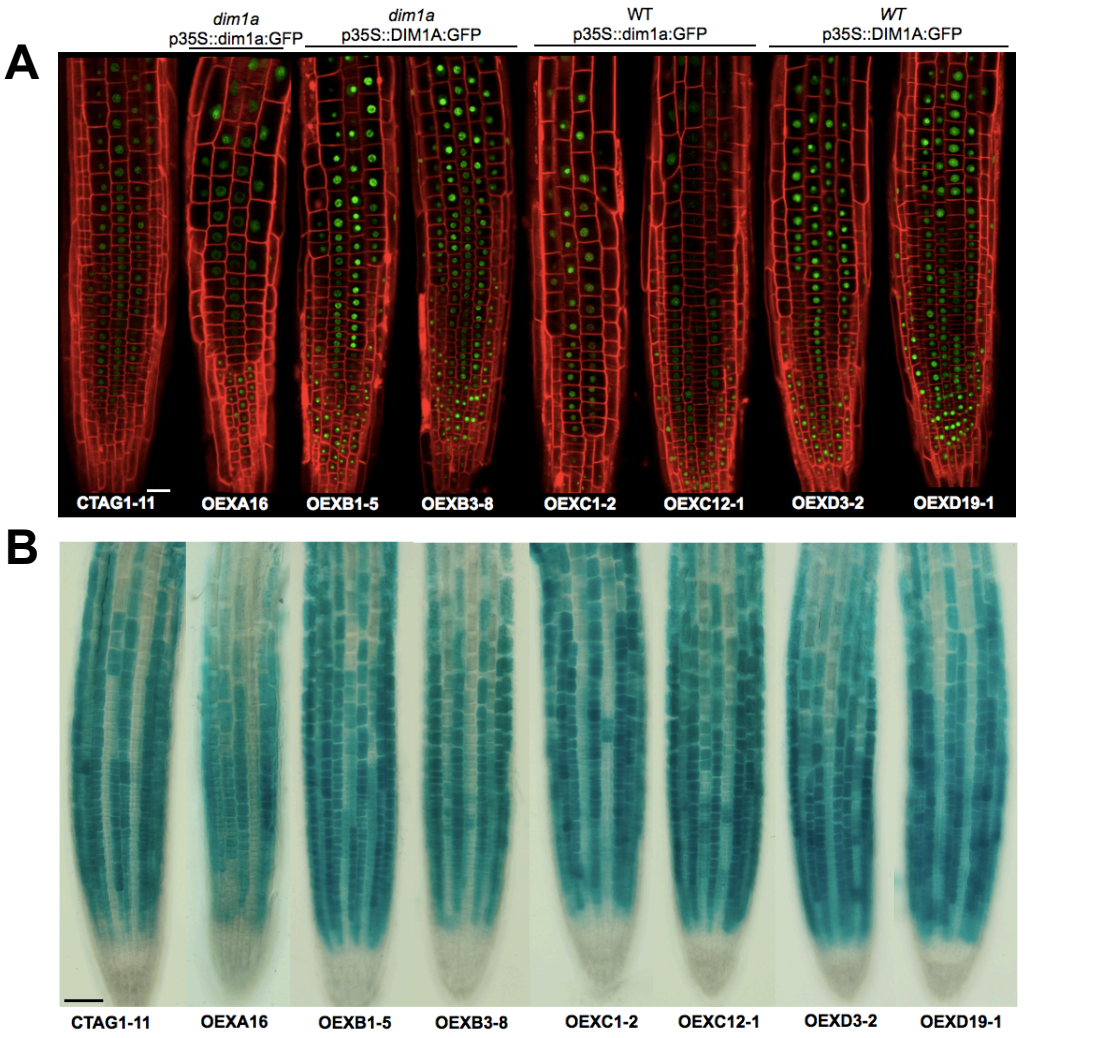
A
dim1a
p35S::dim1a:GFP
dim1a
p35S::DIM1A:GFP
WT
p35S::dim1a:GFP
WT
p35S::DIM1A:GFP
CTAG1-11
OEXA16
OEXB1-5
OEXB3-8
OEXC1-2
OEXC12-1
OEXD3-2
OEXD19-1
B
CTAG1-11
OEXA16
OEXB1-5
OEXB3-8
OEXC1-2
OEXC12-1
OEXD3-2
OEXD19-1
C
GL2::GUS-expressing cells in H position
GL2::GUS-nonexpressing cells in N position
% Cells
25
20
15
10
5
0
WT
dim1A
Ctag1-11
OEX: A1-6
OEX: B1-5
OEX: B3-8
OEX: C1-2
OEX: C12-1
OEX: D3-2
OEX: D19-1
D
WT
dim1A
A1-6
B1-5
B3-8
C1-2
C12-1
D3-2
D19-1
Number of epidermal cells (% WT)
140
120
100
80
60
40
20
0
H-File Cells
N-File Cells
Cell File Counted

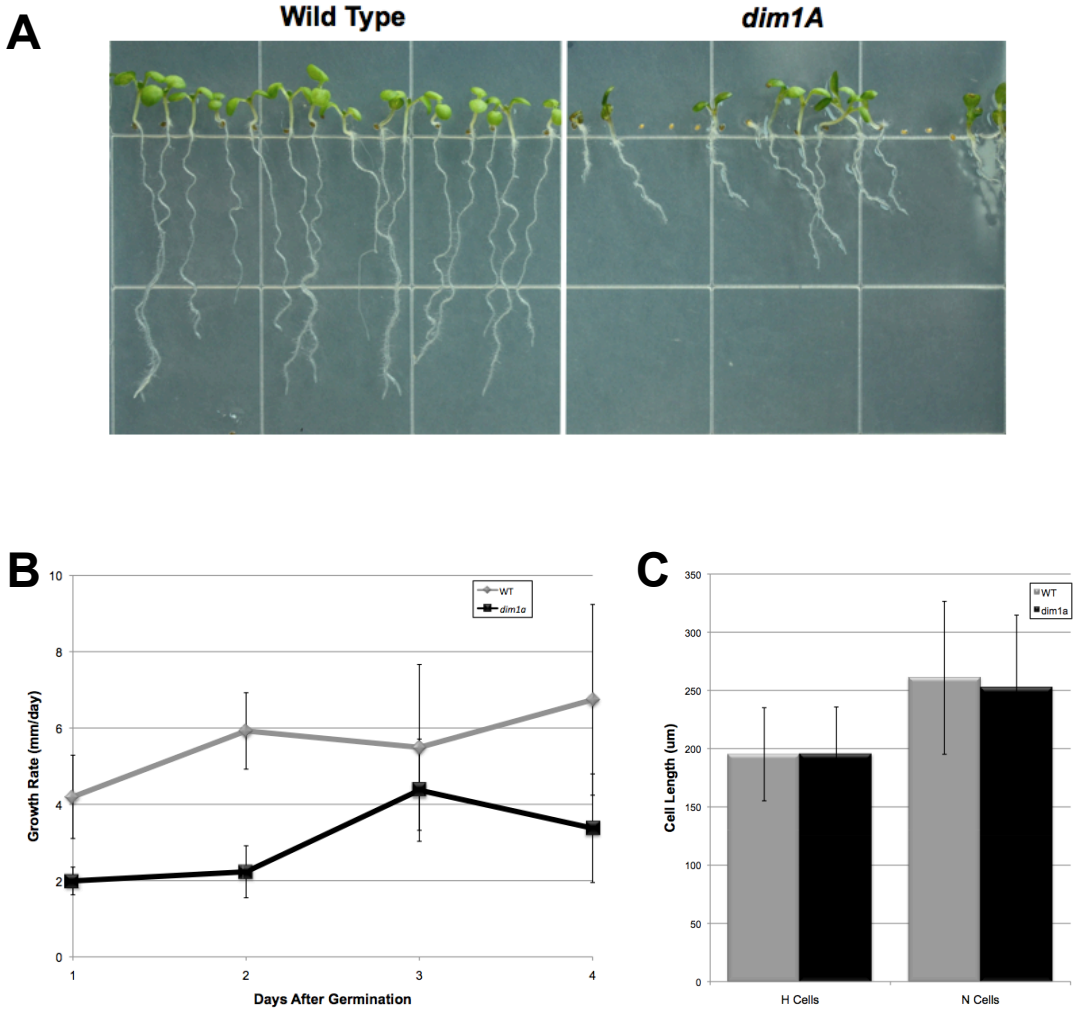

Figure 2.14. *dim1A* displayed reduced root length, and root growth rate, but mature epidermal cell length was unaffected

(A) Five-day-old seedlings grown on vertically-oriented nutrient-media containing petri dishes. (B) Root growth rate measurements of wild-type (grey line) and *dim1A* (black line) seedlings up to four days post-germination. (C) Length of mature, fully elongated, epidermal cells measured from roots of six-day-old seedlings. In (B) and (C) data represents the mean and standard deviation of measurements from 96 wild-type and 75 *dim1A* seedlings (A) or at least 90 individual cells (B)

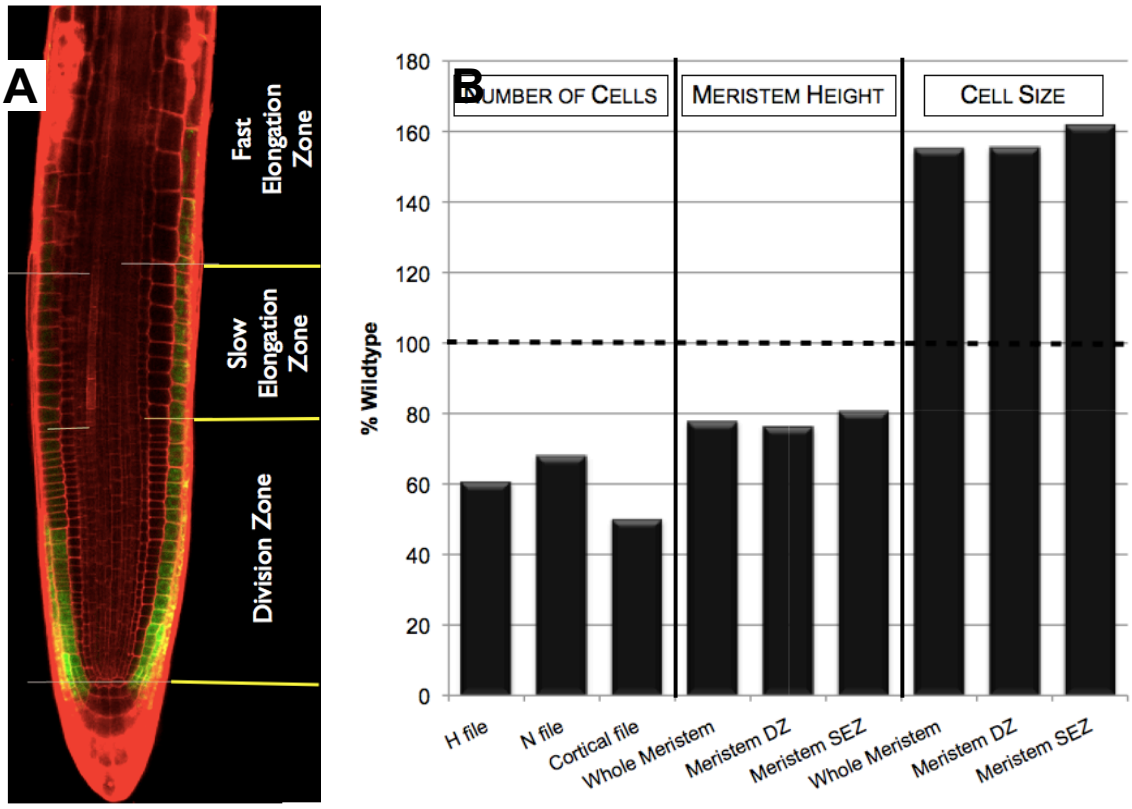

Figure 2.15. *dim1A* roots have fewer and larger cells than wild-type

(A) The root meristem can be broken up into two zones; (1) the division zone, characterized by cells that are much wider than tall, indicative of rapid cell division with minimal expansion and (2) the slow elongation zone, characterized by cells of equal width and height, resulting from slowing cell division and increased expansion. (B) The number of epidermal cells in the H position and N position as well as cortical cells present in the meristem (left panel); meristem dimensions (center panel) and meristem cell size (right panel) as measured for the whole meristem, as well as separately for the division zone (DZ) and slow elongation zone (SEZ). Data shown in (B) is for *dim1A* and is expressed as percent wild-type.

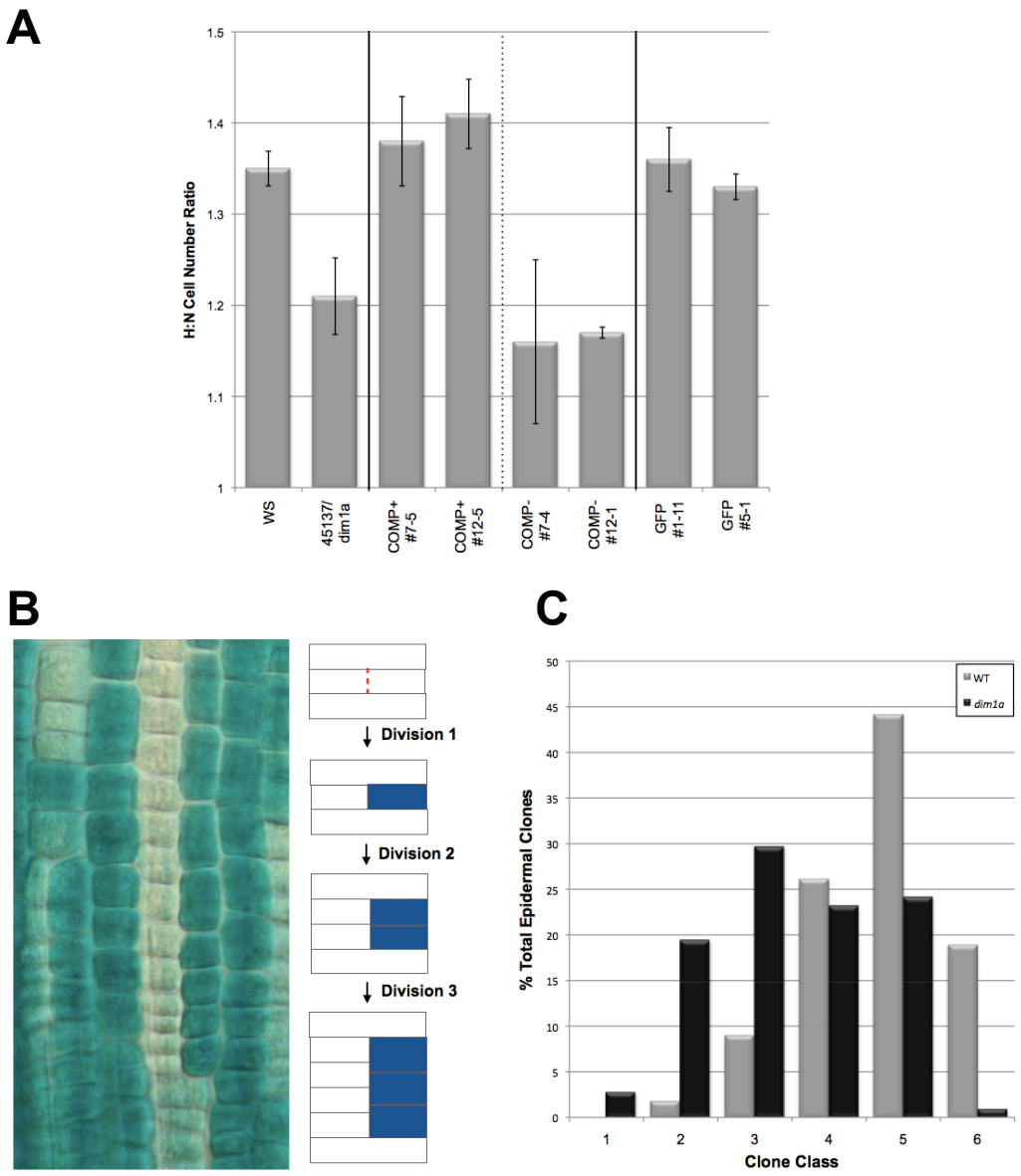

Figure 2.16. *dim1A* has a reduced epidermal cell H/N ratio and division rate

(A) Ratio of the number of epidermal cells in the H position to the number in the N position (H/N ratio) in wild-type, *dim1A* and *dim1A* complementation lines. The mean and standard deviation are indicated for each line. (B) Image depicting an epidermal clone derived from an cell in the H position (left). Diagram (right) illustrating how epidermal cell clones arise: An initial anticlinal longitudinal divisions generates the first cell of a new cell file (top right), then subsequent anticlinal transverse divisions generate additional cells. (C) Distribution of epidermal cell clones into different clone classes in wild-type (grey bars) and *dim1A* (black bars). The number for each class corresponds to the maximum number of cell divisions experienced by the original H position cell. Over 100 epidermal clones were analyzed from each line.

Figure 2.17. Reduced epidermal cell division due to antibiotic treatment does not significantly alter cell-type expression of *GL2::GUS*

(A) The number of epidermal cells present in the H position (grey bars) and N position (black bars) of untreated wild-type and *dim1A* roots as well as wild-type roots exposed to five different treatment conditions (25 µg/ml hygromycin, 100 µg/ml streptomycin, 50 µg/ml puromycin, 5 µg/ml tetracycline, and 20 µg/ml tetracycline). (B) Quantification of the epidermal cell-type pattern, showing frequencies of ectopic *GL2::GUS*-expressing cells in the H cell position (gray bars) and ectopic non-*GL2::GUS*-expressing cells in the N cell position (black bars) in wild-type, *dim1A*, wild-type roots exposed to the five different treatment conditions shown to reduce epidermal cell number to levels comparable to the *dim1A* mutant. The mean and standard deviation are indicated for each line. (C) *GL2::GUS* expression in four-day-old roots of untreated wild-type and *dim1A* as well as treated wild-type roots. Note: seedlings were either germinated on the various media (G) or transferred from nutrient media plates to treatment media at two days post-germination (T).

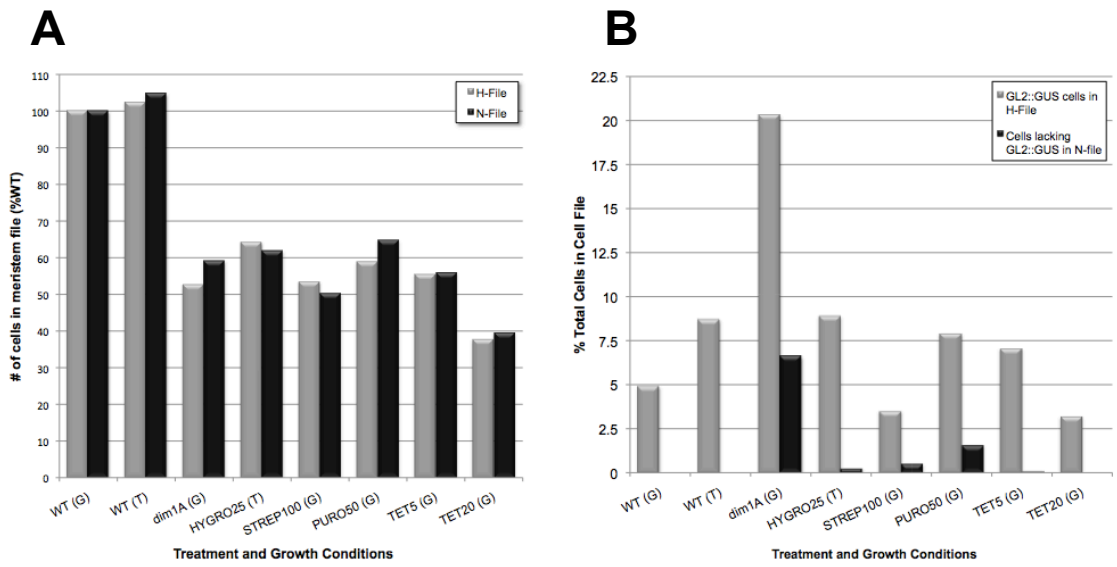
A
B
H-File
N-File
# of cells in meristem file (%WT)
Treatment and Growth Conditions
WT (G)
WT (T)
dim1A (G)
HYGRO25 (T)
STREP100 (G)
PURO50 (G)
TET5 (G)
TET20 (G)
GL2::GUS cells in H-File
Cells lacking GL2::GUS in N-file
% Total Cells in Cell File

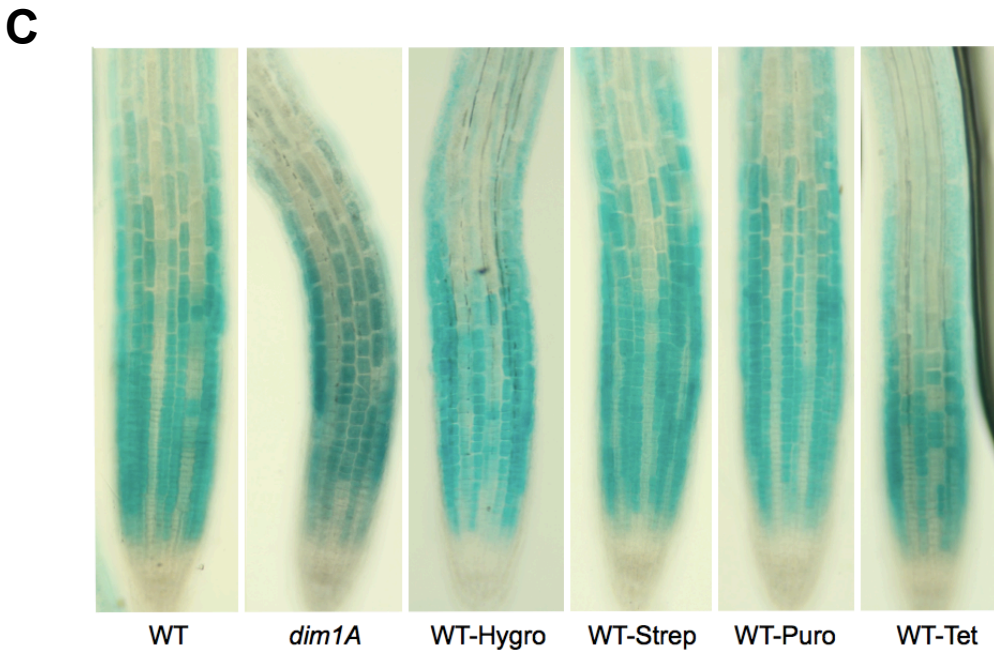
C
WT
dim1A
WT-Hygro
WT-Strep
WT-Puro
WT-Tet

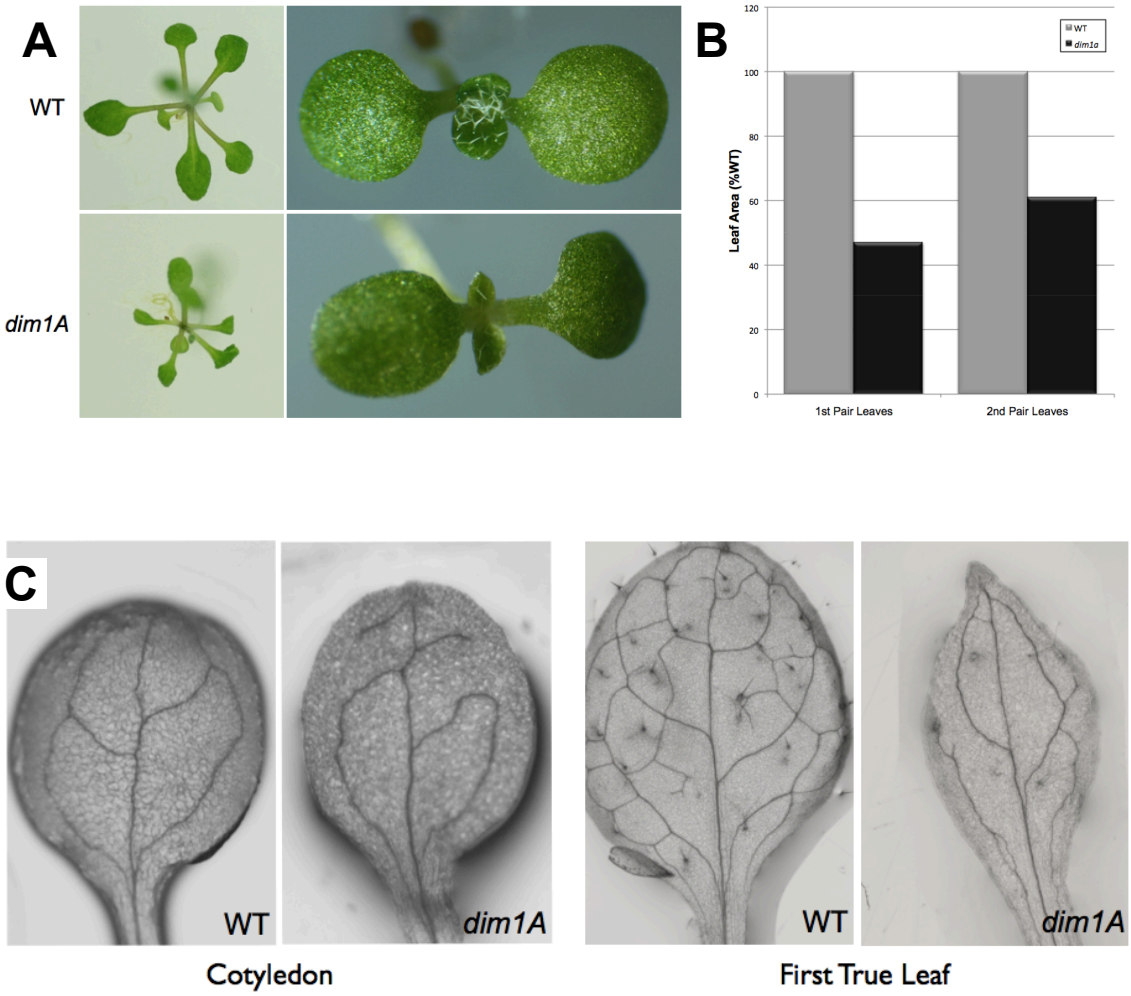

Figure 2.18. Abnormal leaf shape, size and venation in the *dim1A* mutant

(A) Relative sizes of wildtype (top) and *dim1A* mutant (bottom) fourteen-day-old seedlings (left panel). Leaf shape characteristics of the first pair of true leaves emerging in six-day-old seedlings (right panel). (B) Quantification of the surface area of the first pair of true leaves (left) and second pair of true leaves (right) in wild-type (grey bars) and *dim1A* (black bars) seedlings. (C) Leaf vein patterning in cleared cotyledons and first true leaves of wildtype and *dim1A*. Note: with the exception of the images in the left panels of (A), all other *dim1A* images were magnified compared to wildtype for ease of comparison .

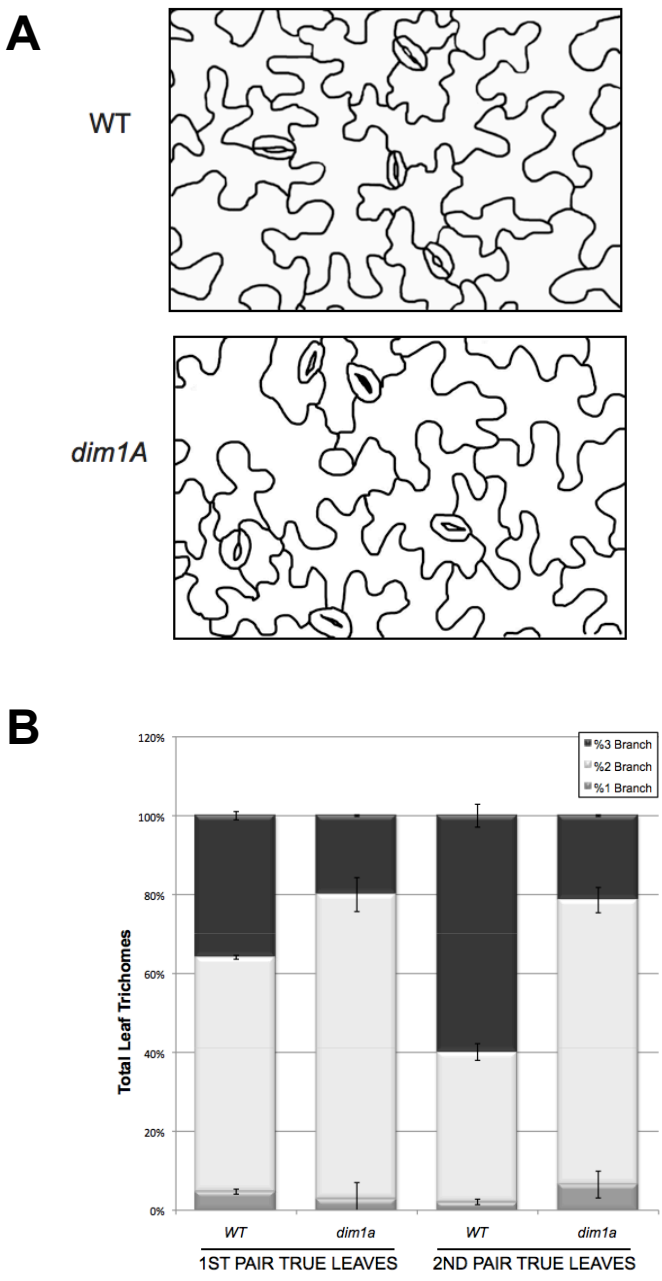

Figure 2.19. Higher-order trichome branching, but not leaf epidermal shape or stomatal patterning, is affected in *dim1A*
(A) Adaxial surface of wild-type and *dim1A* leaves. (B) The distribution of trichomes based on number of branches.

Genes shared between "*dim1A* vs. WT" and "208" lists				
	AGI Number	"Hair" or "Non-hair" gene	Description and GO molecular/biological function	Fold Change, (*dim1A* -vs- WT)
1	AT3G15760	HAIR	Unknown Protein	-2.64
2	AT2G02630	HAIR	DC1 domain-containing protein	-3.05
3	AT1G16260	HAIR	protein kinase family protein	+4.63
4	AT4G15390	HAIR	transferase family protein	+2.69
5	AT2G20520	HAIR	FLA6 (FASCICLIN-LIKE ARABINOGALACTAN 6)	-4.76
6	AT1G07795	HAIR	Unknown Protein	-3.05
7	AT5G57540	HAIR	putative xyloglucan:xyloglucosyl transferase	-3.94
8	AT2G47540	HAIR	pollen Ole e 1 allergen and extensin family protein	-2.25
9	AT5G19800	HAIR	hydroxyproline-rich glycoprotein family protein	-2.97
10	AT2G48080	HAIR	oxidoreductase, 2OG-Fe(II) oxygenase family protein	-2.85
11	AT4G28850	HAIR	putative xyloglucan:xyloglucosyl transferase	-3.53
12	AT3G56000	HAIR	ATCSLA14; cellulose synthase/ transferase,	-2.03
13	AT3G46760	HAIR	protein kinase family protein	-2.83
14	AT1G16440	HAIR	kinase	-2.79
15	AT2G37440	HAIR	endonuclease/exonuclease/phosphatase family protein	-2.10
16	AT2G04680	HAIR	DC1 domain-containing protein	-2.27
17	AT1G69240	HAIR	MES15 (METHYL ESTERASE 15); hydrolase	-2.68
18	AT4G07960	HAIR	ATCSLC12; cellulose synthase/ transferase,	-2.35
19	AT4G25220	HAIR	transporter, putative	-2.41
20	AT4G25790	HAIR	allergen V5/Tpx-1-related family protein	-3.20
21	AT4G19680	HAIR	IRT2; iron ion transmembrane transporter	-3.05
22	AT1G65180	HAIR	DC1 domain-containing protein	-2.50
23	AT2G29740	HAIR	UGT71C2; UDP-glycosyltransferase/ quercetin	-2.11
24	AT2G46860	HAIR	AtPPa3; inorganic diphosphatase/ pyrophosphatase	-2.28
25	AT5G61650	HAIR	CYCP4;2 (CYCLIN P4;2); cyclin-dependent protein kinase	-2.35
26	AT1G30990	HAIR	major latex protein-related / MLP-related	-2.23
27	AT5G65090	HAIR	MRH3, BST1; phosphatidylinositol phosphatase	-2.08
28	AT1G54970	HAIR	ATPRP1 (PROLINE-RICH PROTEIN 1); constituent of cell wall	-2.46
29	AT3G07070	HAIR	protein kinase family protein	-2.39
30	AT1G22500	HAIR	zinc finger (C3HC4-type RING finger) family protein	-2.01
31	AT5G23030	HAIR	TET12 (TETRASPANIN12)	-2.55
32	AT1G63450	HAIR	catalytic	-2.03
33	AT2G18690	HAIR	Unknown Protein	+2.33
34	AT1G34510	HAIR	peroxidase, putative	-2.64
35	AT4G33730	HAIR	pathogenesis-related protein, putative	-2.60
36	AT2G39690	HAIR	unknown protein	-2.51
37	AT4G22640	HAIR	Unknown; membrane achored; expressed in male gameto., root.	+2.62
38	AT1G34330	HAIR	pseudogene, putative peroxidase	-2.28
39	AT5G22410	HAIR	peroxidase, putative	-2.17

Table 2.2. Microarray comparison differentially expressed genes in *dim1A* and root hair and non-hair specification genes

Comparison of 975 genes differentially expressed in the *dim1A* mutant to a list of 208 genes identified through transcriptome analysis as being important for cell-type differentiation in the root. 39 of 145 "hair genes" overlapped between the two lists and 90% of the 39 were found to be downregulated in the *dim1A* mutant.

Rough Mapping Primers										
				Primer Sequences			*PCR Product Size*			
Chr.	**Position (Kb)**	**Name**	**TYPE**	**Forward**	**Reverse**	**Tm**	**COL**	**LER**	**WS**	**Reference**
1	8.60	NGA59	SSLP	TTAATACATTAGCCCAGACCCG	GCATCTGTGTTCACTCGCC		111	115	141	SB Lab Primer/Genomics1994
1	3.21	F21M12	SSLP	TTACTTTTTGCCTCTTGTCATTG	GGCTTTCTCGAAATCTGTCC	56	200	~140	215	SB Lab Primer/Genomics1994
1	11.79	F6N18	SSLP	GATGAACTGAAACTGAGATG	TGCCTAGGCCTATTGATTTC	55	142	121	142	SB Lab Primer (Amy Riley)
1	17.90	CER465523	SSLP	CCTAAAGCTGATGATGATGG	GGTTTCTCGATGAATCGATG	55	254	200	254	SB Lab Primer
1	24.00	CER464623	SSLP	GCGAAGTGGAAGAGAAAAAAG	TTGCTGTGGAGTGTTAGTTGAG	55	138	112	138	SB Lab Primer
2	7.20	CER448739	SSLP	ACACATTACCGAGACTTAC	TTTAAAGGTGCCGAGACAAAG	58	144	92	144	SB Lab Primer
2	8.96	PLS4	SSLP	CCACCCTCTAGACTTATTACG	AAGAGGCAAAAACTGTCATTAG	55	113	>COL,WS	113	SB Lab Primer/Unknown
2	17.01	CER459187	SSLP	CTTCTCCACCCCACAAAGGT	ATGATGGCAGCAGACGAAAC	55	197	183	197	SB Lab Primer
3	9.80	CIW11	SSLP	CCCCGAGTTGAGGTATT	GAAGAAATTCCTAAAGCATTC	54	179	230	240	SB Lab Primer/Steward Gilmor
3	19.1	F24M12-TGF	SSLP	GTTCTCTGCATTCCACACATACTCT	CTTGGGTATTCTGAAGAGCATAAAT	58	151	141	131	SB Lab Primer/ Tanya Falbel
4	4.59	NGA8	SSLP	TGGCTTTCGTTTATAAACATCC	GAGGGCAAATCTTTATTTCGG	55	154	198	166	SB Lab Primer/Genomics1994
4	11.60	CIW7	SSLP	AATTTGGAGATTAGCTGGAAT	CCATGTTGATGATAAGCACAA	55	130	123	150	TAIR/ Stewart Gilmor
4	18.50	DHS1	SSLP	GAGCTTTGTAAATCAACAACC	GATATTTTTCAGGCGACGTGGAAGC	55	194	194	165	TAIR/ Pierre Berthomieu
5	1.84	NGA158	SSLP	ACCTGAACCATCCTCCGTC	TCATTTTGGCCGACTTAGC	55	108	104	120	SB Lab Primer/Genomics1994
5	11.16	NGA76	SSLP	AGGCATGGGAGACATTTACG	GGAGAAAATGTCACTCTCCACC	55	234	250	199	SB Lab Primer/Genomics1994
5	24.80	CER455033	SSLP	AGCTCATGCTTCCCTACACTG	AACAACTAGCATTAGCAACAATCA	55	130	100	130	TAIR/ Andrew Millar

Table 2.3. Rough mapping primers

Primers used for bulk segregant analysis mapping of the 45-137. Primers were either previously designed or lab stocks generated by previous lab members mutation

Fine Mapping Primers - SSLPs

				Primer Sequences				*PCR Product Size*			
Chr.	**Position (Kb)**	**Name**	**TYPE**	**Forward**	**Reverse**	**Tm**	**Enzyme**	**COL**	**LER**	**WS**	**Reference**
2	15.420	F13K3	SSLP	GACATTGGCTCTTTCTACGATTTC	TGCGTGCATGTAATATCTTATCAG	52	-	129	177	187	from TAIR
2	16.259	T7F6	SSLP	TAGAGATTGGACCCACAAGAGA	CGCTTCGACTCACAAATATTTTATG	52	-	178	178	135	from TAIR
2	17.400	CER458027	SSLP	ATTATGATTGCAGAACCAAACA	AATTCCCTCCTTTCCAAGTG	55	-	104	95	104	SB Lab Primer
2	19.326	CER449260	SSLP	TTGTCGTCAAGTCAATTTTATAAT	CATCGGAATTTGTTTGGTTTAC	52	-	139	128	139	Yana's design
2	19.338	CER449256	SSLP	GTAACCAGACCAGTTCAATTTGT	GTTCCGAGGGGCGAGGGAT	52	-	211	191	211	Yana's design
2	19.552	CER460253	SSLP	GGGTTAGTTATGAGTCTGGTTCG	CCGCCTTCTGACATCCAGTT	52	-	240	209	240	Yana's design
2	19.633	CER461445	SSLP	CTTCCTCAGTCCTTCGGGTTC	GTAACATCCCGAACTTCTGAAG	52	-	212	192	212	Yana's design

Fine Mapping Primers - CAPS & dCAPS

Chr.	**Position (Kb)**	**Name**	**TYPE**	**Forward**	**Reverse**	**Tm**	**Enzyme**	**PCR Size**	**COL**	**LER**	**WS**	**Reference**
2	19.341	F4-PK	dCAPS	TGGTGTGAAGGAAATGATGCAAGGCACCACCGAG	AATTCCCATCAACACAGTAGC	55	HinfI	431	226, 205	205, 191, 35	226, 205	Lita Po Yu
2	19.353	dYMW01	dCAPS	AGGAACGGATATGGCCACCCG	CGAATGGGATATTTCGTGCT	55	SmaI	180	180	180	159, 21	Yana's design
2	19.408	CER447606	dCAPS	GATCATAGTAATGCTGAGCAACGTC	CTCGGAATTTCATACGCACT	55	SalI	159	136, 23	159	136, 23	Yana's design
2	19.424	MTO2	CAPS	TGTATGAAGATATGTGTCTTGATTTTC	TGGGGAACCTAGAGATCCAA	55	AatII	895	~600, 295	895	~600, 295	Yana's design
2	19.434	T8I13	dCAPS	TCTTCCATTTAAAGACGAAATAGATTCGCAGGAC	GCTGCAACAATGCTTGAGGTT	52	Sau961	410	410	379, 31	410	Lita Po Yu
2	19.436	CER447619	dCAPS	GAATCGTCCATCCTATTGATCTGCA	GAGGCTAGATTTGCTGGTGA	55	PstI	181	181	156, 25	181	Yana's design
2	19.445	CER447622	dCAPS	TTCGTCTTCTCTCTGTTTCTTCGCT	CGATGCTGACATGTGGATAA	55	TaqI	154	99, 25, 30	124, 30	99, 25, 30	Yana's design
2	19.449	CER447624	dCAPS	CTGGTCGGGACTTGTATCTG	ACACCAAGTTATCACTGAATTGGTT	55	XmnI	247	226, 21	247	226, 21	Yana's design
2	19.467	CER446007	dCAPS	CCTTCTTGCTTTGGACTTGA	GTGACATGAAAGTGAGACAGGATAT	55	EcoRI	160	133, 27	160	133, 27	Yana's design
2	19.490	CER446003	dCAPS	AATTCTTCCCAAAGGACAACACAGC	AGTGGGAAATGGTGATTCTG	55	PvuII	171	147, 24	171	147, 24	Yana's design
2	19.510	DNA-BP	dCAPS	TAGAAGAACTTGGTCGTCAAG	GTCGGCAACCGGAATCTGATA	55	HinfI	708	≠LER, WS	≠COL, WS	≠COL, LER	Lita Po Yu
2	19.534	MTO4	CAPS	CGGAAAATCTCTCCCGTGAT	GACGTGAAAAGAAACAGATTTTTAGA	55	BamHI	1281	~950, 331	1281	~950, 331	Yana's design

Table 2.4. Fine mapping primers

Fine mapping SSLP, CAPS and dCAPS primers were generated specifically for mapping the 450137 mutation. CAPS markers were designed using Marker Tracker database from the University of Toronto (http://bbc.botany.utoronto.ca/markertracker/index.spy). Polymorphisms utilized for designing SSLP and dCAPS markers were designed from the CER database by comparing the COL genome on BACs T9J23, F17A22, T8I13, F14M4, F11C0 and T3F17 to Ler genome. Novel polymorphisms identified from sequencing WS DNA were used to design dCAPS primer set dYMW01. All dCAPS

AT2G47420 Sequencing Primers		
	Left Primer	***Right Primer***
Set 1	TGTTGTCACAAAAATGACATCATAA	GAAGGGAGTTCCTTGAAAACG
Set 2	GGTCCCGGTACTGGAAACTT	ACGAAGCTAGTACGGCCTGA
Set 3	AAGGAGTGGGATGGGTTCTT	TGACGATGTCATAGCAGTTTTC
AT2G47420 Cloning Primers		
	Left Primer	***Right Primer***
45137COMP	CACCCCCTGGGAAAAATCTACCATC	AGTGGGAAAGAAGCTTTGAGATT
45137PRO	CACCTCAGCAAGCATCAGGTTTGT	TGTTGCTCACTTTGCTTCTTCG
45137GFP	CACCTGGGAAAAATCTACCATCGAA	CGCTGTGAAGTGAATACCAGAC
45137OEX	CACCGAAGAAGCAAAGTGAGCAACA	CGCTGTGAAGTGAATACCAGACTTG

RT-PCR Primers			
	Left Primer	***Right Primer***	**Reference**
45137-1	AAGAACCCTCTGCTTGTGGA	AAGCTCCGTCTTGAGCACAT	
45137-2	CGAACCATTACCAAGGAGGA	GGTGGGAGACTCTGGCATAA	
EF1alphaA4	TCTTCTTGCTTTCACCCTTG	AACAACCATACCAGGCTTGA	
RT-PCR 45S rRNAProcessing Assay Primers			
	Left Primer	***Right Primer***	**Reference**
18S rRNA	GTGACGGGTGACGGAGAATTA	ACACTAAGCGCCCGGTATTG	ATRH36 PAPER
U1+U2	CGTAACGAAGATGTTCTTGGC	ATGCGTCCCTTCCATAAGTC	SWA1 paper
U3	GGGAATTGCCTGATCGATG		DEAD36 paper
IS1 + IS2	CAGCTCGCGTTGACTACGTC	GGTCGTTCTGTTTTGGACAG	DEAD 36 paper
Primer Extension Primer			
18sPE	CAATGATCCTTCCGCA		

Table 2.5. Miscellaneous primers used in this study

Primers used for sequencing At2g47420, cloning, RT-PCR and primer extension.

Literature Cited

Abbasi, N, Kim, HB, Park, N-I, Kim, H-S, Kim, Y-K, Park, Y-I & Choi, S-B (2010) APUM23, a nucleolar Puf domain protein, is involved in pre-ribosomal RNA processing and normal growth patterning in *Arabidopsis*. *Plant J.,* 64**,** 960-976.

Ahmad, Y, Boisvert, F-M, Gregor, P, Cobley, A & Lamond, AI (2009) NOPdb: Nucleolar Proteome Database--2008 update. *Nuc. Acids Res.,* 37**,** D181-D184.

Apirion, D & Saltzman, L (1974) Functional interdependence of 50S and 30S ribosomal subunits. *Mol Gen Genet,* 135**,** 11-8.

Beemster, GT & Baskin, TI (1998) Analysis of cell division and elongation underlying the developmental acceleration of root growth in Arabidopsis thaliana. *Plant Physiol.,* 116**,** 1515-26.

Berger, F, Hung, CY, Dolan, L & Schiefelbein, J (1998) Control of cell division in the root epidermis of *Arabidopsis thaliana*. *Dev. Biol.,* 194**,** 235-45.

Berleth, T, Mattsson, J & Hardtke, CS (2000) Vascular continuity and auxin signals. *Trends Plant Sci.,* 5**,** 387-93.

Bernhardt, C, Lee, MM, Gonzalez, A, Zhang, F, Lloyd, A & Schiefelbein, J (2003) The bHLH genes *GLABRA3 (GL3)* and *ENHANCER OF GLABRA3 (EGL3)* specify epidermal cell fate in the *Arabidopsis* root. *Development,* 130**,** 6431-6439.

Bernhardt, C, Zhao, M, Gonzalez, A, Lloyd, A & Schiefelbein, J (2005) The bHLH genes *GL3* and *EGL3* participate in an intercellular regulatory circuit that controls cell patterning in the *Arabidopsis* root epidermis. *Development,* 132**,** 291-298.

Birnbaum, K, Shasha, DE, Wang, JY, Jung, JW, Lambert, GM, Galbraith, DW & Benfey, PN (2003) A gene expression map of the *Arabidopsis* root. *Science,* 302**,** 1956-1960.

Boschetti, A & Bogdanov, S (1973) Binding of dihydrostreptomycin to ribosomes and ribosomal subunits from streptomycin-resistant mutants of Chlamydomonas reinhardi. *FEBS letters,* 38**,** 19-22.

Brown, JWS & Shaw, PJ (1998) Small Nucleolar RNAs and Pre-rRNA Processing in Plants. *Plant Cell,* 10**,** 649-657.

Byrne, M (2009) A role for the ribosome in development. *Trends Plant Sci.,* 14**,** 512-519.

Carter, AP, Clemons, WM, Brodersen, DE, Morgan-Warren, RJ, Wimberly, BT & Ramakrishnan, V (2000) Functional insights from the structure of the 30S ribosomal subunit and its interactions with antibiotics. *Nature,* 407**,** 340-8.

Clough, SJ & Bent, AF (1998) Floral dip: a simplified method for Agrobacterium-mediated transformation of Arabidopsis thaliana. *The Plant journal : for cell and molecular biology,* 16**,** 735-43.

Connolly, K, Rife, JP & Culver, G (2008) Mechanistic insight into the ribosome biogenesis functions of the ancient protein KsgA. *Mol. Microbiol.,* 70**,** 1062-75.

Creff, A, Sormani, R & Desnos, T (2010) The two *Arabidopsis RPS6* genes, encoding for cytoplasmic ribosomal proteins S6, are functionally equivalent. *Plant Mol. Biol.,* 73**,** 533-546.

Decatur, W & Fournier, M (2002) rRNA modifications and ribosome function. *Trends in Biochemical Sciences,* 27**,** 344-351.

Degenhardt, RF & Bonham-Smith, PC (2008) *Arabidopsis* ribosomal proteins RPL23aA and RPL23aB are differentially targeted to the nucleolus and are disparately required for normal development. *Plant Physiol.,* 147**,** 128-42.

Demirci, H, Murphy, F, Belardinelli, R, Kelley, AC, Ramakrishnan, V, Gregory, ST, . . . Jogl, G (2010) Modification of 16S ribosomal RNA by the KsgA methyltransferase restructures the 30S subunit to optimize ribosome function. *RNA,* 16**,** 2319-2324.

Di Cristina, M, Sessa, G, Dolan, L, Linstead, P, Baima, S, Ruberti, I & Morelli, G (1996) The *Arabidopsis* Athb-10 (GLABRA2) is an HD-Zip protein required for regulation of root hair development. *Plant J.,* 10**,** 393-402.

Dolan, L, Duckett, CM, Grierson, C, Linstead, P, Schneider, K, Lawson, E, . . . Roberts, K (1994) Clonal relationships and cell patterning in the root epidermis of *Arabidopsis*. *Development,* 120**,** 2465-2474.

Dolan, L, Janmaat, K, Willemsen, V, Linstead, P, Poethig, S, Roberts, K & Scheres, B (1993) Cellular organisation of the *Arabidopsis thaliana* root. *Development,* 119**,** 71-84.

Dragon, F, Gallagher, JEG, Compagnone-Post, PA, Mitchell, BM, Porwancher, KA, Wehner, KA, . . . Osheim, Y (2002) A large nucleolar U3 ribonucleoprotein required for 18S ribosomal RNA biogenesis. *Nature,* 417**,** 967-970.

Fatica, A & Tollervey, D (2002) Making ribosomes. *Current Opinion in Cell Biology,* 14**,** 313-318.

Fujikura, U, Horiguchi, G, Ponce, MR, Micol, JL & Tsukaya, H (2009) Coordination of cell proliferation and cell expansion mediated by ribosome-related processes in the leaves of *Arabidopsis thaliana*. *Plant J,* 59**,** 499-508.

Gabashvili, IS, Gregory, ST, Valle, M, Grassucci, R, Worbs, M, Wahl, MC, . . . Frank, J (2001) The polypeptide tunnel system in the ribosome and its gating in erythromycin resistance mutants of L4 and L22. *Molecular Cell,* 8**,** 181-8.

Galway, ME, Massucci, JD, Lloyd, A, Walbot, V, Davis, RW & Schiefelbein, J (1994) The *TTG* Gene is Required to Specify Epidermal Cell Fate and Cell Patterning in the *Arabidopsis* Root. *Dev. Biol.,* 166**,** 740-754.

Ganot, P, Bortolin, M-L & Kiss, T (1997) Site-specific pseudouridine formation in preribosomal RNA is guided by small nucleolar RNAs. *Cell,* 89**,** 799-809.

Gendreau, E, Traas, J, Desnos, T, Grandjean, O, Caboche, M & Hofte, H (1997) Cellular basis of hypocotyl growth in Arabidopsis thaliana. *Plant Physiol.,* 114**,** 295-305.

Hagenbuchle, O, Santer, M, Steitz, JA & Mans, RJ (1978) Conservation of the primary structure at the 3' end of 18S rRNA from eucaryotic cells. *Cell,* 13**,** 551-63.

Helser, TL, Davies, JE & Dahlberg, JE (1972) Mechanism of kasugamycin resistance in *Escherichia coli*. *Nature New Biol,* 235**,** 6-9.

Huang, CK, Huang, LF, Huang, JJ, Wu, SJ, Yeh, CH & Lu, CA (2010) A DEAD-Box Protein, AtRH36, is Essential for Female Gametophyte Development and is Involved in rRNA Biogenesis in *Arabidopsis*. *Plant and Cell Physiology,* 51**,** 694-706.

Ito, T, Kim, GT & Shinozaki, K (2000) Disruption of an *Arabidopsis* cytoplasmic ribosomal protein S13-homologous gene by transposon-mediated mutagenesis causes aberrant growth and development. *Plant J,* 22**,** 257-64.

Ivanov, VB, Dobrochaev, AE & Baskin, TI (2002) What the Distribution of Cell Lengths in the Root Meristem Does and Does Not Reveal About Cell Division. *J. Plant Growth Reg.,* 21**,** 60.

Jander, G, Norris, SR, Rounsley, SD, Bush, DF, Levin, IM & Last, RL (2002) *Arabidopsis* map-based cloning in the post-genome era. *Plant Physiol,* 129**,** 440-50.

Kawaguchi, R & Bailey-Serres, J (2002) Regulation of translational initiation in plants. *Curr. Opin. Plant Biol.,* 5**,** 460-5.

Kirik, V, Simon, M, Huelskamp, M & Schiefelbein, J (2004) The *ENHANCER OF TRY AND CPC1* gene acts redundantly with *TRIPTYCHON* and *CAPRICE* in trichome and root hair cell patterning in *Arabidopsis*. *Dev. Biol.,* 268**,** 506-513.

Kiss-Laszlo, Z, Henry, Y, Bachellerie, J-P, Caizergues-Ferrer, ML & Kiss, T (1996) Site-specific ribose methylation of preribosomal RNA: a novel function for small nucleolar RNAs. *Cell,* 85**,** 1077-1088.

Kojima, H, Suzuki, T, Kato, T & Enomoto, K (2007) Sugar-inducible expression of the nucleolin-1 gene of *Arabidopsis thaliana* and its role in ribosome synthesis, growth and development. *Plant J.,* 49**,** 1053-1063.

Koornneef, M (1981) The complex syndrome of *ttg* mutants. *Arabid. Inf. Serv.***,** 45-51.

Koshino-Kimura, Y, Wada, T, Tachibana, T, Tsugeki, R, Ishiguro, S & Okada, K (2005) Regulation of *CAPRICE* Transcription by MYB Proteins for Root Epidermis Differentiation in *Arabidopsis*. *Plant Cell Physiol.,* 46**,** 817-826.

Kwak, S-H & Schiefelbein, J (2007) The role of the SCRAMBLED receptor-like kinase in patterning the *Arabidopsis* root epidermis. *Dev. Biol.,* 302**,** 118-131.

Kwak, S-H & Schiefelbein, J (2008) A feedback mechanism controlling SCRAMBLED receptor accumulation and cell-type pattern in *Arabidopsis*. *Curr Biol,* 18**,** 1949-1954.

Kwak, S-H, Shen, R & Schiefelbein, J (2005) Positional signaling mediated by a receptor-like kinase in *Arabidopsis*. *Science,* 307**,** 1111-1113.

Lafontaine, D, Delcour, J, Glasser, AL, Desgres, J & Vandenhaute, J (1994) The *DIM1* Gene Responsible for the Conserved m62Am62A Dimethylation in the 3'-Terminal Loop of 18S rRNA is Essential in Yeast. *J Mol Biol,* 241**,** 492-497.

Lafontaine, D, Preiss, T & Tollervey, D (1998) Yeast 18S rRNA dimethylase Dim1p: a quality control mechanism in ribosome synthesis? *Mol Cell Biol,* 18**,** 2360-70.

Lafontaine, D, Vandenhaute, J & Tollervey, D (1995) The 18S rRNA dimethylase Dim1p is required for pre-ribosomal RNA processing in yeast. *Genes Dev.,* 9**,** 2470-2481.

Lee, MM & Schiefelbein, J (1999) WEREWOLF, a MYB-Related Protein in *Arabidopsis*, Is a Position-Dependent Regulator of Epidermal Cell Patterning. *Cell,* 99**,** 473-483.

Lee, MM & Schiefelbein, J (2002) Cell Pattern in the *Arabidopsis* Root Epidermis Determined by Lateral Inhibition with Feedback. *Plant Cell,* 14**,** 611-618.

Lukowitz, W, Gilmor, CS & Scheible, W-R (2000) Positional Cloning in *Arabidopsis*. Why it Feels Good to Have a Genome Initiative Working For You. *Plant Physiol.,* 123**,** 1795-8051.

Martin, J & Mcmillan, F (2002) SAM (dependent) I AM: the S-adenosylmethionine-dependent methyltransferase fold. *Current Opinion in Structural Biology,* 12**,** 783-793.

Massucci, JD, Rerie, WG, Foreman, DR, Zhang, M, Galway, ME, David Marks, M & Schiefelbein, J (1996) The homeobox gene *GLABRA2* is required for position-dependent cell differentiation in the root epidermis of *Arabidopsis thaliana*. *Development,* 122**,** 1253-1260.

Mccloskey, JA & Rozenski, J (2005) The Small Subunit rRNA Modification Database. *Nuc. Acids Res.,* 33**,** D135-8.

Nishimura, T, Wada, T, Yamamoto, KT & Okada, K (2005) The *Arabidopsis* STV1 protein, responsible for translation reinitiation, is required for auxin-mediated gynoecium patterning. *Plant Cell,* 17**,** 2940-53.

O'connor, M, Thomas, CL, Zimmermann, RA & Dahlberg, AE (1997) Decoding fidelity at the ribosomal A and P sites: influence of mutations in three different regions of the decoding domain in 16S rRNA. *Nuc. Acids Res.,* 25**,** 1185-1193.

O'farrell, H, Scarsdale, J & Rife, JP (2004) Crystal Structure of KsgA, a Universally Conserved rRNA Adenine Dimethyltransferase in Escherichia coli. *J Mol Biol,* 339**,** 337-353.

O'farrell, H, Xu, Z, Culver, G & Rife, JP (2008) Sequence and structural evolution of the KsgA/Dim1 methyltransferase family. *BMC Research Notes,* 1**,** 108.

Ofengand, J (2002) Ribosomal RNA pseudouridines and pseudouridine synthases. *FEBS letters,* 514**,** 17-25.

Ohashi, Y, Oka, A, Rodrigues-Pousada, R, Possenti, M, Ruberti, I, Morelli, G & Aoyama, T (2003) Modulation of Phospholipid Signaling by *GLABRA2* in Root-Hair Pattern Formation. *Science,* 300**,** 1427-1430.

Ohbayashi, I, Konishi, M, Ebine, K & Sugiyama, M (2011) Genetic identification of Arabidopsis RID2 as an essential factor involved in pre-rRNA processing. *Plant J., In press*.

Pesch, M & Hulskamp, M (2004) Creating a two-dimensional pattern de novo during Arabidopsis trichome and root hair initiation. *Curr Opin Genet Dev,* 14**,** 422-7.

Petricka, J & Nelson, T (2007) *Arabidopsis* nucleolin affects plant development and patterning. *Plant Physiol.,* 144**,** 173-186.

Poehlsgaard, J & Douthwaite, S (2005) The bacterial ribosome as a target for antibiotics. *Nature reviews. Microbiology,* 3**,** 870-81.

Poldermans, B, Goosen, N & Van Knippenberg, PH (1979a) Studies on the Function of Two Adjacent N",N"-Dimethyladenosines Near the 3' End of 16 S Ribosomal RNA of *Escherichia coli* I.THE EFFECT OF KASUGAMYCIN ON INITIATION OF PROTEIN SYNTHESIS. *The Journal of Biological Chemistry,* 254**,** 9085-9089.

Poldermans, B, Roza, L & Van Knippenberg, PH (1979b) Studies on the Function of Two Adjacent iV,W-Dimethyladenosines Near the 3' End of 16 S Ribosomal RNA of *Escherichia coli* III. PURIFICATION AND PROPERTIES OF THE METHYLATING ENZYME AND METHYLASE-30S INTERACTIONS. *The Journal of Biological Chemistry,* 254**,** 9094-9100.

Poldermans, B, Van Buul, CPJJ & Van Knippenberg, PH (1979c) Studies on the Function of Two Adjacent N6,N6-Dimethyladenosines Near the 3' End of 16 S Ribosomal RNA of *Escherichia coli*. *The Journal of Biological Chemistry,* 254**,** 9090-9094.

Pontvianne, F, Matia, I, Douet, J, Tourmente, S, Medina, FJ, Echeverria, M & Saez-Vasquez, J (2007) Characterization of *AtNUC-L1* Reveals a Central Role of Nucleolin in Nucleolus Organization and Silencing of *AtNUC-L2* Gene in *Arabidopsis*. *Mol Biol Cell,* 18**,** 369-379.

Pulicherla, N, Pogorzala, L, Xu, Z, O'farrell, H, Musayev, FN, Scarsdale, JN, . . . Rife, JP (2009) Structural and Functional Divergence within the Dim1/KsgA Family of rRNA Methyltransferases. *J Mol Biol,* 391**,** 884-893.

Ramirez-Parra, E, Gutierrez, C & Frundtand, C (2003) A genome-wide identification of E2F-regulated genes in *Arabidopsis*. *Plant J.,* 33**,** 801-811.

Rerie, W, Feldmann, K & David Marks, M (1994) The *GLABRA2* gene encodes a homeo domain protein required for normal trichome development in *Arabidopsis*. *Genes Dev.,* 8**,** 1388-1399.

Richter, U, Kühn, K, Okada, S, Brennicke, A, Weihe, A & Börner, T (2010) A mitochondrial rRNA dimethyladenosine methyltransferase in *Arabidopsis*. *Plant J.,* 61**,** 558-69.

Rosado, A, Sohn, EJ, Drakakaki, G, Pan, S, Swidergal, A, Xiong, Y, . . . Raikhel, NV (2010) Auxin-mediated ribosomal biogenesis regulates vacuolar trafficking in *Arabidopsis*. *Plant Cell,* 22**,** 143-58.

Ryu, KH, Kang, YH, Park, Y-H, Hwang, I, Schiefelbein, J & Lee, MM (2005) The WEREWOLF MYB protein directly regulates CAPRICE transcription during cell fate specification in the Arabidopsis root epidermis. *Development,* 132**,** 4765-4775.

Schellmann, S, Hulskamp, M & Uhrig, J (2007) Epidermal pattern formation in the root and shoot of *Arabidopsis*. *Biochem. Soc. Trans.,* 35**,** 146-148.

Schellmann, S, Schnittger, A, Kirik, V, Wada, T, Okada, K, Beermann, A, . . . Hülskamp, M (2002) TRIPTYCHON and CAPRICE mediate lateral inhibition during trichome and root hair patterning in *Arabidopsis*. *EMBO J.,* 21**,** 5036-5046.

Scheres, B, Wolkenfelt, H, Willemsen, V, Terlouw, M, Lawson, E, Dean, C & Weisbeek, P (1994) Embryonic origin of the *Arabidopsis* primary root and root meristem initials. *Development,* 120**,** 2475-2475.

Schiefelbein, J, Kwak, S-H, Wieckowski, Y, Barron, C & Bruex, A (2009) The gene regulatory network for root epidermal cell-type pattern formation in *Arabidopsis*. *J. Exp. Bot.,* 60**,** 1515-1521.

Schiefelbein, JW & Somerville, C (1990) Genetic Control of Root Hair Development in Arabidopsis thaliana. *Plant Cell,* 2**,** 235-243.

Schluenzen, F, Takemoto, C, Wilson, DN, Kaminishi, T, Harms, JM, Hanawa-Suetsugu, K, . . . Fucini, P (2006) The antibiotic kasugamycin mimics mRNA nucleotides to destabilize tRNA binding and inhibit canonical translation initiation. *Nat Struct Mol Biol,* 13**,** 871-878.

Seshadri, A, Dubey, B, Weber, MHW & Varshney, U (2009) Impact of rRNA methylations on ribosome recycling and fidelity of initiation in Escherichia coli. *Mol. Microbiol.,* 72**,** 795-808.

Shi, D-Q, Liu, J, Xiang, Y-H, Ye, D, Sundaresan, V & Yang, W-C (2005) *SLOW WALKER1*, essential for gametogenesis in *Arabidopsis*, encodes a WD40 protein involved in 18S ribosomal RNA biogenesis. *Plant Cell,* 17**,** 2340-54.

Simon, M, Lee, MM, Lin, Y, Gish, L & Schiefelbein, J (2007) Distinct and overlapping roles of single-repeat MYB genes in root epidermal patterning. *Dev. Biol.,* 311**,** 566-578.

Tokuhisa, J, Vijayan, P, Feldmann, K & Browse, J (1998) Chloroplast Development at Low Temperatures Requires a Homolog of *DIM1*, a Yeast Gene Encoding the 18S rRNA Dimethylase. *Plant Cell,* 10.

Tominaga, R, Iwata, M, Okada, K & Wada, T (2007) Functional analysis of the epidermal-specific MYB genes *CAPRICE* and *WEREWOLF* in *Arabidopsis*. *Plant Cell,* 19**,** 2264-77.

Trimarchi, JM & Lees, JA (2002) Sibling rivalry in the E2F family. *Nat Rev Mol Cell Biol,* 3**,** 11-20.

Tu, C, Tropea, JE, Austin, BP, Court, DL, Waugh, DS & Ji, X (2009) Structural Basis for Binding of RNA and Cofactor by a KsgA Methyltransferase. *Structure/Folding and Design,* 17**,** 374-385.

Udem, SA & Warner, JR (1973) The cytoplasmic maturation of a ribosomal precursor ribonucleic acid in yeast. *Journal of Biological Chemistry,* 248**,** 1412-1416.

Ueda, M, Koshino-Kimura, Y & Okada, K (2005) Stepwise understanding of root development. *Curr. Opin. Plant Biol.,* 8**,** 71-76.

Van Buul, CPJJ, Visser, W & Can Knippenberg, PH (1984) Increased translational fidelity caused by the antibiotic kasugamycin and ribosomal ambiguity in mutants harbouring the *ksgA* gene. *FEBS letters,* 177**,** 119-124.

Van Knippenberg, PH, Van Kimmenade, JMA & Heus, HA (1984) Phylogeny of tbe conserved 3' terminal structure of the RNA of small ribosomal subunits. *Nuc. Acids Res.,* 12**,** 2595-2604.

Van Lijsebettens, M, Vanderhaeghen, R, Block, MD, Bauw, G, Villarroel, R & Van Montagu, M (1994) An S18 ribosomal protein gene copy at the *Arabidopsis PFL* locus affects plant development by its specific expression in meristems. *EMBO J.,* 13**,** 3378-3388.

Venema, J & Tollervey, D (1999) Ribosome synthesis in *Saccharomyces cerevisiae*. *Annual review of genetics,* 33**,** 261-311.

Volarevic, S, Stewart, MJ, Ledermann, B, Zilberman, F, Terracciano, L, Montini, E, . . . Thomas, G (2000) Proliferation, but not growth, blocked by conditional deletion of 40S ribosomal protein S6. *Science,* 288**,** 2045-2047.

Wada, T, Kurata, T, Tominaga, R, Koshino-Kimura, Y, Tachibana, T, Goto, K, . . . Okada, K (2002) Role of a positive regulator of root hair development, *CAPRICE*, in *Arabidopsis* root epidermal cell differentiation. *Development,* 129**,** 5409-5419.

Wada, T, Tachibana, T, Shimura, Y & Okada, K (1997) Epidermal Cell Differentiation in *Arabidopsis* Determined by a Myb Homolog, *CPC*. *Science,* 277**,** 1113-1116.

Weigel, D & Glazebrook, J 2002. *Arabidopsis: A Laboratory Manual.*, Cold Springs Harbor Laboratory Press, Cold Spring Harbor, NY.

Winter, D, Vinegar, B, Nahal, H, Ammar, R, Wilson, GV & Provart, NJ (2007) An "Electronic Fluorescent Pictograph" browser for exploring and analyzing large-scale biological data sets. *PLoS One,* 2**,** e718.

Xu, Z, O'farrell, H, Rife, JP & Culver, G (2008) A conserved rRNA methyltransferase regulates ribosome biogenesis. *Nature Structural and Molecular Biology,* 15**,** 534-536.

Zakrzewska-Placzek, M, Souret, FF, Sobczyk, GJ, Green, PJ & Kufel, J (2010) *Arabidopsis thaliana XRN2* is required for primary cleavage in the pre-ribosomal RNA. *Nuc. Acids Res.,* 38**,** 4487-502.

Zhang, F, Gonzalez, A, Zhao, M, Payne, C & Lloyd, A (2003) A network of redundant bHLH proteins functions in all TTG1-dependent pathways of *Arabidopsis*. *Development,* 130**,** 4859-4869.

Zimmermann, P, Hirsch-Hoffmann, M, Hennig, L & Gruissem, W (2004) GENEVESTIGATOR. Arabidopsis microarray database and analysis toolbox. *Plant Physiol.,* 136**,** 2621-32.

CHAPTER 3

Identification of Novel Epidermal Patterning Genes Using Cell-Type-Specific Microarray Analysis

Abstract

Specialization of different cell types is paramount in the development of multicellular organisms. This cell-type specification depends, to a large degree, on the tissue- or cell-type-specific expression of genes. The *Arabidopsis* root epidermis contains two types of cells, hair cells and non-hair cells, which arise in a stereotyped pattern influenced by cell position. Extensive genetic research has identified a complex molecular network within epidermal cells which is involved in specifying position-dependent cell fate. While much of what is known about the patterning genes necessary for cells to be specified as root-hair or non-hair cells, little is known about the downstream targets of this patterning network. The development of a technique to study transcriptional changes in individual cell types and tissues within plants has provided the opportunity to learn about specific patterns of gene expression.

In this study, we use this specialized technique, which combines microarray analysis and fluorescence activated cell sorting, to compare transcriptomes from unique populations of *Arabidopsis* root epidermal cells. First, we analyzed the transcriptome of the loss-of-function mutant in the gene *SCRAMBLED*, which encodes a leucine-rich repeat receptor-like kinase essential for position-dependent root epidermal cell-type specification. This allowed us to examine the effect of a disruption in the SCM-signaling pathway, which provides essential positional information to the epidermal patterning gene network. Second, we compared the transcriptome of epidermal cells from roots of a genetic background that completely lack hair cells ("hairless") and a genetic background that has root-hair cells specified at every position ("hairy"). Comparison of these two transcriptomes has provided a detailed glimpse into the genetic control of root hair and non-hair cell development.

Introduction

Microarray technology has revolutionized our ability to monitor whole genome expression, greatly enhancing our knowledge and understanding of gene regulatory networks (Long *et al.*, 2008). It is now possible to monitor output of the entire genome within individual cell types, tissues, and organs (Birnbaum *et al.*, 2005, Birnbaum *et al.*, 2003, Brady *et al.*, 2007). Philip Benfey and Kenneth Birnbaum pioneered such analysis in the root of *Arabidopsis thaliana* by combining protoplasting of root tissue expressing specific cell- and tissue-type

fluorescent reporter constructs with Fluorescent Activated Cell Sorting (FACS) to isolate specific populations of cells (Birnbaum *et al.*, 2005, Birnbaum *et al.*, 2003, Brady *et al.*, 2007). Not only did this work pave the way for future research, but their in-depth analysis also provided a high-resolution map of the root transcriptome.

Over the last twenty years, the *Arabidopsis* root epidermis has emerged at the forefront of analysis of transcriptional regulation during development. The *Arabidopsis* root epidermis contains two types of cells, root-hair cells and non-hair cells, which arise in a stereotyped pattern influenced by cell position. Research to date has defined a gene regulatory network involved in specifying the two distinct root epidermal cell fates. Five genes, *WEREWOLF (WER)*, *GLABRA3 (GL3)*, *ENHANCER OF GLABRA3 (EGL3)*, *TRANSPARENT TESTA GLABRA1 (TTG1)* and *GLABRA2 (GL2)* are required to specify the non-hair fate (Bernhardt *et al.*, 2003, Galway *et al.*, 1994, Lee and Schiefelbein, 1999, Massucci *et al.*, 1996). Current models suggest that WER (an R2R3 MYB-domain protein)(Lee and Schiefelbein, 1999), GL3/EGL3 (related bHLH proteins) (Bernhardt *et al.*, 2003, Bernhardt *et al.*, 2005), and TTG1 (a WD40-repeat protein) (Galway *et al.*, 1994) work together as a transcriptional activation complex to influences non-hair cell fate by directly regulating expression *GL2*, a homeodomain transcription factor necessary for non-hair cell specification(Lee and Schiefelbein, 2002, Massucci *et al.*, 1996, Rerie *et al.*, 1994). Three additional epidermal patterning network genes, *CAPRICE (CPC)*, *TRIPTYCHON (TRY)* and *ENHANCER OF CPC AND TRY (ETC1),* which encode single-repeat

R3 MYB-domain proteins, act semi-redundantly to influence hair cell fate (Kirik *et al.*, 2004, Schellmann *et al.*, 2002, Wada *et al.*, 2002, Wada *et al.*, 1997). CPC, TRY, and ETC1 promote root-hair cell fate by competing with WER for binding to the other transcriptional activation complex members (TTG1-GL3/EGL3) (Lee and Schiefelbein, 2002, Tominaga *et al.*, 2007). Interestingly, *CPC*, *TRY* and *ETC1* are expressed in N position cells (Kirik *et al.*, 2004, Simon *et al.*, 2007, Wada *et al.*, 2002) and the proteins then move to cells in the H position, presumably through the plasmodesmata (Kurata *et al.*, 2005, Wada *et al.*, 2002). Furthermore, the transcriptional activation complex in N position cells promotes transcription of *CPC*, *TRY* and *ETC1*, suggesting that these single-repeat MYB proteins function as part of a lateral inhibition pathway between epidermal cells (Lee and Schiefelbein, 2002, Simon *et al.*, 2007, Wada *et al.*, 2002).

A potential target of the molecular fate-specification network cells is *ROOT HAIR DEFECTIVE 6 (RHD6)* (Massucci and Schiefelbein, 1994, Menand *et al.*, 2007). Roots of *rhd6* mutant plants contain significantly fewer hairs due to a defect in root hair initiation (Massucci and Schiefelbein, 1994), which functions dowstream of the cell-type patterning network (Menand *et al.*, 2007). *RHD6* is one of six members of the bHLH transcription factor subfamily VIIIc, which include *RHD6-LIKE 1 (RSL1),* a recently identified gene involved in root hair development (Menand *et al.*, 2007). *RHD6* is also related to bHLH protein encoding patterning network genes *GL3* and *EGL3*, which belong to bHLH subfamily IIIf (Heim *et al.*, 2003). The bHLH subfamily IIIf also includes *MYC1*, which is believed to play a role in root hair patterning (C.Bernhardt., M. Sridharan

and J.Schiefelbein., unpublished). While multiple members of bHLH subfamily IIIf have been shown to have similar functions in epidermal patterning, the role of the four other subfamily VIIIc (in addition to RHD6 and RSL1) as well as members of other closely related subfamilies in root cell-type development have not yet been investigated.

SCRAMBLED (SCM), which encodes a leucine-rich repeat receptor-like kinase (LRR-RLK), is necessary for the position-dependence of root epidermal cell fate specification (Kwak *et al.*, 2005). Loss-of-function mutations in *SCM* make a similar frequency of hair cells as wild-type, however there is a remarkable disconnect between cell fate and position (Kwak *et al.*, 2005). As *SCM* encodes a receptor-like kinase localized to the plasma membrane of epidermal cells it is likely to receive a positional signal and translate it to underlying epidermal cells (Kwak and Schiefelbein, 2008). Surprisingly, biochemical and genetic evidence indicates that while the carboxyl-terminal kinase domain is necessary for function, it appears to be catalytically inactive (Chevalier *et al.*, 2005). Thus, it is likely that SCM acts as an atypical receptor-like kinase, functioning through protein-protein interactions with yet-to-be-determined signaling partners (Chevalier *et al.*, 2005). Detailed genetic analysis has determined that SCM likely influences the molecular network within epidermal cells by repressing *WER* transcription in H position cells (Kwak and Schiefelbein, 2007). However, to date the mechanism of *WER* regulation by SCM is currently unknown.

The wealth of information gleaned from transcriptome studies of individual

tissue and cell types as well as in different mutant backgrounds has provided an immeasurable amount of data available for more thorough analysis. While a lot can be inferred from systems biology analysis of gene regulatory network, investigation of specific genes identified through these large-scale analyses is necessary to verify the methodology used and to reveal the function of individual gene-products.

The discovery of *SCM* has greatly enriched our knowledge of the molecular network governing position-dependent cell-fate specification in the *Arabidopsis* root epidermis, however there is a clear need for further analysis. In addition, an emerging view of the role of related bHLH transcription factors in root epidermal cell fate specification and root hair development warrants further analysis of related family members of unknown function. In this study we used available microarray data from two separate comparisons, *scm-2* vs. wild-type and "hairless" (*cpc try etc1* triple mutant) vs. a "hairy" (*wer myb23* double mutant), to identify genes involved in root epidermal cell-type patterning and differentiation.

Materials and Methods

Microarray analysis

Microarray analysis of root epidermal cells was conducted according to a modified version of the protocol described in (Birnbaum *et al.*, 2003) and as laid out in the Materials and Methods section of Chapter Two of this thesis. Microarray analysis from wild-type and *scm-2* (a putative null-allele (Kwak *et al.*,

2005)) was conducted by both our lab and the Benfey Lab (Duke University) from both whole root tissue as well as *WER::GFP*-sorted epidermal cells. Microarray analysis of the "hairy" and "hairless" genetic backgrounds was conducted using *WER::GFP*-sorted root epidermal cells of the *wer myb23* double mutant (hairy) and *cpc try etc1 triple* mutant (hairless) lines (Kang *et al.*, 2009, Simon *et al.*, 2007).

Bioinformatic analysis

After statistical analysis, we screened the resulting microarray data for genes that were differentially expressed between the wild-type and *scm-2*. Insertion lines for genes of interest were identified from the SALK database (http://signal.salk.edu/cgi-bin/tdnaexpress) and were ordered through the Arabidopsis Biological Resource Center (ABRC; http://abrc.osu.edu/).

Plant work

Seeds received from ABRC were surface-sterilized using a 30% sodium hypochlorite/1% tritonX-100 solution, stratified for two days in water at 4°C and subsequently germinated and grown in petri dishes on agarose-solidified MS media (0.433% MS salts, 1% sucrose, 0.02 % MES, 0.6% agarose, pH 5.8) under 24h light (Schiefelbein and Somerville, 1990). Plants grown on plates were transferred seven to ten days post germination to soil supplemented with Osmocote (Scotts). Unless otherwise specified, *Arabidopsis* soil-grown plants were incubated at 22°C under long-day conditions in growth chambers.

Genotyping

DNA was extracted from pools of ten to twelve seedlings by grinding tissue with a pestle in an micro-centrifuge tube containing DNA extraction buffer (200 mM Tris-HCl pH 7.5, 250 mM NaCl, 25 mM EDTA, 0.5% SDS). After centrifugation to remove debris, DNA was precipitated with an equal volume of 100% isopropanol and resuspended in water.

Primers for genotyping insertion lines were designed using the T-DNA primer design software from SALK (http://signal.salk.edu/tdnaprimers.2.html). Primer sequences and further genotyping information can be found in Table 3.3.

Microscopy

The pattern of epidermal cell types was determined by staining seedling roots with Toluidine Blue, followed by examination at 160X magnification to determine locations of epidermal cells relative to the anticlinal cortical cell wall. The pattern of root-hair and non-hair cell types in the epidermis was determined by examining at least 20 seedlings from each strain. Ten cells in both the hair position (H position) and non-hair position (N position) were counted for each seedling root. An epidermal cell was scored as a root-hair cell if any protrusion was visible, regardless of its length. Analysis of hair branching was conducted by analyzing 50 hairs per root for ten individual roots.

Results and Discussion

Analysis of genes from *scm-2* vs. wild-type microarray analysis.

To identify new genes essential for position-dependent cell fate specification in the root epidermis, we investigated the gene expression changes in the *scm-2* mutant at the transcriptome level. Six individual microarray analyses, three biological repeats each with one wild-type and one *scm-2*, were conducted. Genes of interest were identified due to either a significant increase or decrease in transcript levels in the *scm-2* mutant when compared to the wild-type background. An initial list of genes of interest was compared to the SALK database and adequate mutant lines were ordered for 43 different loci. Root epidermal cell fate specification was analyzed for confirmed homozygous insertion lines (Table 3.1).

Root cell-type patterning analysis of insertion mutant lines resulted in four categories of patterning: (1) wild-type pattern, (2) hairy pattern (due to increased specification of hair cells), (3) hairless pattern (due to increased specification of non-hair cells), and (4) *scrambled*-like pattern (*i.e*. a disruption in the position-dependent aspect of cell-type patterning). While a majority of the insertion lines displayed a wild-type pattern of root-hair and non-hair cells in the epidermis, a few were identified to have either a hairy, hairless or *scrambled*-like pattern of epidermal cells.

Primary screening identified two insertion lines showing mild hairy-root phenotypes. The insertion line in loci At2g45420 (SALK_112078) and

At4g26540/At4g26554 (SALK_ 053167) had increased hair cells specified in the N position (22% and 25%, respectively, compared to 0% in wild-type). This suggests that the two genes represented by At2g45420 and At4g26540 may function to repress specification or differentiation of the root-hair cell fate or promote specification on the non-hair cell fate in the root epidermis. The At2g45420 loci corresponds to the *LBD18/ASL20* (*LOB-domain containing 18/ASYMMETRIC LEAVES 2-LIKE 20*) gene which has been shown to be involved in formation of lateral roots (Lee *et al.*, 2009). *LBD18/ASL20* is highly expressed in lateral root primordia and was shown to function together with *LBD16*, which encodes a related LOB-domain protein, upstream of auxin-response genes in promoting lateral root emergence (Lee *et al.*, 2009). The second insertion line to show a mild hairy-root phenotype, SALK_053167, contains a T-DNA insertion in two overlapping genes, the gene at locus At4g26540, which encodes a putative leucine-rich repeat receptor-like kinase, and At4g26542, which encodes a potential natural antisense gene. Further analysis is needed to confirm and investigate the role of these genes in epidermal cell-type patterning.

In addition, we identified three insertion lines exhibiting mild hairless-root phenotypes. The insertion lines in loci At4g23670 (SALK_088249), At3g05630 (SALK_ 119085), and At2g46790 (SALK_106072) all had increased non-hair cells in the H position (13%, 15%, and 17%, respectively, compared to 5% in wild-type). This suggests that the three genes represented by At4g23670, At3g05630, and At2g46790 may function to repress specification or

differentiation of the non-hair cell fate in the root epidermis. The gene represented by At4g23670 encodes a putative polyketide cyclase/dehydrase and lipid transport superfamily protein involved in response to stress. Interestingly, according to microarray analysis databases At4g23670 is not normally expressed in the root (eFP: Winter et al 2007). The microarray comparison between wild-type and *scm-2* root tissue showed that At4g23670 is up regulated by 48.1 fold in the *scm-2* background. Thus, it is possible that At4g23670 is not normally expressed in the root, but is upregulated in the absence of functional *SCM*. The second line identified as having a mild hairless-root phenotype has an insertion in the phospholipase Dζ2 gene *PLDζ2*, which is though to be involved in phosphate recycling, auxin response (Cruz-Ramirez *et al.*, 2006, Li and Xu, 2007, Li *et al.*, 2006) as well as root gravitropism and hydrotropism (Taniguchi *et al.*, 2010). Interestingly, *PLDζ1* is a known target of GL2 and has been shown to be involved in root hair morphogenesis (Ohashi *et al.*, 2003). The third gene identified as having a mild hairless phenotype, *PSEUDO-RESPONSE REGULATOR 9 (PPR9),* encodes a circadian clock regulator implicated in a temperature-sensitive circadian system (Salome *et al.*, 2010). While it is difficult to explain why these genes are differentially expressed between wild-type and the *scm-2* mutant, there general role in stress response and adaptation to environmental conditions may suggest a rationale for the hairless-root phenotypes seen in their corresponding insertion mutants. Root hairs are important for nutrient absorption, and thus as a response to less-than desirable environmental conditions plants may alter their root hair density or morphology to better acquire

necessary nutrients and water (Hofer, 1991).

Finally, we identified one line with a mild *scrambled*-like patterning defect. The insertion line in locus At1g20770 (SALK_102662), displayed a mild patterning defect characterized by an increase in hair cells specified in the N position (5.7%, compared to 0% in wild-type) and non-hair cells specified in the H position (14.3%, compared to 5% in wild-type). The gene at locus At1g20770 encodes an unknown protein that is expressed moderately throughout the plant, with the highest levels seen in the root meristem, shoot meristems and pollen (eFP database (Winter *et al.*, 2007)). While At1g20770 insertion line showed a consistent patterning phenotype in further phenotypic analysis (data not shown), we were never able to identify the presence of a T-DNA insert. Further analysis is needed to determine the nature of the mutation in line SALK_102662 and to determine the relation of At1g20770 to root epidermal patterning.

Using data collected from microarray analysis of root tissue from wild-type and the *scm-2* mutant, we identified five genes which may contribute to the position-depend specification of root-hair and non-hair cells in the root epidermis. However, our root epidermal cell-type patterning analysis was preliminary. Further analysis is needed to not only confirm the phenotypes observed in this study, but also to further implicated these genes in root cell-type patterning.

Analysis of genes from hairy vs. hairless microarray analysis

RHD6, identified for its role in hair-fate specification, was recently cloned and found to encode a bHLH protein (Heim *et al.*, 2003, Menand *et al.*, 2007).

Genetic analysis has indicated that *RHD6,* which is essential for root hair initiation, acts downstream of the genes involved in epidermal pattern formation (Massucci and Schiefelbein, 1994, Menand *et al.*, 2007).

To date, 162 bHLH proteins have been identified in *Arabidopsis*, making it one of the largest known families of transcription factors in the model plant (Bailey *et al.*, 2003, Heim *et al.*, 2003, Toledo-Ortiz *et al.*, 2003). *RHD6* is a member of bHLH subfamily VIIIc, which is composed of six total members (*bHLH83/RHD6, bHLH054, bHLH084, bHLH085, bHLH086/RSL1*) (Heim *et al.*, 2003). Recently, bHLH VIIIc subfamily member *RHD6-LIKE1 (RSL1)* was observed to act semi-redundantly with RHD6 in the process of root-hair cell differentiation (Menand *et al.*, 2007). In addition, microarray analysis comparing the transcriptomes of a hairy root mutant (*cpc try etc1*) and hairless root mutant (*wer myb23*) identified both *RHD6* and an additional VIIIc subfamily member *bHLH054* as being differentially expressed in the two genetic backgrounds. Together, this suggests that *RHD6* and related bHLH transcription factors may be involved in *Arabidopsis* root fate specification and/or cell fate development. In support of this notion, known root hair patterning genes *GL3*, *EGL3* and *MYC1* are members of the closely related bHLH subfamily IIIf (Heim *et al.*, 2003). Unfortunately, the other members of the VIIIc family, *bHLH084*, *bHLH085* and *bHLH086*, are not represented on the ATH1 chip and thus expression data in the hairless and hairy mutant genetic backgrounds was unavailable. However, members of the closely related subfamilies XI were also found to be differentially expressed between the hairy root and hairless root backgrounds. Therefore, we

decided to more closely examine root hair patterning, hair length and hair morphology in mutants for all bHLH subfamily VIIIc and XI genes.

To investigate the role of the bHLH families VIIIc and XI in root hair patterning and morphogenesis, we screened the SALK insertion line library for potential mutant lines. At least one line was identified for each gene and homozygous mutant plants were analyzed for potential root cell fate, hair length and hair morphogenesis phenotypes. Interestingly, an insertion line in the bHLH subfamily VIIIc gene *bHLH084* (SALK_06429) and two in *bHLH085* (SAIL_514_C04, SALK_016855) showed moderate increases in branched root hairs (Table 3.2). As for the other three subfamily VIIIc members, *bHLH 086/RSL1* and RHD6 wer not analyzed as they have previously been shown to be necessary for root hair cell development (Menand *et al.*, 2007), and *bHLH054* was analyzed in another study (A. Bruex and J. Schiefelbein, unpublished).

Root cell-fate specification and hair morphogenesis did not differ in insertion lines in the bHLH subfamily XI genes *bHLH007* (SALK_005407, this study) and the *bHLH059* (A. Bruex and J. Schiefelbein, unpublished). However, insertion lines for the other three members of subfamily XI did show significant branching (*bHLH066, bHLH069*) and short hair (*bHLH 066, bHLH069* and *bHLH082*) phenotypes (A. Bruex and J. Schiefelbein, unpublished). Together, this suggests that not only are bHLH transcription factors within subfamilies IIIf and VIIIc involved in root hair development, but related members from subfamily XI may also be involved.

The *RHD6* enhancer trap line expresses *GUS* in cells in the H position

(Menand *et al.*, 2007), implying that *RHD6* likely influences hair-cell fate specification in a cell-autonomous manner. This expression spreads to the cells in the N position in the *wer*, *ttg*, and *gl2* mutant backgrounds, indicating that *WER*, *TTG*, and *GL2* negatively regulate transcription of *RHD6* in the N position (Menand *et al.*, 2007). Together, this suggests that *RHD6* may positively regulate transcription of genes involved in hair outgrowth. According to phylogenetic analysis, *bHLH086/RSL1* is the closest homolog of *RHD6*, and the two genes likely result from a recent duplication event (Heim *et al.*, 2003). The other three bHLH VIIIc family genes cluster together in a sister-clade, hinting at the potential for redundant function (Menand *et al.*, 2007). Thus, it will be interesting to determine if double or triple mutants of mutations in *bHLH084*, *bHLH085* and *bHLH086* result in mutant phenotype enhancement.

In addition to bHLH families VIIIc and XI, five other transcription factors which were differentially expressed in hairless and hairy mutant roots according to microarray analysis were also analyzed. Mutations in *ICE1/bHLH116/SCREAM*, which encodes a bHLH transcription factor involved in transcriptional activation of cold-responsive genes (Chinnusamy *et al.*, 2003) and GBF6, a sucrose-regulated bZIP transcription factor (Rook *et al.*, 1998a, Rook *et al.*, 1998b), both resulted in moderate increases in root hair branching (Table 3.2). Interestingly, in addition to it's role in cold acclimation, *ICE1/bHLH116/SCREAM* is also required for stomatal cell differentiation (Kanaoka *et al.*, 2008). While cold acclimation and stomatal cell differentiation seem relatively unrelated, it is possible that *ICE1/SCREAM* may play a role in

acclimation of the plant to environmental changes (Kanaoka *et al.*, 2008), which may include alterations in root hair patterning. A insertion mutant in *ANAC013* (At1g32870), which was identified in both microarray experiments as being down-regulated in hairless roots, did not show a root epidermal cell phenotype and thus was not further analyzed.

While an insertion line in *MYB20* did not show a phenotype, an insertion lines in *BPC2* found to have branched as well as wavy hairs. These two genes will not be discussed here as they are part of a separate study (A. Bruex and J. Schiefelbein, unpublished).

Altogether, this work not identified potential new transcription factors involved in root hair development, but also legitimized the use of tissue-specific microarray analysis for identifying genes involved in regulation of specific developmental processes. Future analysis is needed to not only screen further genes of interest, but to unveil the function of the above-verified genes in root development.

Acknowledgements

Root epidermal cell specification analysis and insertion-line genotyping was done with the help of two very talented undergraduate students, Luay Almassalha and Asha Radhamohan. Analysis of hairy vs. hairless lines was done in conjunction with Angela Bruex and will be submitted as a paper.

	LOCI	GENE	Microarray Comparison	Fold Change	Salk Line	Insert Location	H Cell File (%)	N Cell File (%)
	-	Wild-type	-	-	-	-	95	100
1	At2g26560	PATATIN-LIKE PROTEIN 2, PHOSPHOLIPASE A 2A	*scm-2* vs. WT	+48.8	SALK_059119	INTRON	95.5	97.5
2	At2g41370	Cytoplasmic and nuclear-localized NPR1 like protein with BTB/POZ domain and ankyrin repeats	*scm-2* vs. WT	+10.3	SALK_075879	5'UTR	94.6	98.6
3	At4g23670	Major latex protein-related	*scm-2* vs. WT	+48.1	SALK_088249	5'UTR	87.0	100
4	At2g45420	Lateral organ boundaries domain protein	*scm-2* vs. WT	+14.0	SALK_112078	5'UTR	98.0	78.0
5	At3g05630	Encodes a member of the PXPH-PLD subfamily of phospholipase D proteins	*scm-2* vs. WT	+7.0	SALK_119084	INTRON	85.0	95.0
6	AT4G26540	Protein kinase family protein	*scm-2* vs. WT	-14.5	SALK_053167	EXON	96.0	75.0
7	AT5G13790	AGAMOUS-LIKE 15, expressed during embryogenesis	*scm-2* vs. WT	-1.38	SALK_093946	INTRON	100	96.0
8	AT1G20770	similar to Os04g0509200	*scm-2* vs. WT	-2.57	SALK_102662	5'UTR*	85.7	94.3
9	AT2G46790	Pseudo-response regulator PRR9	*scm-2* vs. WT	-11.4	SALK_106072	INTRON	83.0	100
10	AT3G21340	LRR-protein kinase	*scm-2* vs. WT	-2.1	SALK_110696	PROMOTER	97.0	100
11	At3g09600	MYB family transcription factor	*scm-2* vs. WT	-53.1	SALK_016333	INTRON	100	95.0
12	At3g15540	IAA-induced protein	*scm-2* vs. WT	+8.1	SALK_034924	INTRON	100	97
13	At3g55840	unknown; similar to putative Hs1pro-1-like receptor	*scm-2* vs. WT	+13.8	SALK_076686	EXON	97.6	91.3
14	At3g28390	P-GLYCOPROTEIN 18 ATPase, transmembrane movement of substances	*scm-2* vs. WT	+26.9	SALK_130155	EXON	91.0	97.0
15	At2g37050	Protein Kinase	*scm-2* vs. WT	+8.4	SALK_143700	EXON	96.0	97.0
16	At2g28100	Alpha-fucosidase (AtFUC1)	*scm-2* vs. WT	-42.1	SALK_072441	EXON	94	88
17	At3g45450	clpC-like protein, ATPase involved in protein metabolism	*scm-2* vs. WT	-15.0	SALK_127435	INTRON	98	97
18	At1g24620	Putative polcalcin/calmodulin-binding pollen allergen.	*scm-2* vs. WT	-13.0	SALK_000164	EXON	100	99
19	At4g25450	Non-Intrinsic ABC protein 8); member of the NAP subfamily of integral membrane proteins	*scm-2* vs. WT	-12.7	SALK_151551	INTRON	98	98
20	At3g11220	Elongata 1; subunit "A" of Elongator, a histone acetyl transferase complex.	*scm-2* vs. WT	-11.8	SALK_079193	EXON	98	92
21	At5g15780	Allergen and extensin family protein	*scm-2* vs. WT	-11.5	SALK_032656	EXON	96	100
22	At2g39130	Amino Acid Family Transporter, transmembrane protein.	*scm-2* vs. WT	-11.4	SALK_068456	INTRON	96	100
23	At2g43090	3-isopropylmalate dehydratase, small subunit	*scm-2* vs. WT	-11	SALK_119351	EXON	98	100
24	At4g26430	Cop9 Signalosome subunit 6B, CSN6B. Involved in ubiquitin-dependent protein catabolism	*scm-2* vs. WT	-9.8	SALK_036965	INTRON	100	100
25	At5g58550	EOL2- Paralog (Ethylene Overproducer 1), a negative regulator of ACS5	*scm-2* vs. WT	-9.3	SALK_114207	EXON	98	96
26	At5g56870	Putative beta-galactosidase/ lactase	*scm-2* vs. WT	+9.4	SALK_022796	EXON	100	86

	LOCI	GENE	Microarray Comparison	Fold Change	Salk Line	Insert Location	H Cell File (%)	N Cell File (%)
27	At1g69490	NAC transcription factor family protein.	*scm-2* vs. WT	+9.8	SALK_005010	EXON	93	99
28	At5g14180	AtLIP2 (Triacylglycerole lipase 2), lipase family protein	*scm-2* vs. WT	-17.8	SALK_031227	EXON	98	98
29	At2g40180	AtPP2C5 - serine/threonine phosphatase complex	*scm-2* vs. WT	+26.0	SALK_015191	EXON	100	100
30	At1g52890	NAC transcription factor; similar to No Apical Meristem	*scm-2* vs. WT	+8.4	SALK_096310	EXON	98	100
31	At5g65890	ACT (amino acid binding) domain containing protein	*scm-2* vs. WT	+8.6	SALK_072160	EXON	99	95
32	At4g25300	Oxidoreductase, 20g-Fe (II) oxygenase family protein.	*scm-2* vs. WT	+9.1	SALK_101182	INTRON	100	94
33	At1g74000	SS3; strictosidine synthase 3.	*scm-2* vs. WT	+9.3	SALK_032305	INTRON	91	91
34	At1g07160	Protein phosphatase 2c (putative)	*scm-2* vs. WT	+11.8	SALK_060018	PROMOTER	100	100
35	At1g19520	Expressed protein - unknown	*scm-2* vs. WT	-23.7	SALK_139536	5'UTR	90	94
36	At3g15357	Zinc-finger protein related	*scm-2* vs. WT	-13.1	SALK_009195	5'UTR	94	94
37	At5g13080	WRKY-like protein	*scm-2* vs. WT	+9.8	SALK_004954	5'UTR	94	100
38	AT1G52690	putative LEA protein	scm vs. WT (whole root)	-	CS119690	EXON	92.0	100.0
39	AT4G38350	hedgehog/patched receptor-like	scm vs. WT (whole root)	-	CS805038	INTRON	93.5	98.5
					CS859451c	INTRON	96.7	97.3
40	AT5G37740	C2 domain containing	scm vs. WT (whole root)	-	SALK_080173c	EXON	94.0	98.4
					SALK_038968c	EXON	92.7	100.0
41	AT1G52240	ROP GEF II, KPP (kinase partner protein) family	scm vs. WT (whole root)	-	SALK_126725c	EXON	92.7	96.9
					CS835623	INTRON	95.0	99.0
42	AT3G11490	Rac GTPase activator	scm vs. WT (whole root)	-	SALK_068684c	EXON	94.4	98.1
					SALK_152535	EXON	94.7	99.3
					SALK_038694c	EXON	88.3	99.2
43	AT5G24240	phosphatidylinositol 3,4-kinase family	*scm-2* vs. WT	-	SALK_048798c	EXON	95.7	100.0
44	AT1G33930	avirulence response protein	*scm-2* vs. WT	-	SALK_060790c	INTRON	-	-
					SALK_089489	300-UTR5	-	-

Table 3.1. Analysis of genes differentially expressed in root tissue of *scm-2* when compared to wild-type

Results from the analysis of genes of interest identified in a comparison of microarray analysis of wild-type and the *scm-2* mutant. Fold change (center column) represents the comparison of average transcript levels (from three biological repeats) of *scm-2* to wild-type. Unless otherwise indicated, the microarray comparison analyzed used RNA isolated from *WER::GFP*-sorted epidermal cells. Results of root cell-type patterning analysis of at least one insertion line for each gene of interest is presented (right). Data indicates the percent of appropriately specified cells in each position (aka - hair cells in the H position, non-hair cells in the N position).

#	LOCI	Gene Family	GENE	Fold Change (hairless - vs- hairy)	Insertional Line	Insert Location	Phenotype Analysis
45	AT2G14760	**bHLH VIIIc**	bHLH 084	-	SALK_06429c	EXON	branched hairs (38%)
46	AT4G33880	**bHLH VIIIc**	bHLH 085	-	CS874457	INTRON	branched hairs (51%)
					SALK_016855	3' Region	branched hairs (35%)
47	AT1G03040	**bHLH VIIIc**	bHLH007	0.8 (UM) / 0.7 (Duke)	SALK_005407c	EXON	Not analyzed
					SALK_079917	EXON	Not analyzed
48	AT3G26744	**Other TF**	ICE1/ SCREAM	0.2 (UM) / 0.4 (Duke)	SALK_003155	EXON	branched hairs (27%)
49	AT1G32870	**Other TF**	ANAC013	0.3 (UM) / 0.4 (Duke)	SALK_096150	5'UTR	Not analyzed
50	AT4G34590	**Other TF**	GBF6/ AtZIP11	0.3 (UM) / 0.3 (Duke)	SALK_018229	EXON	branched hairs (25%)

Table 3.2. Analysis of genes encoding transcription factors and bHLH proteins identified as differentially expressed in hairless vs. hairy roots

Results from the analysis of genes of interest identified in a comparison of microarray analysis of WER::GFP-sorted root epidermal tissue from a hairless root (*cpc try etc1* triple mutant background) and from a hairy root (*wer myb23* double mutant background). Fold change (center column) represents the comparison of average transcript level (from three biological repeats) in experiments conducted at Duke University (courtesy of the Benfey Lab) and at Michigan (A. Bruex and J. Schiefelbein, unpublished). Results of root cell-type patterning and root-hair cell morphogenesis analysis of insertion lines for each gene of interest are presented (right).

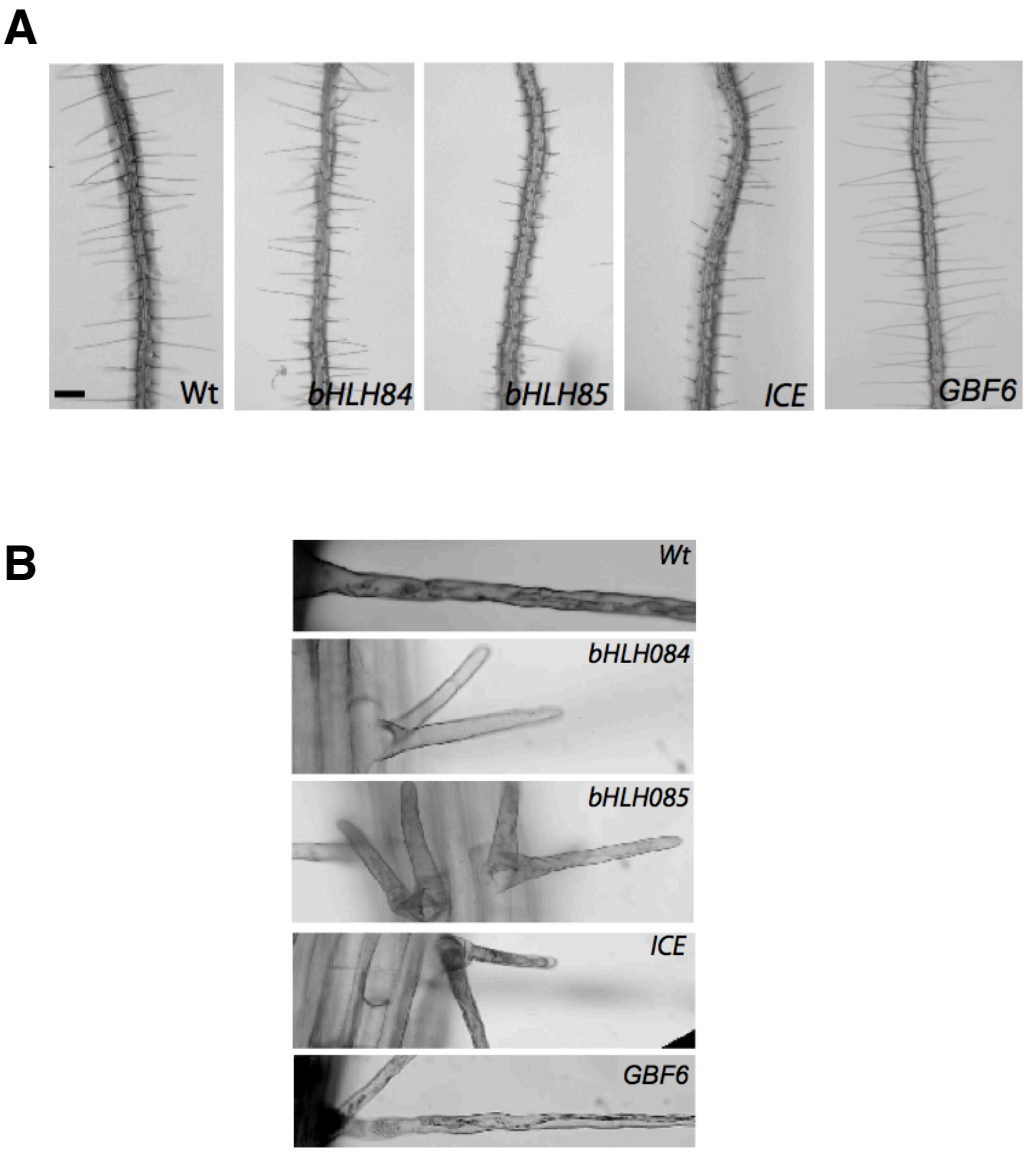

Figure 3.1. Root-hair phenotypes of insertion lines in the *bHLH84*, *bHLH85*, *ICE1* and *GBF6* genes

(A) Root-hair length and density and (B) morphology of individual root hairs in wildtype and T-DNA insertion lines for *bHLH084* (SALK_06429c), *bHLH085* (CS874457), *ICE1* (SALK_003155) and *GBF6* (SALK_081229).

	LOCUS	INSERTION LINE	LEFT PRIMER	RIGHT PRIMER	LB Primer
1	At2g26560	SALK_059119	TGGTTGGGGACTATTGAATTG	CGTGCATTAGTGAAACAAACG	LBb1
2	At2g41370	SALK_075879	CTGGTATAATTCCAGCTGGGG	CGGTTCATCCATTCAAATCTC	LBb1
3	At4g23670	SALK_088249	TTGTATGGGCCCATAAATGAC	TTGTCGTCGCTAGCTCATAGG	LBb1
4	At2g45420	SALK_112078	CTTGCTCGGAGTCAAAGTACG	TGATGGCTAATTTAAGTTGGACC	LBb1
5	At3g05630	SALK_119084	TTTTAATTGGTATTCTCTGTTTTTGG	TCATCGCCAGTGAAAAATCTC	LBb1
6	At4g26540	SALK_053167	ACTAGTCTCCGGAGCCTCAAG	TTTCCCAACGAGATTGTTCTG	LBb1
7	At5g13790	SALK_093946	CTTGAGGCGTGATTCTTCAAG	GATCGAGAATGCGAATAGCAG	LBb1
8	At1g20770	SALK_102662	GTGCGAGAACGAGAGAGACAG	CACGCAATCCTTTTTAATCCC	LBb1
9	At2g46790	SALK_106072	TTCTGCTGACTTGCTTTCCTC	TCAAACCAATGAGGAAAAACG	LBb1
10	At3g21340	SALK_110696	CCATGGAAGTGAGTCACTTCG	TCGTACGTATGCATAATGCAC	LBb1
11	At3g09600	SALK_016333	GGAAACTTGAAGTGGCATTTG	GAAAAATAACCGATGAGCTCG	LBb1
12	At3g15540	SALK_034924	CGGATATGTAGTAACCGAAACCTC	AGCTGTAAGGAAGCTTCGACC	LBb1
13	At3g55840	SALK_076686	CACTGATCGTTAGATGCTTCC	TCGGTTTAGGAGAACCAAACC	LBb1
14	At3g28390	SALK_130155	GATCGCGATTCTCTGTTTTTG	CGAACCATTACAGCTTTCTCG	LBb1
15	At2g37050	SALK_143700	TAGCAACAACCCTTGGTTGTG	GATAAATTTCGGGGCTGAAAG	LBb1
16	At2g28100	SALK_072441	AAAACATTTGGGCCGAGTTAC	TTCAGCGAAATGAAGAACTCC	LBb1
17	At3g45450	SALK_127435	TGGTTCAGGTACCTTCACAGG	CGTGTCTTATTGGAAAGCCTG	LBb1
18	At1g24620	SALK_000164	GAGAATCATCCGCTTCCTTTG	CGGAGAATTCAGTTTCAGCAG	LBb1
19	At4g25450	SALK_151551	GAAGGGTTTTGATCCAGAAGG	ACAGCTTTTGAGATTTGACCG	LBb1
20	At3g11220	SALK_079193	CCTGAGCAATGGAAAGATCTG	GTCTGGTTTTGGGGCTAAAAG	LBb1
21	At5g15780	SALK_032656	ATCAAATCTAATCGACACGCG	GCGCTTGTCTGTTTTCACTTC	LBb1
22	At2g39130	SALK_068456	TGACATGACAAGACCTGCAAG	TGGAATTCACAGCAAAGGAAC	LBb1
23	At2g43090	SALK_119351	GGAGTTTCTCACTCTCGTCCC	TTTGCATCGTTCAATTCAATG	LBb1
24	At4g26430	SALK_036965	CAGAGAGGTCGTACGGTTGAG	TGGCTTAAGATGTGCAACATG	LBb1
25	At5g58550	SALK_114207	CTCCCTCTACAAGCAGCAATG	TGTTGATTCCACGAAAGAACC	LBb1
26	At5g56870	SALK_022796	ATACCGGGAACAAATTTGAGC	AGCACCCCTGAGGTAACAATC	LBb1
27	At1g69490	SALK_005010	ACCCAAACCTTCTCTGCTTTC	TACTTCGTCCATGAAACCCTC	LBb1
28	At5g14180	SALK_031227	TCACACTGATCATCCCTCCAC	GTTGTCTCTTTCCCCCATCTC	LBb1
29	At2g40180	SALK_015191	ATTTCACGTGATCACCGAGTC	TGGTCGTTTCCTTTTCAACAC	LBb1
30	At1g52890	SALK_096310	ATTCGATCCATGGGTTTTACC	ATGCGGTTTGGGTTAGAAAAC	LBb1
31	At5g65890	SALK_072160	CTTTTTGGGTACTTTTGGACG	ATCCTCTCGCATCTTCCTCTC	LBb1
32	At4g25300	SALK_101182	CCATGAAGTCGAAGCAGAGAG	TCCATTCCATGGTTTACAAGC	LBb1
33	At1g74000	SALK_032305	TAGGTTGCATGGAGGCAGTAG	TCATTTCAAAAACTTCCGGTG	LBb1
34	At1g07160	SALK_060018	TAACCATCACCTTCCCTCTCC	TGGCTCTGCAAATAAAACGAC	LBb1
35	At1g19520	SALK_139536	TTTCTAAAACCAATTACAAGTAGAAAGC	TAGTGAAATACGGTGGATCGC	LBb1
36	At3g15357	SALK_009195	TCCTCTTCCTCATCATCTTCG	GCCTCAATTTTCTGAGCTACC	LBb1
37	At5g13080	SALK_004954	CGGATAAAATGATGACGTTCG	AAAAGGAGCATACAACGACCC	
38	At1g52690	CS119690/ SM_3_32979	GAACTGTAGGAGAAAACTGGGGAAGCTAT	GATTAAATTTGACTCCGTCTTCCAGAGTT	Sm32
39	At4g38350	CS805038/ SAIL_104_H11	CTGCAGTTTTGTTCTAAGGCG	CTTTTCTGGTCGTGTTTCCAC	LB3
		CS859451c/ SALK_031865	TCGGAGTTCCGTACATACCAC	TCATCTGCATTTGAAGCAGTG	LBb1.3

40	At5g37740	SALK_080173c	ATCTGATGGACTCATGATCGG	AACTTGTGTTGTCGCCTTTTG	LBb1.3
		SALK_038968c	TGGTGGAACCAGAAGAGATTG	TCTTCGGTTTCTCAACGTTTG	LBb1.3
41	At1g52240	SALK_126725c	TCAGAGAGAGGTCAAAATTGAGG	TACCTGCGAGATTGGTAATGG	LBb1.3
		CS835623/ SAIL_796_B05	TTTCCCCTGAAGAATCTGACC	TCGAGTTTCTTAAGTGCAGGG	LB3
42	AT3G11490	SALK_068684c	TGTGTGTGGTACATTCATCCG	ATCATTGATGTCAGGGGACAC	LBb1.3
		SALK_152535	TCTGATCACCATTATGGTCCC	GCAATTAGTGTGTCCCCTGAC	LBb1.3
		SALK_038694c	TCCCTTCTTTCACCCTTTTTG	CTGCCATTCAATGTGATGATG	LBb1.3
43	At5g24240	SALK_048798c	AAAAGGCTCCACGAAGAACTC	TCCATGACTGATTCCTGTGATC	LBb1.3
44	At1g33930	SALK_060790c	TTTGAACTGCGGTAAATCCTC	TCACACATTTTCTCTTAGCTTTGTC	LBb1.3
		SALK_089489	TTTTCCTTGATGTTTTGCAGG	CAATCACATTGATTATGGGGC	LBb1
45	At2g14760	SALK_06429c	GCAAAACAAAAATATTAAACCGAC	GCAGATCCAGACTCGATTCTG	LBb1.3
46	At4g33880	CS874457/ SAIL_514_C04	TTGTCAGACCTTTCTTCATTCG	TACAAAATCTCGTCCCCAATG	LB3
		SALK_016855	TGGATATGCTATTCCAGCCAC	TTTAATATTCTCCGCCTTCGG	LBb1.3
47	At1g03040	SALK_005407c	TTTTTGGCTCAGATTGGTGAG	GGGACCAAGGATTTACACCAC	LBb1.3
		SALK_079917	TCCATGAGTGCTAAATTTCGG	CGTCTTGGAAACGTTTACCAG	LBb1.3
48	At3g26744	SALK_003155	TGTGCAAATGTTTTGTCTGTC	TGAGGAAGAGGCTCGTGATAG	LBb1.3
49	At1g32870	SALK_096150	AACCCACAGTTTTTGTAGGCC	CGGATGAAACCTAAAACCTGG	LBb1.3
50	At4g34590	SALK_018229	TCTTCGTTTTTCGTCATCTGG	AGCGTACGTTACATGCGAAAC	LBb1.3

Table 3.3. Insertional line genotyping primers

Gene specific primer sequences and left-border insertion primer used to genotype each line used in this study. Primers were designed using T-DNA express online primer design software (http://signal.salk.edu/tdnaprimers.2.html).

Literature Cited

Bailey, P, Martin, C, Toledo-Ortiz, G, Quail, PH, Huq, E, Heim, MA, . . . Weisshaar, B (2003) Update on the basic helix-loop-helix transcription factor gene family in *Arabidopsis thaliana*. *Plant Cell,* 15**,** 2497-2501.

Bernhardt, C, Lee, MM, Gonzalez, A, Zhang, F, Lloyd, A & Schiefelbein, J (2003) The bHLH genes *GLABRA3 (GL3)* and *ENHANCER OF GLABRA3 (EGL3)* specify epidermal cell fate in the *Arabidopsis* root. *Development,* 130**,** 6431-6439.

Bernhardt, C, Zhao, M, Gonzalez, A, Lloyd, A & Schiefelbein, J (2005) The bHLH genes *GL3* and *EGL3* participate in an intercellular regulatory circuit that controls cell patterning in the *Arabidopsis* root epidermis. *Development,* 132**,** 291-298.

Birnbaum, K, Jung, JW, Wang, JY, Lambert, GM, Hirst, JA, Galbraith, DW & Benfey, PN (2005) Cell type-specific expression profiling in plants via cell sorting of protoplasts from fluorescent reporter lines. *Nat Methods,* 2**,** 615-9.

Birnbaum, K, Shasha, DE, Wang, JY, Jung, JW, Lambert, GM, Galbraith, DW & Benfey, PN (2003) A gene expression map of the *Arabidopsis* root. *Science,* 302**,** 1956-1960.

Brady, SM, Orlando, DA, Lee, J-Y, Wang, JY, Koch, J, Dinneny, JR, . . . Benfey, PN (2007) A high-resolution root spatiotemporal map reveals dominant expression patterns. *Science,* 318**,** 801-806.

Chevalier, D, Batoux, M, Fulton, L, Pfister, K, Yadav, RK, Schellenberg, M & Schneitz, K (2005) STRUBBELIG defines a receptor kinase-mediated signaling pathway regulating organ development in *Arabidopsis*. *Procl. Natl. Acad. Sci.,* 102**,** 9074-9079.

Chinnusamy, V, Ohta, M, Kanrar, S, Lee, B-H, Hong, X, Agarwal, M & Zhu, J-K (2003) *ICE1*: a regulator of cold-induced transcriptome and freezing tolerance in *Arabidopsis*. *Genes Dev.,* 17**,** 1043-1054.

Cruz-Ramirez, A, Oropeza-Aburto, A, Razo-Hernandez, F, Ramirez-Chavez, E & Herrera-Estrella, L (2006) Phospholipase DZ2 plays an important role in extraplastidic galactolipid biosynthesis and phosphate recycling in Arabidopsis roots. *Proc Natl Acad Sci U S A,* 103**,** 6765-70.

Galway, ME, Massucci, JD, Lloyd, A, Walbot, V, Davis, RW & Schiefelbein, J (1994) The *TTG* Gene is Required to Specify Epidermal Cell Fate and Cell Patterning in the *Arabidopsis* Root. *Dev. Biol.,* 166**,** 740-754.

Heim, M, Jakoby, M, Werber, M, Martin, C, Weisshaar, B & Bailey, PC (2003) The basic helix–loop–helix transcription factor family in plants: a genome-wide study of protein structure and functional diversity. *Molecular biology and evolution,* 20**,** 735-747.

Hofer, R-M 1991. Root hairs. *In:* WAISEL Y., EA, KAFKAFI U. (ed.) *Plant Roots: The Hidden Half.* 1 ed.

Kanaoka, M, Pillitteri, L, Fujii, H, Yoshida, Y, Bogenschutz, N, Takabayashi, J & Torii, K (2008) *SCREAM/ICE1* and *SCREAM2* specify three cell-state transitional steps leading to *Arabidopsis* stomatal differentiation. *Plant Cell,* 20**,** 1775-1785.

Kang, YH, Kirik, V, Hulskamp, M, Nam, K, Hagely, K, Lee, MM & Schiefelbein, J (2009) The *MYB23* gene provides a positive feedback loop for cell fate specification in the *Arabidopsis* root epidermis. *Plant Cell,* 21**,** 1080-1094.

Kirik, V, Simon, M, Huelskamp, M & Schiefelbein, J (2004) The *ENHANCER OF TRY AND CPC1* gene acts redundantly with *TRIPTYCHON* and *CAPRICE* in trichome and root hair cell patterning in *Arabidopsis*. *Dev. Biol.,* 268**,** 506-513.

Kurata, T, Ishida, T, Kawabata-Awai, C, Noguchi, M, Hattori, S, Sano, R, . . . Wada, T (2005) Cell-to-cell movement of the CAPRICE protein in *Arabidopsis* root epidermal cell differentiation. *Development,* 132**,** 5387-5398.

Kwak, S-H & Schiefelbein, J (2007) The role of the SCRAMBLED receptor-like kinase in patterning the *Arabidopsis* root epidermis. *Dev. Biol.,* 302**,** 118-131.

Kwak, S-H & Schiefelbein, J (2008) A feedback mechanism controlling SCRAMBLED receptor accumulation and cell-type pattern in *Arabidopsis*. *Curr Biol,* 18**,** 1949-1954.

Kwak, S-H, Shen, R & Schiefelbein, J (2005) Positional signaling mediated by a receptor-like kinase in *Arabidopsis*. *Science,* 307**,** 1111-1113.

Lee, H, Kim, N, Lee, DJ & Kim, J (2009) *LBD18/ASL20* regulates lateral root formation in combination with *LBD16/ASL18* downstream of *ARF7* and *ARF19* in *Arabidopsis*. *Plant Physiol.,* 151**,** 1377-1389.

Lee, MM & Schiefelbein, J (1999) WEREWOLF, a MYB-Related Protein in *Arabidopsis*, Is a Position-Dependent Regulator of Epidermal Cell Patterning. *Cell,* 99**,** 473-483.

Lee, MM & Schiefelbein, J (2002) Cell Pattern in the *Arabidopsis* Root Epidermis Determined by Lateral Inhibition with Feedback. *Plant Cell,* 14**,** 611-618.

Li, G & Xu, H (2007) Arabidopsis PLDZ2 regulates vesicle trafficking and is required for auxin response. *Plant Cell,* 19.

Li, M, Qin, C, Welti, R & Wang, X (2006) Double knockouts of phospholipases DZ1 and DZ2 in Arabidopsis affect root elongation during phosphate-

limited growth but do not affect root hair patterning. *Plant Physiol.,* 140**,** 761-770.

Long, TA, Brady, SM & Benfey, PN (2008) Systems approaches to identifying gene regulatory networks in plants. *Annual Review of Cell and Developmental Biology,* 24**,** 81-103.

Massucci, JD, Rerie, WG, Foreman, DR, Zhang, M, Galway, ME, David Marks, M & Schiefelbein, J (1996) The homeobox gene *GLABRA2* is required for position-dependent cell differentiation in the root epidermis of *Arabidopsis thaliana*. *Development,* 122**,** 1253-1260.

Massucci, JD & Schiefelbein, J (1994) The *rhd6* mutation of *Arabidopsis thaliana* alters root-hair initiation through an auxin-and ethylene-associated process. *Plant Physiol.,* 106**,** 1335-1346.

Menand, B, Yi, K, Jouannic, S, Hoffmann, L, Ryan, E, Linstead, P, . . . Dolan, L (2007) An Ancient Mechanism Controls the Development of Cells with a Rooting Function in Land Plants. *Science,* 316**,** 1447-1480.

Ohashi, Y, Oka, A, Rodrigues-Pousada, R, Possenti, M, Ruberti, I, Morelli, G & Aoyama, T (2003) Modulation of Phospholipid Signaling by *GLABRA2* in Root-Hair Pattern Formation. *Science,* 300**,** 1427-1430.

Rerie, W, Feldmann, K & David Marks, M (1994) The *GLABRA2* gene encodes a homeo domain protein required for normal trichome development in *Arabidopsis*. *Genes Dev.,* 8**,** 1388-1399.

Rook, F, Gerrits, N, Kortstee, A, Kampen, MV, Borrias, M, Weisbeek, P & Smeekens, S (1998a) Sucrose-specific signalling represses translation of the *Arabidopsis ATB2* bZIP transcription factor gene. *Plant J.,* 15**,** 253-263.

Rook, F, Weisbeek, P & Smeekens, S (1998b) The light-regulated *Arabidopsis* bZIP transcription factor gene *ATB2* encodes a protein with an unusually long leucine zipper domain. *Plant Mol. Biol.,* 37**,** 171-178.

Salome, P, Weigel, D & Mcclung, CR (2010) The role of the *Arabidopsis* morning loop components *CCA1*, *LHY*, *PRR7*, and *PRR9* in temperature compensation. *Plant Cell,* 22**,** 3650-3661.

Schellmann, S, Schnittger, A, Kirik, V, Wada, T, Okada, K, Beermann, A, . . . Hülskamp, M (2002) TRIPTYCHON and CAPRICE mediate lateral inhibition during trichome and root hair patterning in *Arabidopsis*. *EMBO J.,* 21**,** 5036-5046.

Schiefelbein, JW & Somerville, C (1990) Genetic Control of Root Hair Development in Arabidopsis thaliana. *Plant Cell,* 2**,** 235-243.

Simon, M, Lee, MM, Lin, Y, Gish, L & Schiefelbein, J (2007) Distinct and overlapping roles of single-repeat MYB genes in root epidermal patterning. *Dev. Biol.,* 311**,** 566-578.

Taniguchi, Y, Taniguchi, M, Tsuge, T, Oka, A & Aoyama, T (2010) Involvement of *Arabidopsis thaliana* phospholipase Dζ2 in root hydrotropism through the suppression of root gravitropism. *Planta,* 231**,** 491-497.

Toledo-Ortiz, G, Huq, E & Quail, PH (2003) The *Arabidopsis* basic/helix-loop-helix transcription factor family. *Plant Cell,* 15**,** 1749-1770.

Tominaga, R, Iwata, M, Okada, K & Wada, T (2007) Functional analysis of the epidermal-specific MYB genes *CAPRICE* and *WEREWOLF* in *Arabidopsis*. *Plant Cell,* 19**,** 2264-77.

Wada, T, Kurata, T, Tominaga, R, Koshino-Kimura, Y, Tachibana, T, Goto, K, . . . Okada, K (2002) Role of a positive regulator of root hair development, *CAPRICE*, in *Arabidopsis* root epidermal cell differentiation. *Development,* 129**,** 5409-5419.

Wada, T, Tachibana, T, Shimura, Y & Okada, K (1997) Epidermal Cell Differentiation in *Arabidopsis* Determined by a Myb Homolog, *CPC*. *Science,* 277**,** 1113-1116.

Winter, D, Vinegar, B, Nahal, H, Ammar, R, Wilson, GV & Provart, NJ (2007) An "Electronic Fluorescent Pictograph" browser for exploring and analyzing large-scale biological data sets. *PLoS One,* 2**,** e718.

CHAPTER 4

Conclusions and Future Directions

The goal of my thesis research was to identify and investigate novel components in the *Arabidopsis* root epidermal cell-type patterning system. Previous to my joining the lab, a forward-genetic screen was conducted using EMS-mutagenized plants containing the *GL2::GUS* transcriptional reporter. Through this screen, our lab identified *SCRAMBLED*, a leucine-rich repeat receptor-like kinase essential for position-dependent cell fate specification (Kwak *et al.*, 2005). A second interesting mutant isolated was *45-137*, which I identified as corresponding to the *DIM1A* gene. By characterizing the *45-137/dim1A* mutant phenotypes a new connection was established between root epidermal patterning and ribosome biogenesis. The significance of this research is threefold. First, the results presented here make a clear connection between ribosome biogenesis and establishment of distinct gene expression patterns in the *Arabidopsis* root during cell-type patterning. Second, it furthered our knowledge of the molecular mechanism of root epidermal patterning, strengthening the evidence for the importance of the balance between WER and

CPC levels in epidermal cells and also hinted at a possible additional mechanism involved in *GL2* transcriptional regulation. Lastly, it provided the first insight into the importance of a highly conserved ribosomal RNA base modification in multicellular organisms.

Ribosome Biogenesis and Epidermal Cell-Type Patterning

The overarching conclusion from my analysis of the effect of *dim1A* on root epidermal patterning was that functional DIM1A is required to ensure cells in the H position adopt the hair cell fate. Altogether, it appears that the main effect of *dim1A* mutation on the epidermal patterning gene network is misregulation of *WER* gene expression. While in wild-type roots, *WER* expression is much higher in N position cells than H position cells (Lee and Schiefelbein, 1999), the *dim1A* mutation causes a significant increase in *WER* expression in H position cells. Together with other genetic analysis, I suggest that a decreased N/H ratio of *WER* expression may reduce the ability of CPC to compete with WER for binding to TTG1-GL3/EGL3, increasing the likelihood of a functional transcriptional activation complex in H position cells. The functional activation complex in H position cells of the *dim1A* mutant results in *GL2* expression and subsequently non-hair fate specification.

An interesting question – that of the mechanism of *WER* gene regulation – remains to be answered. Due to the nature of the DIM1A gene product, it is likely that DIM1A regulation of *WER* is indirect via translational regulation of

another transcription factor. However, my analysis did not address this, so it remains to be confirmed.

Additionally, while it is possible to connect many of the *dim1A* epidermal patterning phenotypes to misregulation of *WER* expression, it remains difficult to explain some. For one, the small increase in non-*GL2::GUS*-expressing cells in root epidermal cells in the N position is not consistent with increased *WER* expression, as *WER* promotes *GL2* expression (Lee and Schiefelbein, 1999). Secondly, the partial rescue of the *scm-2 GL2::GUS* patterning defect was rather unexpected, and is inconsistent with and increase in *WER* expression. Since SCM downregulates expression of *WER* in H position cells (Kwak and Schiefelbein, 2007), and *WER* expression equally throughout the epidermis causes a "scrambled" pattern of *GL2::GUS* expression (Lee and Schiefelbein, 2002, Ryu *et al.*, 2005), we would have expected to see a more extreme *scm*-like phenotype in the *dim1A scm* double mutant. Thirdly, the increase in *GL2::GUS* expressing cells in the *dim1A wer* double mutant (compared to the *wer GL2::GUS* single mutant) is difficult to connect with an increase in *WER* expression caused by *dim1A*. Altogether this suggests that *dim1A* may affect a yet-to-be determined player in the epidermal-patterning network.

An interesting possibility that was suggested in Chapter Two is the potential effect of *dim1A* on translation reinitiation and uORF-mediated translational regulation. A potentially simple way to test the general effect of *dim1A* on uORF read-through is using the a reporter construct for the gene *ATB2*, which is translationally-regulated in response to sugar by four uORFs in its

5‘ leader sequence (Rook *et al.*, 1998, Wiese *et al.*, 2004). In a system developed by Kim et al (2007), uORF read-through is examined by comparing translation of the luciferase reporter driven by either the native *ATB2* promoter or an altered promoter in which uORFs within the 5’ leader sequence are mutated. A second way to determine uORF read-through is the measure RNA accumulation in addition to protein level of the reporter construct and compare these results to wild-type. In a background where translation reinitiation is affected, RNA accumulation will be unaffected but protein level will be significantly lower than in wild-type. This is precisely what was observed in the loss-of-function mutant of eIF3h, a subunit of the *Arabidopsis* translational initiation factor 3 (eIF3) complex shown to be important for efficient translation of 5’ leader sequences harboring uORFs (Kim *et al.*, 2004, Kim *et al.*, 2007). A second parallel experiment would be to introduce the *eif3h* mutation, which is known to affect uORF read-through, into the *GL2::GUS*, *WER::GFP*, *CPC::GUS* and patterning gene mutant backgrounds. If *dim1A* affects translation of 5’ leader sequences containing uORFs and this influences epidermal cell-type patterning, the *eif3h* mutation would be expected similarly effect patterning gene expression and cell-type specification as the *dim1A* mutation.

A **Highly Conserved Ribosomal RNA Methylation**

To the best of my knowledge, this is the first report of an investigation of the two highly conserved 3’-terminal loop adenosine dimethylation in the 18S rRNA subunit of the cytosolic ribosomes from a multicellular organism. This

rRNA base modification has been extensively studied in *E. coli* (Helser *et al.*, 1972, Poldermans *et al.*, 1979a, Poldermans *et al.*, 1980, Van Buul and Van Knippenberg, 1985, O'Farrell *et al.*, 2004, Demirci *et al.*, 2010) and *S. cerevisiae* (Lafontaine *et al.*, 1994, Lafontaine *et al.*, 1995, Lafontaine *et al.*, 1998, Pulicherla *et al.*, 2009), and has been reported in *Arabidopsis* chloroplast 16S rRNA (Tokuhisa *et al.*, 1998) and mitochondria 16S rRNA (Richter *et al.*, 2010). While the homolog of KsgA/Dim1A, the enzyme that catalyzes the formation of the two adjacent dimethyladenosines, has been annotated in the human genome, this enzyme or the rRNA modifications have not been investigated. Thus, my work not only furthers our knowledge of the function of these highly conserved rRNA nucleotide modifications, but also provides insight into their evolution.

In addition, this is only the fourth report (and first in a multicellular organism) of a catalytically inactive KsgA/Dim1 methyltransferase. Connolly et al (2008) identified E66A, a methylation-dead *ksgA* mutant, which, when overexpressed in wild-type *E. coli*, results in a highly deleterious effect on growth. However, the *ksgaΔ* knockout mutant, which lacks the 16S dimethyladenosines, shows only mild affects on organism fitness (Helser *et al.*, 1972, Poldermans *et al.*, 1979a, Van Buul *et al.*, 1984, O'Connor *et al.*, 1997). This suggests that the KsgA enzyme and the dimethyladenosines are not essential for ribosome function, but that in the case where the enzyme is present, methylation activity is crucial for ribosome biogenesis. Interestingly, two independent methylation-dead alleles of yeast Dim1p were reported to result in mild (*dim1-2*) or no (E85A)

growth defects (Connolly *et al.*, 2008, Pulicherla *et al.*, 2009). The mild growth defects in *dim1-2* have been suggested to result from additional mutations in the *DIM1* gene (six in total), suggesting that catalytically inactive Dim1p does not affect yeast growth (Lafontaine 1998, Pulicherla 2009). Primer extension revealed that the *Arabidopsis dim1A* mutant lacks the 18S rRNA 3'-end dimethyladenosines, suggesting that the G66E point mutation affects methylation activity. As additional rRNA biogenesis defects were not detected, my results suggest that the mutant phenotypes of the *dim1A* mutant may be attributable to the presence of a catalytically inactive DIM1A protein and subsequent lack of the highly conserved rRNA dimethyladenosines. In addition, by expressing the catalytically inactive *dim1a* in the wild-type background my results suggest that, unlike in *E. coli* and similar to yeast, methylation may not be required for ribosome biogenesis.

However, further research is needed to elucidate the mechanism of *dimA*s effect. For one, it is important to distinguish between the effect of lack of the 18S 3'-terminal loop dimethyladenosines and the presence of DIM1A protein that is unable to methylate. Previous research in *E. coli* suggests that the KsgA/Dim1 proteins are not able to bind the cofactor SAM until it binds to RNA (O'Farrell *et al.*, 2004, Poldermans *et al.*, 1979b, Thammana and Held, 1974) and that KsgA may remain bound to the ribosome until the action of methylation releases it (Connolly *et al.*, 2008). However, this contradicts what is seen in yeast. Thus, it is possible that in *Arabidopsis* catalytically inactive DIM1A protein may remain bound to the ribosome and interfere with translation, thus causing the *dim1A*

phenotype. However, if this were the case I suspect that the *dim1A* mutation would have had a more severe defect on growth. Structural analysis in *E. coli* has shown that KsgA binds to the decoding center of the ribosome, preventing initiation factor 3 (IF-3) from binding and likely preventing translation initiation (Xu *et al.*, 2008). Thus, if mutant *dim1A* remain bound to the *Arabidopsis* cytosolic enzyme, it would likely result a severe translational defect that would likely cause more than moderate root and leaf development phenotypes.

Identification of Novel Genes Involved in Epidermal Cell-type Patterning

While investigating the role of *DIM1A* in root development and cell-type patterning, I also worked on a few projects with the goal of identifying new players in the root epidermal-patterning network. Shortly after I joined the lab, we embarked on a new project looking at the transcriptome of root cells in different patterning mutant backgrounds. Using a technique developed by the Benfey lab at Duke University (Birnbaum *et al.*, 2005, Birnbaum *et al.*, 2003) which combines protoplasting of root tissue expressing specific cell- and tissue-type fluorescent reporter constructs, fluorescent activated cell sorting (FACS) and microarray analysis, we are now able to obtain transcriptome information from single types of root cells.

Forty-three genes of interest were chosen for analysis based on their differential expression in root tissue of the *scm-2* mutant compared to wild-type. With the help of two talented undergraduates, Asha Radhamohan and Luay Almassalha, I analyzed the cell-type patterning of T-DNA insertion mutants for

each of the forty-three genes. From this analysis, mutant lines for five genes were identified as putatively playing a role in the position-dependent specification of root-hair and non-hair cells in the root epidermis. However, our root epidermal cell-type patterning analysis was preliminary. Further analysis is needed to not only confirm the phenotypes observed in this study, but also to further implicate these genes in root cell-type patterning.

In addition, I worked with Dr. Angela Bruex analyzing a group of transcription factor genes identified from microarray analysis conducted on "hairy" and "hairless" roots. The aforementioned microarray analysis identified a subset of bHLH transcription factors from subfamilies VIIIc and XI as being differentially expressed in the two genetic backgrounds. As subfamily VIIIc members RHD6 and RSL1 (Menand *et al.*, 2007), as well as members of related subfamily IIIf GL3, EGL3 and MYC1 (Bernhardt *et al.*, 2003), are known to be involved in root epidermal cell-type patterning we set out to further analyze remaining subfamily VIIIc and XI genes. Homozygous T-DNA insertion mutants were identified in all subfamily VIIIc bHLH genes not previously analyzed, as well as in the subfamily XI genes. While none of the mutant lines displayed root hair phenotypes as striking as other bHLH subfamily VIIIc and IIIf, such as *GL3* (Bernhardt *et al.*, 2003) and *RHD6* (Massucci *et al.*, 1996, Menand *et al.*, 2007), plant lines with insertions in *bHLH 84, bHLH85, bHLH66, bHLH69* and *bHLH82* had mild root hair morphology and/or hair branching phenotypes.

The bHLH transcription factor subfamily VIIIc that comprises six members, including *RHD6* (Heim *et al.*, 2003). An additional member, *RSL1*, is very similar

to *RHD6* and was recently shown to have somewhat redundant functions in root hair initiation (Menand *et al.*, 2007). In our study, we identified homozygous insertion lines in the other for subfamily VIIIc bHLH transcription factor genes. While alone they have mild root epidermal phenotypes, it will be interested to see if there is a genetic interaction between these mutants and the *rhd6* and/or rsl1 mutations.

In addition to the bHLH transcription factors, microarray analysis identified five other transcription factors as differentially expressed in the hairy and hairless root backgrounds.

Conclusions

After narrowing down the region containing the *45-137* mutation to 41 genes I began systematically sequencing genes of interest, based on their annotation and predicted function, to look for the mutation. By the time I had sequenced 39 of the 41, and was left only with a "putative rRNA dimethyladenosine transferase" and another gene I thought could never be what I was looking for, I was pretty convinced that I had missed the mutation. Through the wonders of forward genetics, my thesis research took an unexpected turn into the world of ribosome biogenesis. This not only gave me the opportunity to investigate this truly amazing process, which is often overlooked but so essential to life, but also established a new connection between epidermal patterning and ribosome biogenesis.

In addition, my work analyzing root cell-type patterning in insertion mutant lines of genes of interest identified in microarray analysis not only identified putative regulators of root epidermal development. In addition, by identifying root epidermal cell phenotypes in mutant lines for genes identified as important for epidermal cell differentiation using microarray analysis, I helped to validate the use of microarray analysis in identification of novel regulators of complex transcriptional networks.

Literature Cited

Bernhardt, C, Lee, MM, Gonzalez, A, Zhang, F, Lloyd, A & Schiefelbein, J (2003) The bHLH genes *GLABRA3 (GL3)* and *ENHANCER OF GLABRA3 (EGL3)* specify epidermal cell fate in the *Arabidopsis* root. *Development,* 130**,** 6431-6439.

Birnbaum, K, Jung, JW, Wang, JY, Lambert, GM, Hirst, JA, Galbraith, DW & Benfey, PN (2005) Cell type-specific expression profiling in plants via cell sorting of protoplasts from fluorescent reporter lines. *Nat Methods,* 2**,** 615-9.

Birnbaum, K, Shasha, DE, Wang, JY, Jung, JW, Lambert, GM, Galbraith, DW & Benfey, PN (2003) A gene expression map of the *Arabidopsis* root. *Science,* 302**,** 1956-1960.

Connolly, K, Rife, JP & Culver, G (2008) Mechanistic insight into the ribosome biogenesis functions of the ancient protein KsgA. *Mol. Microbiol.,* 70**,** 1062-75.

Demirci, H, Murphy, F, Belardinelli, R, Kelley, AC, Ramakrishnan, V, Gregory, ST, . . . Jogl, G (2010) Modification of 16S ribosomal RNA by the KsgA methyltransferase restructures the 30S subunit to optimize ribosome function. *RNA,* 16**,** 2319-2324.

Heim, M, Jakoby, M, Werber, M, Martin, C, Weisshaar, B & Bailey, PC (2003) The basic helix–loop–helix transcription factor family in plants: a genome-wide study of protein structure and functional diversity. *Molecular biology and evolution,* 20**,** 735-747.

Helser, TL, Davies, JE & Dahlberg, JE (1972) Mechanism of kasugamycin resistance in *Escherichia coli*. *Nature New Biol,* 235**,** 6-9.

Kim, BH, Cai, X, Vaughn, JN & Von Arnim, AG (2007) On the functions of the h subunit of eukaryotic initiation factor 3 in late stages of translation initiation. *Genome Biol,* 8**,** R60.

Kim, TH, Kim, BH, Yahalom, A, Chamovitz, DA & Von Arnim, AG (2004) Translational regulation via 5' mRNA leader sequences revealed by mutational analysis of the Arabidopsis translation initiation factor subunit eIF3h. *Plant Cell,* 16**,** 3341-56.

Kwak, S-H & Schiefelbein, J (2007) The role of the SCRAMBLED receptor-like kinase in patterning the *Arabidopsis* root epidermis. *Dev. Biol.,* 302**,** 118-131.

Kwak, S-H, Shen, R & Schiefelbein, J (2005) Positional signaling mediated by a receptor-like kinase in *Arabidopsis*. *Science,* 307**,** 1111-1113.

Lafontaine, D, Delcour, J, Glasser, AL, Desgres, J & Vandenhaute, J (1994) The *DIM1* Gene Responsible for the Conserved m62Am62A Dimethylation in the 3'-Terminal Loop of 18S rRNA is Essential in Yeast. *J Mol Biol,* 241**,** 492-497.

Lafontaine, D, Preiss, T & Tollervey, D (1998) Yeast 18S rRNA dimethylase Dim1p: a quality control mechanism in ribosome synthesis? *Mol Cell Biol,* 18**,** 2360-70.

Lafontaine, D, Vandenhaute, J & Tollervey, D (1995) The 18S rRNA dimethylase Dim1p is required for pre-ribosomal RNA processing in yeast. *Genes Dev.,* 9**,** 2470-2481.

Lee, MM & Schiefelbein, J (1999) WEREWOLF, a MYB-Related Protein in *Arabidopsis*, Is a Position-Dependent Regulator of Epidermal Cell Patterning. *Cell,* 99**,** 473-483.

Lee, MM & Schiefelbein, J (2002) Cell Pattern in the *Arabidopsis* Root Epidermis Determined by Lateral Inhibition with Feedback. *Plant Cell,* 14**,** 611-618.

Massucci, JD, Rerie, WG, Foreman, DR, Zhang, M, Galway, ME, David Marks, M & Schiefelbein, J (1996) The homeobox gene *GLABRA2* is required for position-dependent cell differentiation in the root epidermis of *Arabidopsis thaliana*. *Development,* 122**,** 1253-1260.

Menand, B, Yi, K, Jouannic, S, Hoffmann, L, Ryan, E, Linstead, P, . . . Dolan, L (2007) An Ancient Mechanism Controls the Development of Cells with a Rooting Function in Land Plants. *Science,* 316**,** 1447-1480.

O'connor, M, Thomas, CL, Zimmermann, RA & Dahlberg, AE (1997) Decoding fidelity at the ribosomal A and P sites: influence of mutations in three different regions of the decoding domain in 16S rRNA. *Nuc. Acids Res.,* 25**,** 1185-1193.

O'farrell, H, Scarsdale, J & Rife, JP (2004) Crystal Structure of KsgA, a Universally Conserved rRNA Adenine Dimethyltransferase in Escherichia coli. *J Mol Biol,* 339**,** 337-353.

Poldermans, B, Bakker, H & Van Knippenberg, PH (1980) Studies on the function of two adjacent N6, N6-dimethyladenosines near the 3' end of 16 S ribosomal RNA of Escherichia coli. IV . The effect of the methylgroups on ribosomal subunit interaction. *Nuc. Acids Res.,* 8**,** 143-151.

Poldermans, B, Goosen, N & Van Knippenberg, PH (1979a) Studies on the Function of Two Adjacent N",N"-Dimethyladenosines Near the 3' End of 16 S Ribosomal RNA of *Escherichia coli* I.THE EFFECT OF KASUGAMYCIN ON INITIATION OF PROTEIN SYNTHESIS. *The Journal of Biological Chemistry,* 254**,** 9085-9089.

Poldermans, B, Roza, L & Van Knippenberg, PH (1979b) Studies on the Function of Two Adjacent iV,W-Dimethyladenosines Near the 3' End of 16 S Ribosomal RNA of *Escherichia coli* III. PURIFICATION AND PROPERTIES OF THE METHYLATING ENZYME AND METHYLASE-

30S INTERACTIONS. *The Journal of Biological Chemistry,* 254**,** 9094-9100.

Pulicherla, N, Pogorzala, L, Xu, Z, O'farrell, H, Musayev, FN, Scarsdale, JN, . . . Rife, JP (2009) Structural and Functional Divergence within the Dim1/KsgA Family of rRNA Methyltransferases. *J Mol Biol,* 391**,** 884-893.

Richter, U, Kühn, K, Okada, S, Brennicke, A, Weihe, A & Börner, T (2010) A mitochondrial rRNA dimethyladenosine methyltransferase in *Arabidopsis*. *Plant J.,* 61**,** 558-69.

Rook, F, Gerrits, N, Kortstee, A, Van Kampen, M, Borrias, M, Weisbeek, P & Smeekens, S (1998) Sucrose-specific signalling represses translation of the Arabidopsis ATB2 bZIP transcription factor gene. *The Plant journal : for cell and molecular biology,* 15**,** 253-63.

Ryu, KH, Kang, YH, Park, Y-H, Hwang, I, Schiefelbein, J & Lee, MM (2005) The WEREWOLF MYB protein directly regulates CAPRICE transcription during cell fate specification in the Arabidopsis root epidermis. *Development,* 132**,** 4765-4775.

Thammana, P & Held, WA (1974) Methylation of 16S RNA during ribosome assembly in vitro. *Nature,* 251**,** 682-686.

Tokuhisa, J, Vijayan, P, Feldmann, K & Browse, J (1998) Chloroplast Development at Low Temperatures Requires a Homolog of *DIM1*, a Yeast Gene Encoding the 18S rRNA Dimethylase. *Plant Cell,* 10.

Van Buul, CPJJ & Van Knippenberg, PH (1985) Nucleotide sequence of the *ksgA* gene of *Escherichia coli*: comparison of methyitransferases effecting dimethylation of adenosine in ribosomal RNA. *Gene,* 38**,** 65-72.

Van Buul, CPJJ, Visser, W & Can Knippenberg, PH (1984) Increased translational fidelity caused by the antibiotic kasugamycin and ribosomal ambiguity in mutants harbouring the *ksgA* gene. *FEBS letters,* 177**,** 119-124.

Wiese, A, Elzinga, N, Wobbes, B & Smeekens, S (2004) A conserved upstream open reading frame mediates sucrose-induced repression of translation. *Plant Cell,* 16**,** 1717-29.

Xu, Z, O'farrell, H, Rife, JP & Culver, G (2008) A conserved rRNA methyltransferase regulates ribosome biogenesis. *Nature Structural and Molecular Biology,* 15**,** 534-536.

APPENDIX

The Expression Pattern of *WER::GFP* in the Root Epidermis in Patterning and Root Hair Morphogenesis Gene Mutants

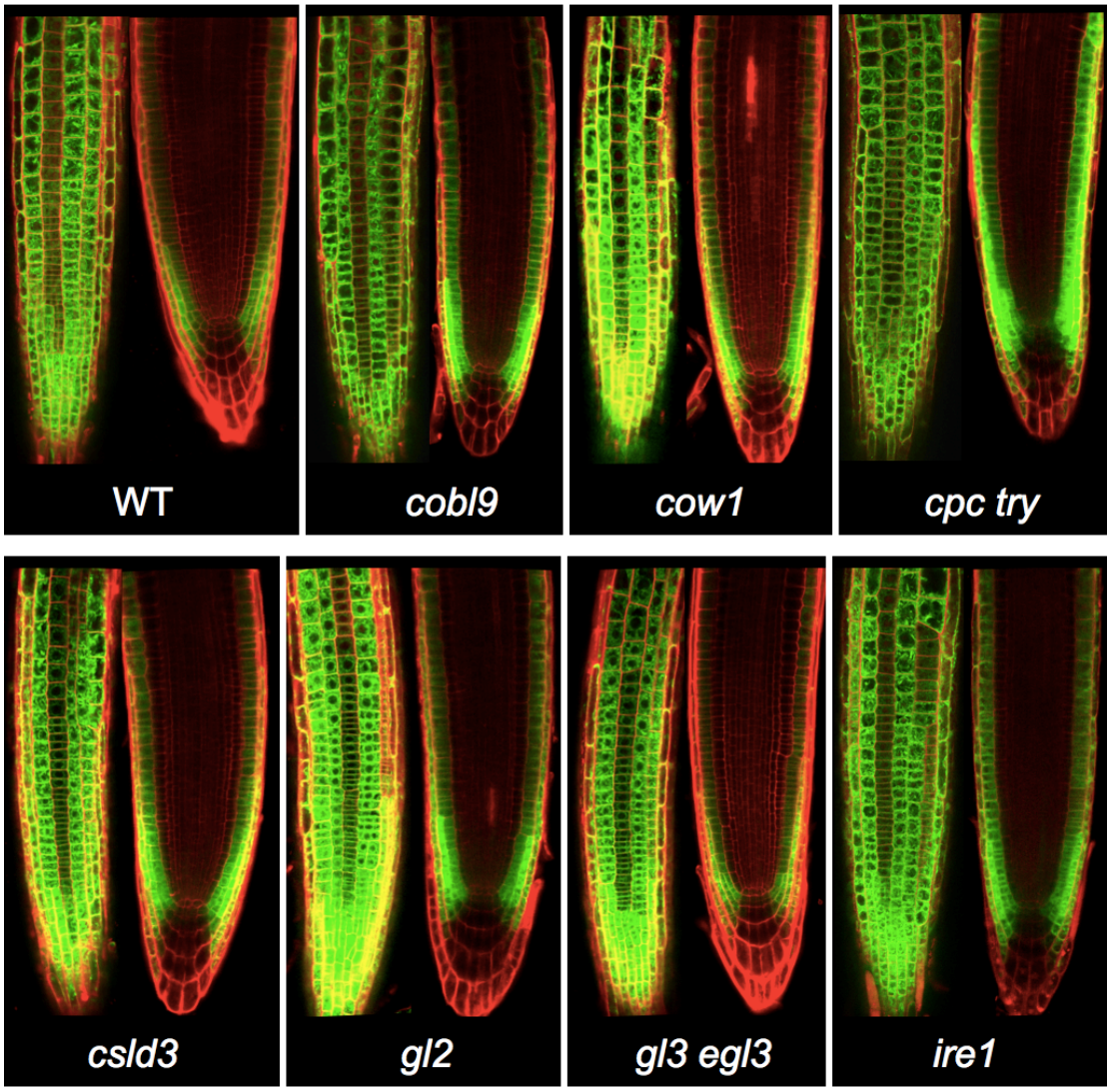

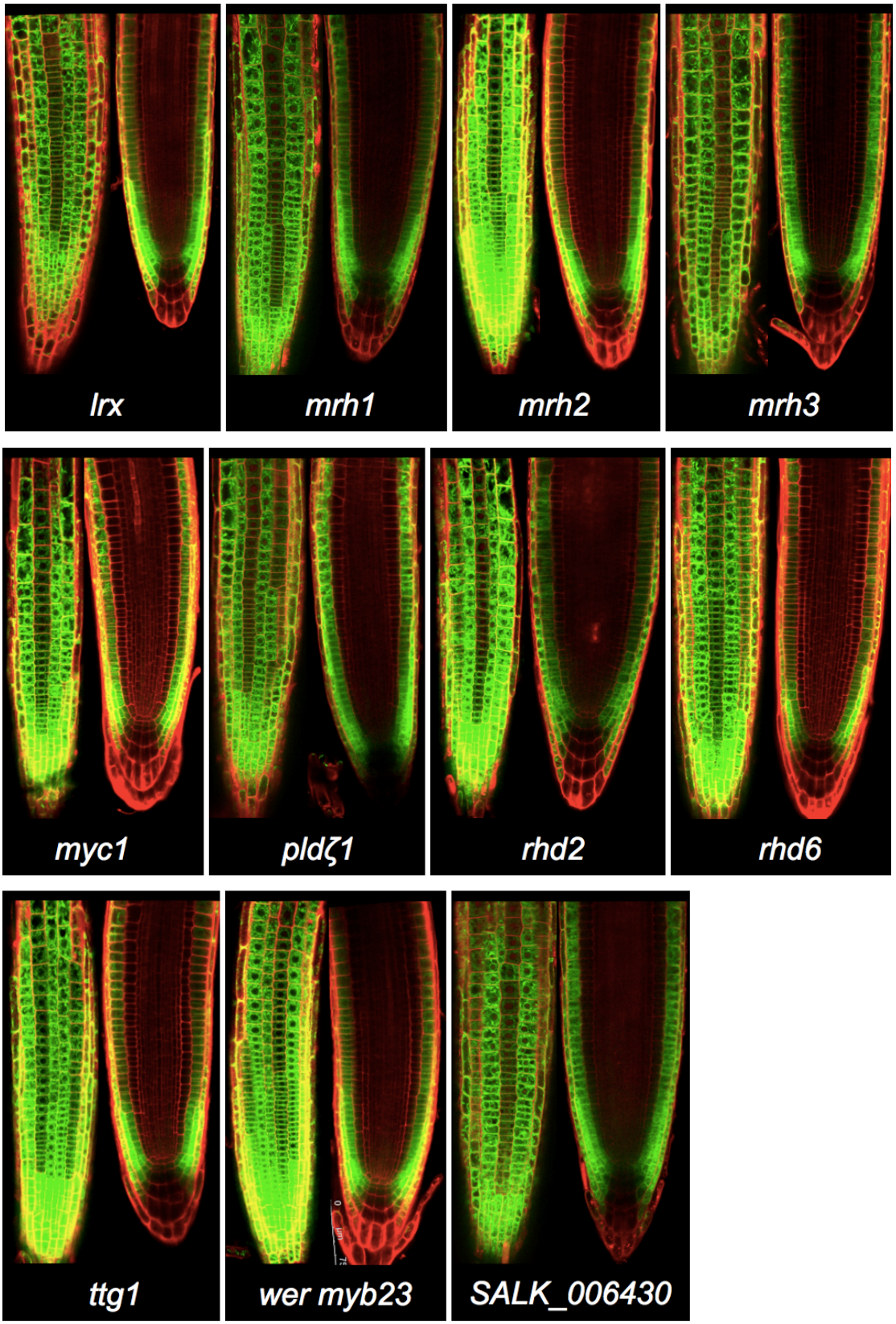
lrx
mrh1
mrh2
mrh3
myc1
pldζ1
rhd2
rhd6
ttg1
wer myb23
SALK_006430